

The FORS1 catalogue of stellar magnetic field measurements*

S. Bagnulo¹, L. Fossati^{2,3}, J.D. Landstreet^{1,4}, and C. Izzo⁵

¹ Armagh Observatory, College Hill, Armagh BT61 9DG, Northern Ireland, U.K. e-mail: sba@arm.ac.uk, jls@arm.ac.uk

² Space Research Institute, Austrian Academy of Sciences, Schmiedlstrasse 6, A-8042 Graz, Austria.
e-mail: luca.fossati@oeaw.ac.at

³ Argelander Institut für Astronomie, Auf dem Hügel 71, Bonn D-53121, Germany.

⁴ Physics & Astronomy Department, The University of Western Ontario, London, Ontario, Canada N6A 3K7.
e-mail: jlandstr@uwo.ca

⁵ Deceased

Received: 2015-05-11 / Accepted: 2015-08-03

ABSTRACT

Context. The FORS1 instrument on the ESO Very Large Telescope was used to obtain low-resolution circular polarised spectra of nearly a thousand different stars, with the aim of measuring their mean longitudinal magnetic fields. Magnetic fields were measured by different authors, and using different methods and software tools.

Aims. A catalogue of FORS1 magnetic measurements would provide a valuable resource with which to better understand the strengths and limitations of this instrument and of similar low-dispersion, Cassegrain spectropolarimeters. However, FORS1 data reduction has been carried out by a number of different groups using a variety of reduction and analysis techniques. Our understanding of the instrument and our data reduction techniques have both improved over time. A full re-analysis of FORS1 archive data using a consistent and fully documented algorithm would optimise the accuracy and usefulness of a catalogue of field measurements.

Methods. Based on the ESO FORS pipeline, we have developed a semi-automatic procedure for magnetic field determinations, which includes self-consistent checks for field detection reliability. We have applied our procedure to the full content of circular spectropolarimetric measurements of the FORS1 archive.

Results. We have produced a catalogue of spectro-polarimetric observations and magnetic field measurements for ~ 1400 observations of ~ 850 different objects. The spectral type of each object has been accurately classified. We have also been able to test different methods for data reduction in a systematic way. The resulting catalogue has been used to produce an estimator for an upper limit to the uncertainty in a field strength measurement of an early type star as a function of the signal-to-noise ratio of the observation.

Conclusions. While FORS1 is not necessarily an optimal instrument for the discovery of weak magnetic fields, it is very useful for the systematic study of larger fields, such as those found in Ap/Bp stars and in white dwarfs.

Key words. Polarisation – Stars: magnetic field – Catalogs

1. Introduction

During a full decade of operations, the FORS1 instrument on the ESO Very Large Telescope collected a large number of magnetic field measurements of various kinds of stars. Together with the ESPaDOnS instrument on the Canada-France-Hawaii Telescope, and the MuSiCoS and NARVAL instruments on the 2 m Telescope Bernard Lyot of the Pic-du-Midi Observatory, FORS1 has been one of the workhorse instruments for observational studies of stellar magnetism.

Most, if not all, FORS1 field measurements have been published in the literature in dozens of different articles. Gathering them in a general catalogue would serve to obtain an overview (even though biased at the target selection phase) of the incidence of the magnetic fields in various kinds of stars. However, a catalogue compiled using published material would suffer from the lack of homogeneity in the way data have been treated. Furthermore, over time, new ideas for data reduction and quality checks have improved the reliability of FORS1 magnetic measurements, which calls for a revision of earlier data. We also

note that the literature of FORS magnetic field measurements includes a certain number of controversial detections. These problems have been thoroughly discussed by Bagnulo et al. (2012) and Bagnulo et al. (2013), and a discussion on the quality of the non-controversial FORS1 measurements of magnetic Ap stars was presented by Landstreet et al. (2014).

Here we publish our full catalogue of FORS1 measurements and explore experimental relationships between signal-to-noise (S/N) ratios and error bars achieved in stars with different spectral characteristics.

2. Instrument and instrument settings

FORS1 is a multi-purpose instrument equipped with polarimetric optics capable of performing imaging and low-resolution spectroscopy in the optical. It was attached to the Cassegrain focus of one of the 8 m units of the ESO Very Large Telescope (VLT) at the Paranal Observatory from the beginning of operations in 1999 until instrument decommissioning in March 2009. The instrument is described in Appenzeller & Rupprecht (1992) and Appenzeller et al. (1998).

* The full catalogue and the spectra are available in electronic form at the CDS via anonymous ftp to cdsarc.u-strasbg.fr (130.79.128.5) or via <http://cdsweb.u-strasbg.fr/cgi-bin/qcat?J/A+A/>. This paper includes an abridged printable version of the catalogue.

2.1. Polarimetric optics

The polarimetric optics of FORS1 are arranged according to the optical design described by Appenzeller (1967). These components are embedded in the overall optical train of the low-dispersion spectrograph for spectropolarimetric observations as follows. The Cassegrain focal plane of the telescope coincides with a mask containing 18 parallel sets of positionable slit jaws, which in simple spectroscopy allow multi-object spectroscopy of up to 18 objects simultaneously. For spectropolarimetry every second pair of slit jaws is masked to prevent beam overlapping in the camera (following the scheme proposed by Scarrott et al. 1983), so up to nine slits can be used at once. For most observations only a single slit was used, normally (but not always) centred on the optical axis of the telescope and of the spectrograph collimator (“fast” mode), but a number of spectropolarimetric observations using the multi-slit capability were carried out for studies of clustered objects (e.g. stars in an open cluster; “fims” mode). The slits are 22” long and can be adjusted to an arbitrary width.

The slit plane is followed by a dioptric collimator consisting of four UV-transmitting lenses, which takes each diverging beam from the slit plane and converts it into a parallel beam; the collimated beams from different slits have slightly different axes. For spectropolarimetry, these collimated beams are then passed through a rotatable super-achromatic quarter- or half-wave plate, followed by a beam-splitting Wollaston prism which produces two slightly diverging beams that have been divided into two orthogonal linear polarisation states. Each beam pair is analysed into polarisation states parallel to and perpendicular to the plane of the beam divergence produced by the Wollaston prism.

Following the polarimetric optics, the beams pass through a grism, and possibly an order-sorting filter, which disperses each beam into a spectrum. This is followed by a camera lens system (four lenses) that images the dispersed light from each polarised beam into a spectrum along one axis of the CCD detector. The two dispersed beams from each single slit are imaged on neighbouring CCD rows (in the case of multi-slit observations, the various pairs of beams are arranged parallel to one another on the detector). Spectropolarimetry is accomplished (in principle) by comparing the two beams from each single slit to form sum and difference spectra, from which a polarisation Stokes parameter can be deduced.

2.2. CCD and CCD readout

Two detectors have been used in the FORS1 instrument: a 2k×2k SITE CCD (from the beginning of operations to end of February 2007), and a mosaic composed of two 2k × 4k MIT CCDs with a pixel size of $15 \times 15 \mu\text{m}$ (from March 2007 until FORS1 decommissioning in March 2009). The upgrade to the MIT CCD was described by Szeifert et al. (2007).

The older SITE CCD had a pixel scale of 0.20”. For most of the observations obtained with it, the readout mode was set in “low gain” (to minimise the ADU count, and the risk of saturation of the ADC, at typically 2.8 e^- per ADU¹), and with a window of 400 or 500 pixel rows centred about the spectrum, to

¹ The conversion from ADU to electron is recorded in the fits-header keyword DET.OUT1.CONAD. However, in the QC1 database, the same quantity is called gain, while the QC1 entry CONAD gives the number of ADU per electron. Conversely, the fits-header keyword DET.OUT1.GAIN represents the conversion factor from electrons to ADUs, but corresponds to the entry CONAD in the QC1 database <http://www.eso.org/observing/dfo/quality/>.

Table 1. Summary of the characteristic of the grisms+CCD most commonly employed for magnetic field measurements.

Grism	CCD	Wavelength range (Å)	dispersion (\AA px^{-1})	spectral res. (1’’)
600B	SITE	3470–5900	1.20	780
600B	MIT	3300–6210	0.70	800
1200B	SITE	3800–4960	0.61	1420
1200B	MIT	3660–5110	0.43	1420
1200g	SITE	4290–5470	0.58	1400
600R	SITE	5250–7420	1.08	1160

minimise CCD readout overheads, which represent a consistent fraction of the total overhead time necessary to achieve high S/N ratio spectropolarimetric measurements.

The MIT detector, composed of two chips, had a 0.125” pixel scale, although in many observations a 2×2 rebinning was adopted for the readout. The quantum efficiency of the MIT CCD in the blue was higher than that of the SITE CCD, but the MIT CCD suffered from heavy fringing in the red. One of the advantages of the MIT CCD compared to the SITE CCD was its better cosmetic character. Figure 1 shows the raw image of a spectropolarimetric frame obtained in fast-mode with the MIT CCD. An internal reflection due to the Longitudinal Atmospheric Dispersion Corrector (LADC; Avila et al. 1983), visible in the blue edge of the CCD, has affected many observations.

Most of the observations were obtained in fast-mode, while only a fraction of the observations were obtained in multi-object mode, in which up to nine polarised spectra were obtained with the same frame series. No windowing option was offered for the operations with the MIT CCD, but its typical readout time was comparable to the readout time of the SITE CCD when windowed to 4–500 pixel rows.

2.3. Grisms and slit width

In order of frequency of usage, most of the observations were carried out with grisms 600B (~ 1000 observations), 1200g (~ 100), 1200B (~ 100), 600R (~ 150), and only very rarely with grism 300V (~ 25) and 300I (2). The slit width was generally set to 0.4” or 0.5”, and very rarely > 1”. The systematic use of narrow slits suggests that users wanted to have a high spectral resolution and did not care much about slit losses.

Table 1, obtained from the various editions of the FORS User manual, summarises the characteristics of these grisms. We note that grism 1200 g was often used setting the slit close to the right edge of the instrument field of view. For that special setting, the observed wavelength interval was often offset to the blue to include more Balmer lines than in the configuration with the slit at the centre of the field of view. Grism 600R was used together with order separation filter GG 435, while 600B, 1200B and 1200g were always used with no filter.

2.4. Observing strategy

Most of the observations were obtained by setting the retarder waveplate at two position angles relative to the principal plane of the Wollaston prism, and obtaining multiple exposures for the purpose of maximising the S/N ratio and allowing the computation of the null profiles. The most typical observing sequence was $-45^\circ, +45^\circ, +45^\circ, -45^\circ, -45^\circ, +45^\circ, +45^\circ, -45^\circ$. This beam-swapping technique allows one to minimise instrumental effects as explicitly suggested in the FORS1/2 manual, and thor-

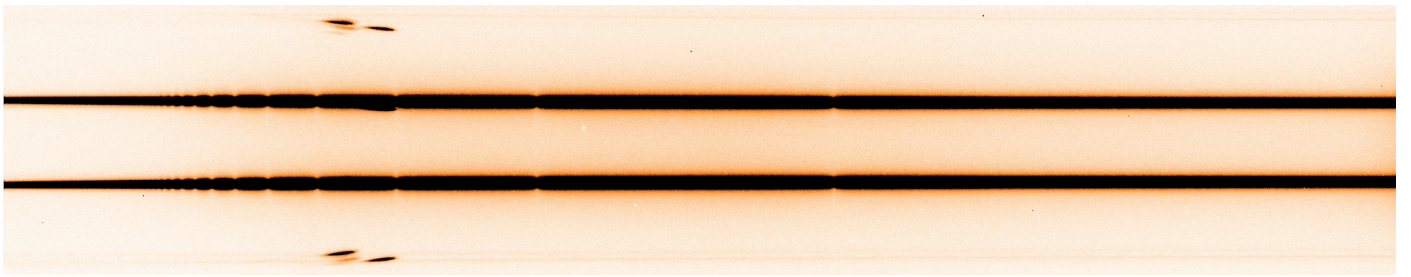


Fig. 1. Raw image of a polarisation spectrum obtained with the MIT CCD. On the blue (left) side reflections from the LADC are visible.

oughly discussed, e.g. by Bagnulo et al. (2009). Bagnulo et al. (2013) have argued that swapping between only two positions of the retarder waveplate may lead to more accurate results than cycling through all four positions in quadrature (i.e. -45° , 45° , 135° , 225°) because the latter sequence is more likely to introduce small instrumental wavelength offsets between different exposures.

3. Data reduction

In this Section we give a detailed description of how we have organised the archive data, and how we have treated them to measure the circular polarisation. We will adopt the same formalism used in Bagnulo et al. (2009), i.e. f^{\parallel} and f^{\perp} are the fluxes in the parallel and in the perpendicular beam, respectively, $P_V = V/I$ is the circular polarisation normalised to the intensity, and N_V is the null profile (also normalised to I), a quantity that was introduced by Donati et al. (1997), and, as described by Bagnulo et al. (2009), is representative of the noise of P_V .

We have always obtained P_V profiles from a series of one or more pairs of exposures. Each pair of exposures is composed of two frames obtained with the retarder waveplate at position angles separated by 90° . In Sect. 3.1 we explain the criteria followed to associate the frames retrieved from the archive in series of polarimetric measurements, which in fact may occasionally differ from the original plans of the observers.

For most of the observing series, it was also possible to calculate the null profile. For those cases in which the number of pairs of exposures N was odd and ≥ 3 , the null profile was obtained omitting the last pair of exposures. Obviously, with just one pair of exposure, the null profile was not calculated.

3.1. Organising frames

3.1.1. Scientific frames

As a first step we downloaded from the archive all frames obtained in spectropolarimetric mode with the quarter wave retarder in the optical beam. Then we grouped individual frames according to target pointing and observing night. Target identification was obtained via cross-correlation between RA and DEC keywords and SIMBAD catalogue, although we note that the fits-header keyword `OBS.TARG.NAME`, which is set manually by the observer, turned out to be sufficiently meaningful to identify the observed target in all but a very few cases. Occasionally, the RA and DEC of a target with the same `OBS.TARG.NAME` slightly changed within a consecutive series of exposures. We automatically ascribed a change of RA and DEC within $0.5''$ as due to a change of the guiding star; for larger offsets we visually inspected the Stokes I profile to check whether the observations were in fact pointing to distinct components of a visual multiple system. In the (rare) cases in which the same target was acquired

twice or more times during the same night after an interval of time longer than 1 h, the observations were split and treated as independent field measurements. Most of the observation groups finally included *at least* two pairs of exposures, each pair with the retarder waveplate at position angles $+45^\circ$ and -45° . Some observing sets included an odd number of exposures. In many cases, this was because a short test exposure was obtained prior executing a long series, with the aim of deciding on the exposure time. These short exposures were then discarded. Sets including only one exposure were discarded.

The archive includes a few long time series of exposures that were performed within the same night on rapidly rotating or pulsating stars, and that were aimed at monitoring the target during its rotation or pulsation cycle. Examples of these cases include the roAp stars observed within programme ID 69.D-0210 and 270.D-5023 (see Table 3), or the cataclysmic variables II Peg and V426 Oph observed with programme ID 079.D-0697 and 081.D-0670. In all these cases we had the choice whether to report the field values e.g. for each pair of frames, or to measure the field from the I and P_V profiles obtained adding up all individual frames. For simplicity, we decided to adopt the latter approach. The interpretation of these field measurement has to be given case by case. For instance, since in roAp stars there is no evidence of a variability of the magnetic field with stellar pulsation, the value averaged over several pulsation cycles is still a meaningful estimate of the actual star's longitudinal field at a given rotation phase. If a time series extends over an interval of time that represents a non negligible fraction of the star's rotation cycle, then the averaged measurement may not be representative of the actual field. Long time series may be identified by the of frames used for field identification, which is an entry of our catalogue (see Sect. 6.2).

Any pair of frames where at least one beam in one exposure had an ADU count $\geq 64\,000$ in at least 20 pixels was discarded as saturated. Exceptions to this rule were applied when all pairs of frames of a given series would be discarded, in which case we rescued those spectral regions that were not saturated. A second exception to this rule applies to the observations obtained in the context of the observing programme 073.D-0464. The CCD gain had been set to a very high value (3.5 ADU/e^-), with the consequence that the CCD reached the full well capacity before ADC saturation. For all frames obtained with that CONAD value we set the threshold for saturation to 40,000 ADUs instead of 64 000 ADUs.

3.1.2. Calibration frames

For each set of observations, we retrieved from the archive the corresponding calibration frames, which included at least five bias frames, one arc lamp, and one flatfield, although for each set, we generally used five flatfield frames. Most calibration

frames were obtained the morning after the night in which the scientific frames were obtained. Occasionally, wavelength calibration frames were in fact obtained one or two days later or earlier than science data, and very rarely up to one or two weeks later or earlier. Time gaps between science data and calibration frames longer than one day were found more frequently for flat field calibrations. The reason is that acquiring high S/N ratio flatfield calibrations in the blue with a narrow slit is very time consuming, especially with the polarimetric optics in. Hence, for operational reasons, sometimes flatfield calibrations had to be postponed by one or more days. We note that flatfield frames were used by the pipeline to identify the CCD regions occupied by spectra, but scientific frames were not divided by the flatfield.

3.2. Deriving the Stokes and null spectra

Each individual pairs of raw data were ingested into the FORS pipeline (Izzo et al. 2010) to perform bias subtraction, 2D-wavelength mapping of the frames, and flux extraction without flat-fielding the science data. Crucial for the data reduction was to avoid alignment with the sky lines. Many targets were very bright, and the adopted short-exposure times were not long enough to obtain high S/N ratio sky lines. Furthermore, only one useful line is present in most of the settings. We found that the alignment of each frame to the sky lines would generate differential shifts that would be eventually responsible for spurious signals in the polarisation spectra (see Fig. 1 of Bagnulo et al. 2013).

We did not use the final pipeline products but we combined the various f^{\parallel} and f^{\perp} fluxes output by the ESO pipeline with a dedicated FORTRAN routine, and we obtained P_V and N_V profiles using the formulas of the difference methods given in Eqs. (A2) and (A7) of Bagnulo et al. (2009), which for convenience we reproduce below,

$$\begin{aligned} P_V &= \frac{1}{2N} \sum_{j=1}^N \left[\left(\frac{f^{\parallel}-f^{\perp}}{f^{\parallel}+f^{\perp}} \right)_{\alpha_j} - \left(\frac{f^{\parallel}-f^{\perp}}{f^{\parallel}+f^{\perp}} \right)_{\alpha_j+90^\circ} \right] \\ N_V &= \frac{1}{2N} \sum_{j=1}^N (-1)^{(j-1)} \left[\left(\frac{f^{\parallel}-f^{\perp}}{f^{\parallel}+f^{\perp}} \right)_{\alpha_j} - \left(\frac{f^{\parallel}-f^{\perp}}{f^{\parallel}+f^{\perp}} \right)_{\alpha_j+90^\circ} \right], \end{aligned} \quad (1)$$

where α_j belongs to the set $\{-45^\circ, 135^\circ\}$. The reason for not using the final products of the pipeline was to experiment with different algorithms. For instance, the rectification that we use for P_V and $\langle N_z \rangle$ (explained in Sect. 3.1 of Bagnulo et al. 2012) is carried out on the fluxes f^{\parallel} and f^{\perp} . This rectification is occasionally needed for those cases in which we found the P_V profile clearly offset from zero. This offset was found even when no circular polarisation of the continuum was expected, for instance in Herbig Ae/Be stars by Wade et al. (2007), and in several other cases in the course of the present work. A possible explanation is cross-talk from linear to circular polarisation, as discussed by Bagnulo et al. (2009). Obviously, cross-talk is expected to be a problem only with observations of linearly polarised sources, and it is far more significant for spectra acquired with a slitlet close to the edge of the instrument field of view (as in some series obtained in multi-object mode).

A slight but noticeable circular polarisation signal in the continuum was also found in some of FORS data for sources that are *not* linearly polarised, and that were observed in the centre of the field of view. For these cases, we should probably rule out cross-talk as a mechanism responsible for the observed continuum polarisation. A possible explanation could be that the ratio between the transmission functions in the perpendicular beam h^{\perp} , and the transmission function in the parallel beam, h^{\parallel} , is not

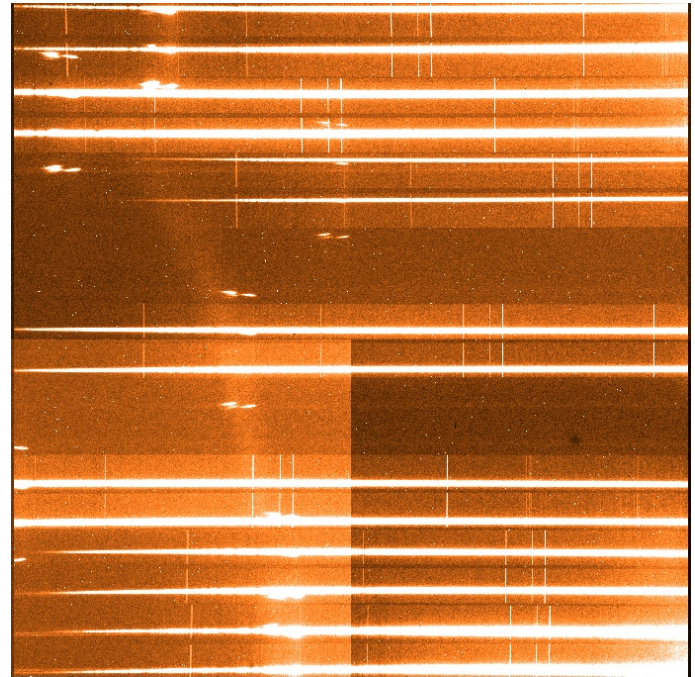


Fig. 2. Raw image of polarisation spectra obtained with the SITE CCD on 2003-02-09. Seven out of nine slitlets are on stars member of an open cluster. The various reflections (presumably from the LADC) hamper the automatic extraction and recombination of the beams by the pipeline.

constant as the retarder waveplate rotates at the different position angles. In either case (cross-talk from linear polarisation, or variability of the ratio $h = h^{\perp}/h^{\parallel}$), the P_V profile should be rectified to zero for a more accurate field determination. Inspection of the null profile may help to discriminate between the two cases. If P_V is offset from zero because of cross-talk from linear polarisation (or simply because the source is intrinsically circularly polarised), the null profile will still be oscillating about zero. If the P_V offset is due to a non-constant ratio of the transmission functions, then also the null profile will be offset from zero.

In this work, the P_V and N_V profiles were rectified to zero as explained in Sect. 3.1 of Bagnulo et al. (2012).

An important difference concerns the treatment of data obtained in multi-objects spectropolarimetric mode. In most of the cases, the ESO pipeline failed to correctly associate the beams, probably due to the presence of strong reflections in the frames. Figure 2 shows an example of a frame obtained in multi-object mode, with seven slits centred on a target, and two slits closed. Some of the data obtained in multi-object mode (mostly those pertaining to a large open cluster survey) were “rescued” through manual data reduction (see Sect. 6.1.1).

Finally, in less than 3 % of the observations obtained in fast mode, the pipeline delivered results of lower quality than expected. Most of these cases were successfully individually treated by performing a data reduction with IRAF tasks (Fossati et al. 2015).

3.3. Magnetic fields determinations

FORS1 magnetic field measurements are obtained by exploiting the relationship

$$\frac{V}{I} = -g_{\text{eff}} C_Z \lambda^2 \frac{1}{I} \frac{dI}{d\lambda} \langle B_z \rangle, \quad (2)$$

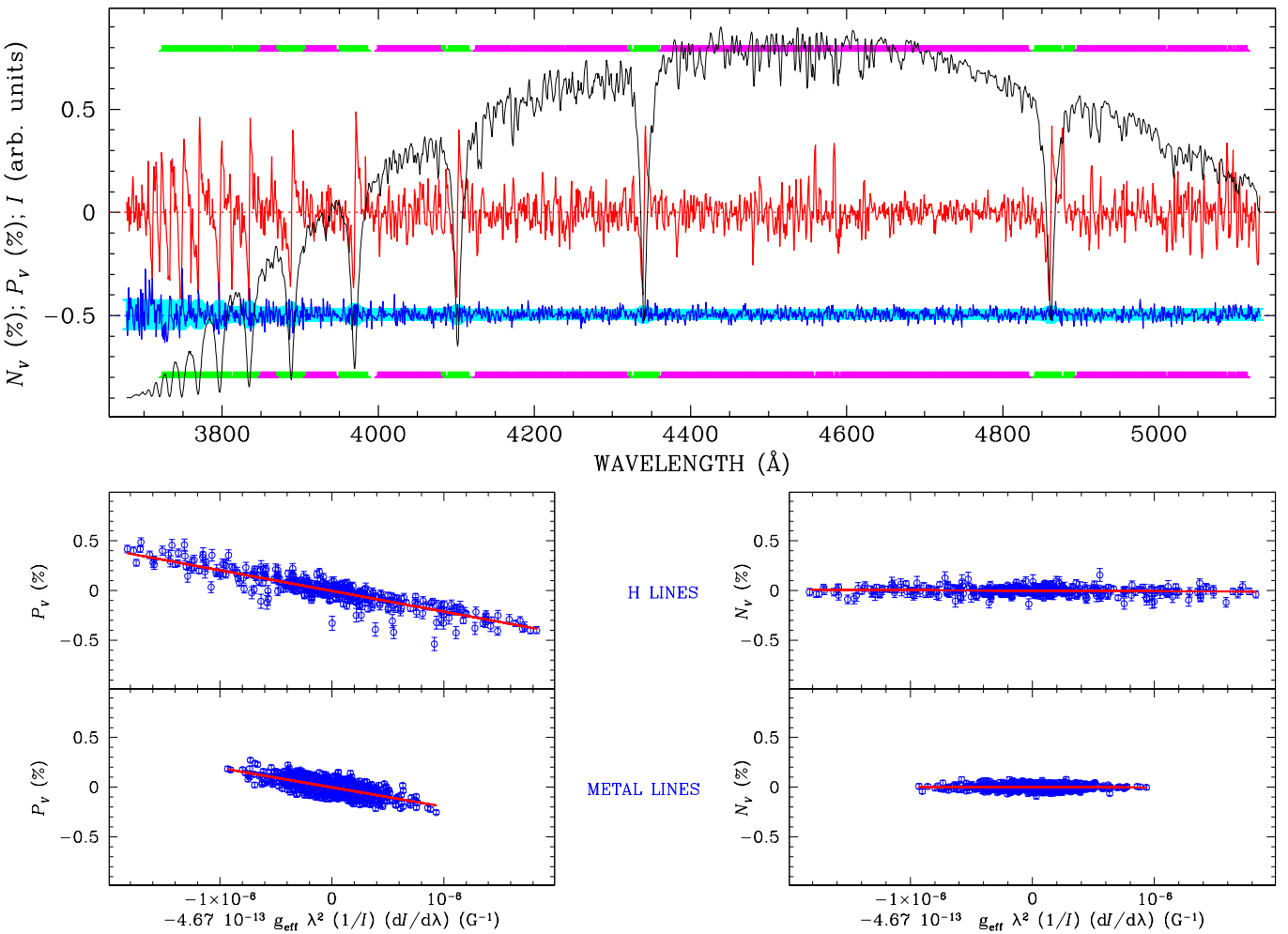


Fig. 3. An example of data reduction: the case of the Ap star HD 94660. In the upper panel, the black solid line shows the intensity profile, the shape of which is heavily affected by the transmission function of the atmosphere + telescope optics + instrument. The red solid line is the P_V profile (in % units) and the blue solid line is the null profile offset by -0.5% for display purpose. Photon-noise error bars are centred around -0.5% and appear as a light blue background. Spectral regions highlighted by green bars have been used to determine the $\langle B_z \rangle$ value from H Balmer lines, and the magenta bars highlight the spectral regions used to estimate the magnetic field from metal lines. The four bottom panels show the best-fit obtained by minimising the χ^2 expression of Eq. (4) using the P_V profiles (left panels) and the N_V profiles (right panels) for H Balmer lines and metal lines as described. The field values ($\langle B_z \rangle \sim -2000$ G and $\langle N_z \rangle \sim 0$ G) are determined with a formal accuracy of ~ 40 G for Balmer lines and ~ 25 G for metal lines.

where g_{eff} is the effective Landé factor, and

$$C_Z = \frac{e}{4\pi m_e c^2} \quad (\simeq 4.67 \times 10^{-13} \text{ Å}^{-1} \text{ G}^{-1}), \quad (3)$$

where e is the electron charge, m_e the electron mass, c the speed of light. We have adopted $g_{\text{eff}} = 1.00$ for the H lines, and 1.25 as an average for the metal lines. Bagnulo et al. (2002) proposed to use a least-squares technique to derive the longitudinal field via Eq. (2), by minimising the expression

$$\chi^2 = \sum_i \frac{(y_i - \langle B_z \rangle x_i - b)^2}{\sigma_i^2}, \quad (4)$$

where, for each spectral point i , $y_i = P_V(\lambda_i)$, $x_i = -g_{\text{eff}} C_Z \lambda_i^2 (1/I_i \times dI/d\lambda)_i$, and b is a constant introduced to account for possible spurious polarisation in the continuum. The limitation of this method is that the spurious polarisation is assumed to be constant in wavelength, which in fact may not be true. The use of profiles rectified as explained in the previous

Section probably makes the introduction of the constant b redundant. The numerical evaluation of the quantity $1/I_i \times (dI/d\lambda)_i$, which appears in the definition of the term x_i , was obtained as

$$\frac{1}{I_i} \left(\frac{dI}{d\lambda} \right)_{\lambda=\lambda_i} = \frac{1}{N_i} \frac{N_{i+1} - N_{i-1}}{\lambda_{i+1} - \lambda_{i-1}}, \quad (5)$$

where N_i is the photon count at wavelength λ_i . $\langle B_z \rangle$ is calculated on points selected after visual inspection either as pertaining to H Balmer lines or to He and metal lines.

We systematically avoided emission lines and spectral lines clearly affected by non-photon noise (e.g. cosmic rays) and we generally avoided using spectral regions judged featureless by means of a visual inspection.

We also obtained null field $\langle N_z \rangle$ in the same way as $\langle B_z \rangle$, but using the null profiles N_V instead of P_V .

Figure 3 illustrates in detail how field is estimated from P_V and N_V profiles.

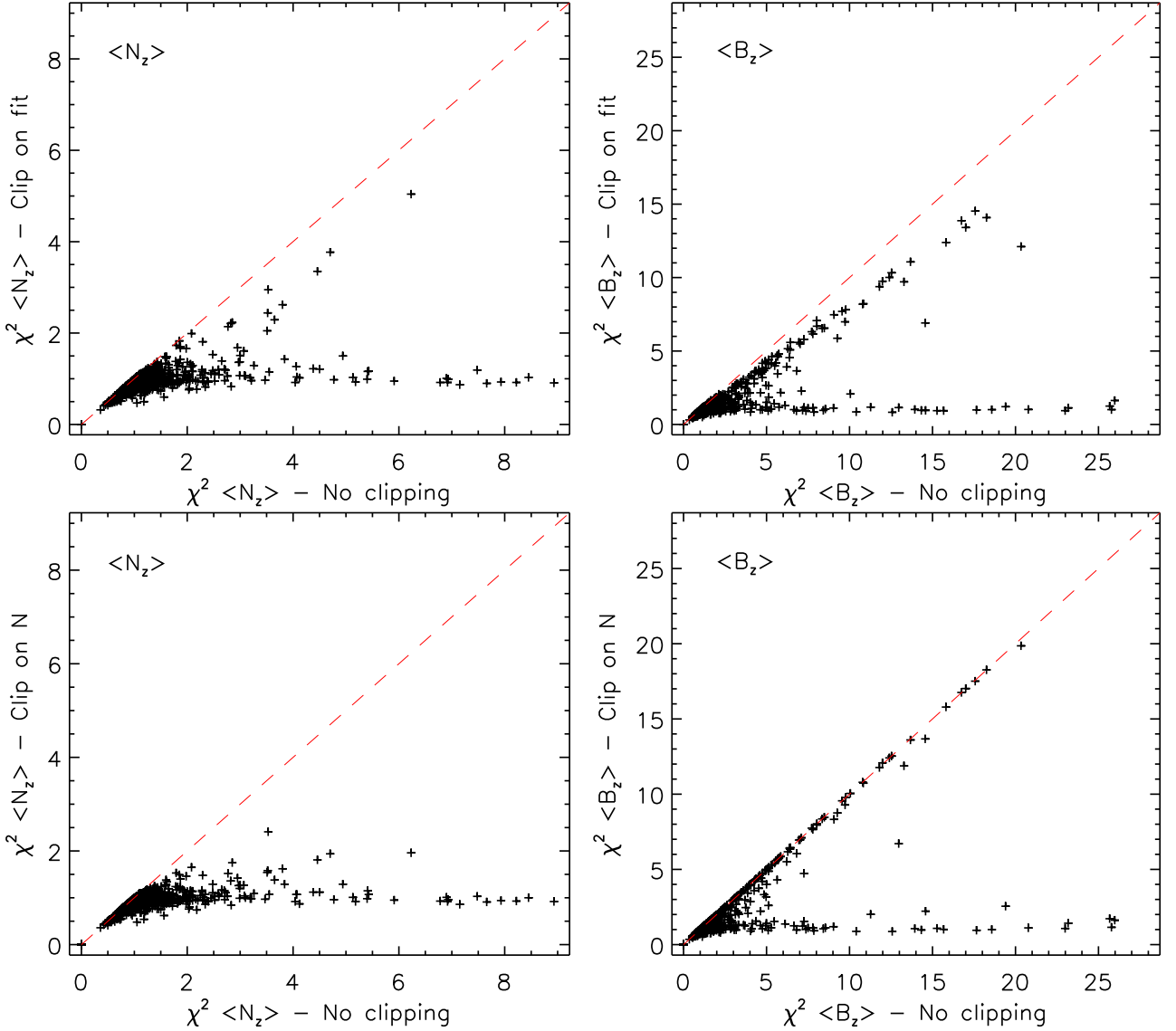


Fig. 4. The reduced χ^2 adopting two different clipping algorithms for field estimates, versus the reduced χ^2 obtained without adopting any clipping algorithm.

3.3.1. Clipping algorithms

It is possible to improve the quality of the field determinations by applying one or more clipping algorithms. For instance, we can reject all spectral points for which the rectified null value exceeds 3σ in absolute value (as proposed by Bagnulo et al. 2012, we call this method N -clipping), or we can rejects all P_V and N_V points that are more than 3σ away from the interpolating line $y = \langle B_z \rangle x + b$ (we will call this method fit-clipping).

Another possible way to improve the precision measurement is to reject all points for which $|x|$ is greater than a certain threshold, as Landstreet et al. (2012a) did. For instance, a point with $|x| > 10^{-6} \text{ G}^{-1}$ in the spectrum of a white dwarf is probably due to a cosmic ray rather than to a real sharp spectral line, hence the motivation for this type of clipping.

Figure 4 shows the effects of some of these algorithms on the final error bars and on the reduced χ^2 , and makes the effect of their use evident.

We noticed that in several cases, a clipping on deviant N_V points would improve the $\langle N_z \rangle$ best-fit, without having a sig-

nificant impact on the quality of the fit used to determine $\langle B_z \rangle$. Conversely, the clipping on the best-fit was found to be more efficient. The reason is that spikes in P_V due to instrumental instabilities, for example, do not necessarily also appear in the null profiles, and vice versa (for a detailed discussion, see Bagnulo et al. 2012). We finally decided to implement a σ clipping on the best-fit, adopting the following specific algorithm (Bagnulo et al. 2006). As a first step, a best-fit is obtained by minimising the expression of the χ^2 given by Eq. (4), considering all (pre-selected) spectral points. Then we calculate the median and the median absolute deviation (MAD) of the distances weighted by the photon-noise error between P_V (or N_V) values and the best-fit. We then reject the P_V (or N_V) points for which the weighted distance from the best-fit is $> 3 \times 1.48 \text{ MAD}$. The procedure is iterated until no points are rejected, but from the second iteration on we reject the points that have distance from the best fit-larger than three times the reduced χ^2 value.

It is important to recognise that for a given dataset it is not possible to associate a uniquely defined longitudinal field estimate. Bagnulo et al. (2012) have thoroughly discussed how two

equally reasonable data reduction procedures produce (slightly) different results. In some cases one may be able to decide that one procedure may be more appropriate than another one, but in most cases we are left with a certain degree of arbitrariness. Among steps that may affect the final results one should consider whether data are flatfielded or not, which method is adopted to extract spectra (average extraction or optimal extraction), if and how Stokes profiles are rebinned and/or rectified, how the derivative is calculated, if and how data are clipped, which spectral regions are used for the field determination, and which effective Landé factor is adopted (the latter choice does not change the relative error measurement). It is not surprising therefore that from the same dataset, different field values are obtained by different authors, or even by the same authors in different epochs. In this respect, data reduction should be somehow considered as a source of noise that adds to photon-noise and instrument instabilities.

3.4. Error bars

Error bars of $\langle B_z \rangle$ and $\langle N_z \rangle$ are calculated using Eqs. (10) and (11) of Bagnulo et al. (2012). Briefly, they are calculated by propagating the photon-noise of the fluxes, and then multiplied by the square root of the reduced χ^2 . When a field is detected, the reduced χ^2 associated with the $\langle B_z \rangle$ estimate tends to be higher than the reduced χ^2 associated with the $\langle N_z \rangle$ estimate. As a consequence of the way they are calculated, the $\langle B_z \rangle$ error bars are also systematically higher than $\langle N_z \rangle$ error bars. Since our error bars are proportional to the square-root of the reduced χ^2 , field error bars are higher in strongly magnetic stars than in weak-field or non-magnetic stars. This phenomenon is not surprising, but is simply a natural consequence of the fact that Eq. (2) is only an approximation, and a lot of effects conspire to deviate from it, such as line blending, breaking of the weak-field approximation in metal lines, Lorentz forces and Stark broadening of the H lines. One could even conclude that a situation where the reduced χ^2 associated with P_V is substantially higher than the χ^2 associated with N_V represents already *per se* an indication that a magnetic field is present.

4. Precision of field measurements versus spectral signal-to-noise ratio

Our catalogue may be used for a number of statistical studies, some of them already discussed by Bagnulo et al. (2012).

An important question for planning observations and for evaluating their success is the extent to which the final magnetic field uncertainty of a measurement may be predicted from the expected S/N ratio of the observation (as estimated for example using the exposure time calculator, or measured after the observation). We here use the catalogue to establish a quantitative link between field error bars and spectral S/N ratio for stars of different spectral classes.

A global overview of the situation is shown in the upper left panel of Figure 5. This panel shows the error bar $\sigma_{\langle N_z \rangle}$ of the null field versus the peak S/N ratio per Å measured in the spectrum for most of the main spectral classes present in the catalogue, using the value of $\sigma_{\langle N_z \rangle}$ computed from the entire (useful) spectrum. The reason to choose $\sigma_{\langle N_z \rangle}$ rather than $\sigma_{\langle B_z \rangle}$ as abscissa is that, as discussed in Sect. 3.4, in stars with strong magnetic fields, $\sigma_{\langle B_z \rangle}$ may be much higher than $\sigma_{\langle N_z \rangle}$, without being representative of the real detection threshold. In this panel the data do show a broad trend of decreasing $\sigma_{\langle N_z \rangle}$ with increasing peak

S/N ratio, and we already see that to obtain measurements with $\sigma_{\langle N_z \rangle} \lesssim 100$ G, it is necessary to obtain spectra with peak S/N ratio $\gtrsim 10^3$.

The data also show a considerable scatter around the mean curve. Part of this scattering occurs because in some spectral classes a more precise field measurement is possible than in others (for example, field measurements are more precise in Ap/Bp stars with their rich line spectra than in O-type stars with far fewer, weaker lines). Part of this scatter seems to be intrinsic to each main spectral class.

The scatter around the mean curve may be better understood by restricting the data used. In the upper right panel of Fig. 5, the uncertainty $\sigma_{\langle N_z \rangle}$ is plotted again for normal A and B stars and for Ap/Bp stars, but using only observations with the 600B grism and only the Balmer line regions for the estimate of $\sigma_{\langle N_z \rangle}$. We see that the dispersion around the mean curve (which here is fitted to the data, with somewhat arbitrary omission of some outliers) is dramatically reduced. The tightness of the data around the mean curve reflects the fact that the Balmer line strength and shape do not change very much through this effective temperature range, and are not very different for Ap/Bp stars than for normal stars.

In contrast, the left bottom panel shows $\sigma_{\langle N_z \rangle}$ as determined using only the metallic line regions and grism 600B. Here the scatter is much larger than in the preceding panel, showing the diversity of the metallic spectra in this sample. In this sample, the number of available spectral lines, and their typical depth and breadth, vary with spectral class and with projected rotational velocity, and some stars have many points in the spectra with steep slopes $dI/d\lambda$, while others have few or none. In turn this has a very strong effect on the horizontal distribution of points in correlation diagrams such as the lower panels of Fig. 3, with the consequence that for some stars the field is far more precisely determined from metal lines than for others. At the extremes, $\sigma_{\langle N_z \rangle}$ from metal lines may be much less than half as large as that from the Balmer lines, or twice as large. Thus the scatter in the upper left panel arises essentially from the variations in the metallic line spectrum. For early-type stars, a robust estimation of the field uncertainty expected from the H lines as a function of S/N ratio may be obtained, but the (potentially quite large) improvement in this basic $\sigma_{\langle N_z \rangle}$ coming from the metallic lines cannot even be estimated without knowing in some detail the nature of the metallic line spectrum.

The right bottom panel of Fig. 5 illustrates the special case of DA white dwarfs. Here we have plotted $\sigma_{\langle B_z \rangle}$ instead of $\sigma_{\langle N_z \rangle}$ because with field measurements based only on completely unblended H lines (hardly any DA white dwarfs show lines of any other chemical element), all with the same Landé factor, no extra dispersion enters the evaluation of $\sigma_{\langle B_z \rangle}$ compared to $\sigma_{\langle N_z \rangle}$. It is seen that field measurements of the DA white dwarfs follow a similar relation to the Balmer line relationship for main sequence A and B stars. However, for a given S/N ratio, the field uncertainties are two or three times higher than for main sequence A and B stars. This larger uncertainty is essentially a consequence of the fact that the H lines of white dwarfs are several times broader than those of main sequence stars with similar temperature. Consequently, the slopes $dI/d\lambda$ of various points in the spectrum of a white dwarf are smaller than in a A or B-type star. Since we have essentially $\sigma_{\langle B_z \rangle} \propto \sigma_V (dI/d\lambda)^{-1}$ it is clear that for a given value of the S/N ratio, $\sigma_{\langle B_z \rangle}$ is larger in stars with small $dI/d\lambda$ than in stars with higher $dI/d\lambda$. We also note that there are a few distant outliers in the white dwarf panel, because white dwarfs with very high or very low effective temperatures have very shallow Balmer lines that provide a very poorly constrained slope in Fig. 3.

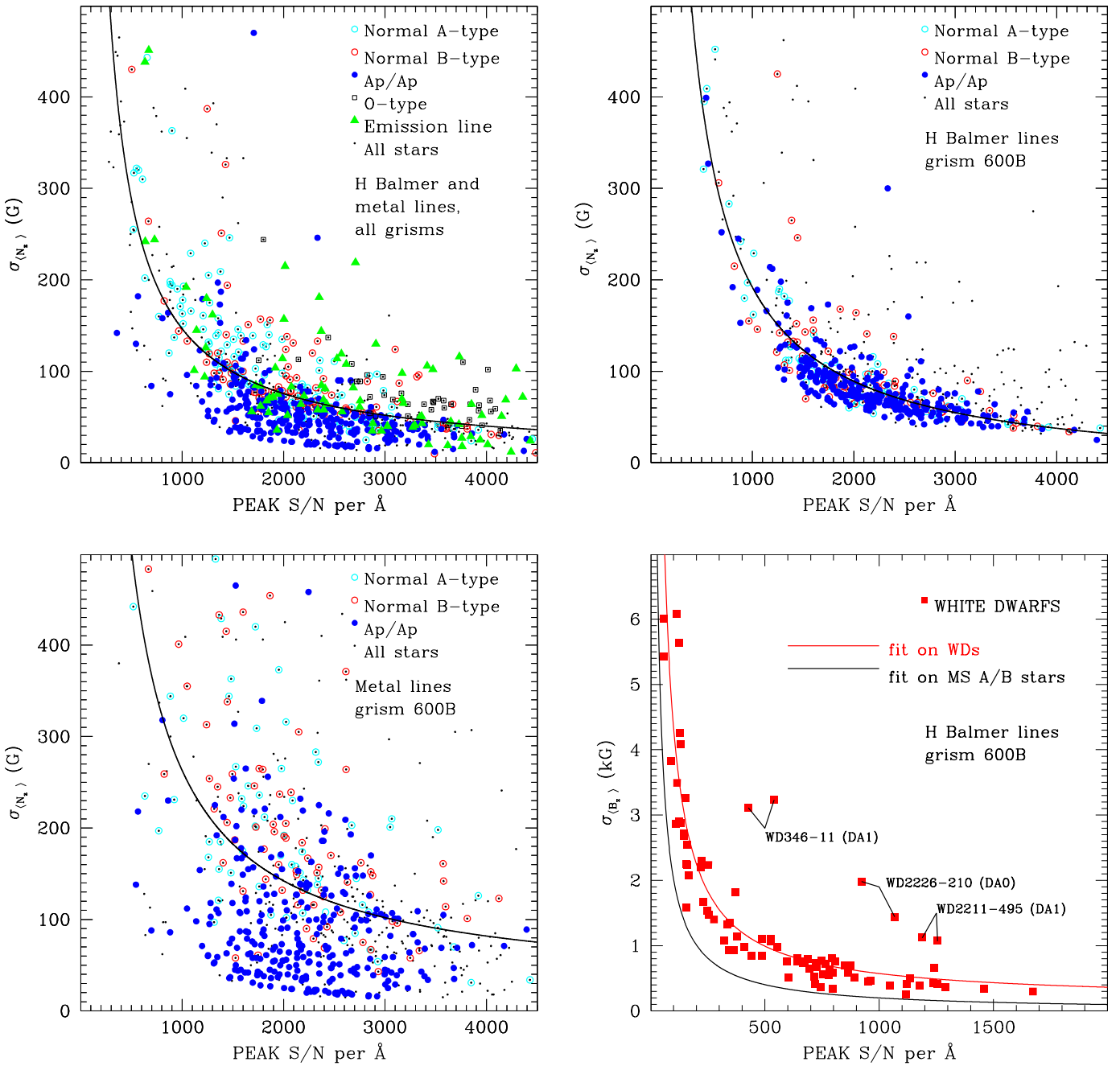


Fig. 5. Error bars versus the peak S/N ratio for different kinds of stars. Left top panel: the error bars on the null field for all stars calculated using both H Balmer and metal lines. Right top panel: same as left panel, but considering only main sequence A- and B-type stars (including Ap/Ap stars) observed using grism 600B, and using H Balmer lines only. Left bottom panel: same as right top panel, but using metal lines only. Right bottom panel: the errors $\sigma_{\langle B_z \rangle}$ on the longitudinal field measured from H Balmer lines only in white dwarfs; the outliers are the hottest star.

Finally, we note that, with the exception only of the fast rotating G-type star FK Com, FORS1 was never used to observe cool stars. Clearly, from the higher density spectra of cooler stars we expect to measure fields with higher precision than in chemically normal early-type stars (but higher precision does not automatically translate into higher accuracy). Field measurements in FK Com have reached a precision of ~ 20 G for a S/N ratio ~ 3500 , comparable to what is achievable from metal lines of Ap stars.

5. Stellar classification

The stars of the FORS1 archive cover a wide range of spectral types and evolution stages. Many are in some way distinctive or even peculiar. Here we provide a classification to facilitate the identification of all FORS1 measurements of a particular type of star.

In order to maximise the usefulness of these classifications, we went beyond the very inhomogeneous classes that would be obtained, for example, by simply taking the stellar classifications (often on the MK or Henry Draper systems) from the Simbad data archive. One reason for doing this is that the normal spectral classes reported in catalogues are also quite limited in their

Table 2. Symbols used in classification entry to the catalogue of FORS1 magnetic field measurements

Symbol	Description
First field: evolution state	
PM	(probable or certain) pre-main-sequence star
MS	main sequence star, MK luminosity class IV or V
GS	giant star, MK luminosity class III
SG	supergiant star, MK luminosity class I or II
SD	(hot) subdwarf
CP	central star of planetary nebula
WD	white dwarf
??	star of unknown evolutionary state
Second field: temperature class	
A5, B9, etc.	temperature (spectral) class according to MK or HD system
DA7, DB3, etc.	temperature class according to white dwarf system of Sion et al. (1983)
CV	cataclysmic variable system (nova, dwarf nova, etc.)
Third field: distinctive characteristics	
AM	metallic-line (Am) star
AP	star of the Ap (peculiar A) spectroscopic class
BCEP	early B-type β Cep pulsating star
CSD	star showing evidence of a circumstellar debris disk
CV	cataclysmic variable system (nova, dwarf nova, etc.)
DSCT	δ Sct star, a late A-type pulsating main sequence star
E	presence of emission lines, especially in H α
EB	eclipsing binary system
FKCOM	FK Com variable (rapidly rotating cool giant)
FLS	flare star
FP	O stars with the Of?p peculiarity
HES	a star showing abnormally strong He lines for its effective temperature
HEW	a star showing abnormally weak He lines for its effective temperature
HGMN	a late B-type star showing the HgMn class of spectral peculiarities
HIPM	a high proper motion star
LPS	standard of linear polarisation
M	a star in which a magnetic field has definitely been detected (not necessarily with FORS1)
NOV	nova
P	peculiar (often chemically peculiar)
ROAP	rapidly oscillating Ap star (roAp star)
SB	spectroscopic binary system
SPB	slowly pulsating B star
V	variable
XRB	X-ray binary system

intent; most simply describe the morphological class to which an observed classification spectrum belongs. Spectral classification often lacks important information about the nature or evolutionary state of the star, and usually does not contain any information about such important characteristics as pulsation properties.

Our classifications are intended to provide a brief summary of a number of different kinds of information about each of the stars observed. We include information about *a*) the general evolutionary state (pre-main sequence, main sequence, giant, etc.); *b*) the photospheric temperature; *c*) some specific distinctive features of the star such as chemical peculiarity, pulsation properties, presence of a disk, clear presence of a magnetic field in the star, etc. The system we have adopted is to provide a single entry for each observation in the general format:
(evolution state):(effective temperature):(feature 1).(feature 2). . .(feature N).

The choice of classes for the first field (evolution) is a fairly obvious extension of the MK luminosity classes, supplemented

by classes not covered by this system such as CP for the central star of a planetary nebula.

In the second field (effective temperature), we follow the MK classes whenever these provide a useful description of temperature (A5, B0, or simply A or B if the temperature class is rather uncertain). For white dwarfs we use the temperature classification system described by Sion et al. (1983), where the numeral following the spectral type DA, DB, etc., is the quantity $50400/T_{\text{eff}}$ rounded to an integer. Sometimes we have simply provided a class which explains why we cannot give a simple temperature (such as CV for a cataclysmic variable). In the case of SB systems, we have usually given the temperature class of the brightest member.

In the third field (features), we have included a very wide variety of information, including chemical peculiarity (metallic-line Am star, helium-strong star), binary nature, evidence of circumstellar material (classical Be stars, shell stars), pulsation properties (β Cep stars), clear presence of a magnetic field, and/or other miscellaneous information.

The origins of the information contained in these classifications are very diverse. We have naturally made extensive use of the classes provided by the Simbad database, or more specific catalogues such as the revised Henry Draper catalogue of Houk and collaborators (Houk & Swift 1999). The white dwarf catalogue of McCook & Sion (1999) has been consulted extensively. In addition, we have often found useful information in the publications that have been based on the data re-analysed here. A large number of such articles are cited by Bagnulo et al. (2012).

For a few of the spectra in the catalogue, literature spectral classifications appeared to be inconsistent with the observed I spectra. Furthermore, two observing programmes measuring magnetic fields of open cluster stars (68.D-0403 and 70.D-0352) made extensive use of the fims multi-object observing mode in order to observe as large a sample of stars as possible. In these multi-object observations, stars other than the one or two explicitly chosen targets were simply selected from the nearby field. Such stars often have no published classifications at all, even if they have cluster numbers.

For cases of dubious or missing spectral classification in the catalogue, we tried to assign spectral classes based on the observed intensity spectra. We did this by visually comparing each observed spectrum with a grid of spectra of stars of known spectral type, also taken from the catalogue. For B and A stars classification was usually successful, using normal spectral classification criteria such as line strength ratios of lines of H, He and Ca K. We could also often use the width of Balmer lines to assign evolutionary state. The precision of our spectral classes is estimated to be about ± 2 or 3 spectral subclasses, probably about the same as the precision of classes taken somewhat randomly from the literature. However, this procedure usually failed, or produced only very imprecise classification for late type stars, for which very few stars of known spectral type are available in the catalogue. We were also usually unsuccessful in assigning spectral classes to stars for which only spectra around $H\alpha$ are available in the catalogue, as this region lacks the required variety of clear classification indicators.

The full list of symbols and abbreviations adopted for our classifications are given in Table 2. For example, a main sequence A9V star that is a δ Sct variable and a member of a spectroscopic binary system will be classified as MS:A9:DSCT.SB.

6. Description of the catalogue

The FORS1 archive of circular spectro-polarimetric data includes about 1500 observing series, for a total of more than about 12 000 scientific frames, obtained within the context of 59 observing programmes, using more than 2 000 hours of granted telescope time and about 340 hours of shutter time.² The content of the FORS1 archive is presented here in the form of three printed tables, one catalogue online, and one database of intensity spectra available at <http://star.arm.ac.uk/FORS/>. In the following we describe this material.

6.1. List of the observing programmes

Table 3 is the list of the IDs and PIs of the observing programmes, and their general characteristics (i.e. the amount of

telescope time granted, and the scope of the programme). Programme IDs may be readily associated to published papers and to the abstract of the proposals by entering it into the online form available at <telbib.eso.org>. Table 3 is organised as follows: Column 1 gives the programme ID and col. 2 the last name of the Principal Investigator of the observing programme. Column 3 is a brief description of the scope of the observing programme and nature of the observed targets. Column 4 gives the amount of time allocated to the proposal. Column 5 is the most frequently used grism in that programme.

6.1.1. Comments to individual programme IDs

Programmes 060.A-9203 and 060.A-9800 were not granted to users but belonged to Paranal SCIOPS team for ordinary calibrations and for technical tests, including some polarimetric tests on magnetic stars. For instance, the first observation of a magnetic Ap star (HD 94660), used as a proof-of-concept for the method of Sect 3.3 (Bagnulo et al. 2002), was made on 2001-03-23 under programme ID 060.A-9203 (although telescope time was officially granted as DDT).

This catalogue contains little or no reduced data for the programmes IDs 65.H-0293 (PI=Jordan), 65.P-0701 (PI=Wagner), 66.D-0128 (PI=Appenzeller), 072.D-0736 (PI=O'Brien), 072.D-0119 (PI=Marsh), 073.D-0322 and 082.D-0695 (PI=Reinsch) and 277.D-5034 (PI=Greiner), for various different reasons, e.g. because data were taken in multi-object mode (073.D-0322, 082.D-0695) and could not be reduced by the automatic pipeline, or because the S/N ratio was extremely low (e.g. 277.D-05034). Most of data obtained under programme IDs 080.D-0521 (PI=Kawka) 082.D-0736 (PI=Vornanen) could not be used to measure $\langle B_z \rangle$ through the least-square technique of Sect. 3.3, but intensity spectra are still made available (see Sect. 6.4).

Programme IDs 68.D-0403, 70.D-0352, 073.D-0498, 272.D-5026 and 074.D-0488 (PI=Bagnulo) do contain many observations obtained in fims mode, and were not properly reduced by our pipeline. However, it was possible to re-use an older data reduction carried out with IRAF routines by Bagnulo et al. (2006). From this old data reduction we took the extracted wavelength calibrated beams and we recombined them to obtain the P_V and N_V spectra, and measured the $\langle B_z \rangle$ and $\langle N_z \rangle$ values as explained in Sect. 3.2 and 3.3.

6.2. The entries of the catalogue

The general catalogue includes the following entries; the number in parentheses correspond to the fields (columns) of the catalogue.

- 1-7) The coordinates RA and DEC of the frame fits-headers. These may not correspond exactly to Simbad coordinates, but in the large majority of the cases they allow an unambiguous identification of the target.
- 8) The star identifier.
- 9) The star classification as explained in Sect. 5.
- 10) The programme ID.
- 11) The epoch of the observations (at the mid-time of the exposure series), expressed in Modified Julian Date.
- 12-13) Same as 11), but expressed in calendar date and UT.
- 14) The total exposure time in seconds.
- 15) The number of frames used for the field determination.
- 16) The grism used.
- 17) The slit width in arcsec.

² The top right panel of Fig. 6 of Bagnulo et al. (2012) shows that a large fraction of FORS1 magnetic field measurements were obtained with very short exposure times, in some cases even less than 1 s. As a consequence, the execution time of many observing programmes were dominated by overheads.

Table 3. List of observing programmes carried out with FORS1 in circular spectropolarimetric mode.

PR. ID	PI	TARGETS	TIME	YEAR	GRISM
60.A-9203	SCIOPS	(engineering ID)			
60.A-9800	SCIOPS	(engineering ID)			
65.H-0293	Jordan	WD LP 790	6h	2000	150I
65.P-0701	Wagner	Blazars	2N	2000	150I
66.D-0128	Appenzeller	Polar EF Eri	0.7N	2000	600B
67.D-0306	Bagnulo	WD 1953–011 (monitoring)	13h	2001	600R
68.D-0403	Bagnulo	Open cluster Ap stars	2N	2002	600R
69.D-0210	Hubrig	Time series roAp stars	1n	2002	600B
269.D-5044	Hubrig	Mini-survey of roAp stars	10h	2002	600B
70.D-0259	Jordan	Weak fields in white dwarfs	24h	2003	600B
70.D-0352	Bagnulo	Open cluster Ap stars	3h+2N	2003	600B
270.D-5023	Kurtz	Time series of roAp star HD 101065	4h	2003	600B
71.D-0308	Hubrig	Evolution of Ap stars in the field	20h	2003	600B
072.D-0119	Marsh	Polar ES Cet	1N	2003	300V
072.C-0447	Bagnulo	Herbig stars	3HN	2004	600B
072.D-0089	Jordan	Planetary Nebulae	7h	2003	600B
072.D-0290	O'Toole	Hot subdwarfs	1N	2004	600B
072.D-0377	Hubrig	Evolution of Ap stars in the field	30h	2004	600B
272.C-5063	Bagnulo	Herbig stars	4.5h	2004	600B
073.D-0322	Reinsch	Zeeman tomography of WDs	2h+3N	2004	300V
073.D-0356	Jordan	Weak fields in White Dwarfs	24h	2004	600B
073.D-0464	Hubrig	Evolution of Ap stars in the field	30h	2004	600B
073.D-0466	Hubrig	SLP B and Bp stars	30h	2004	600B
073.D-0498	Bagnulo	Open cluster Ap stars	30h	2004	600B
073.D-0516	Bagnulo	Cool White Dwarfs	42h	2004	600B
073.D-0736	O'Brien	X-rays binary	6h	2004	300V
274.D-5025	Mason	Nova V574 Pup	7.1h	2004	300V
272.D-5026	Bagnulo	Open cluster Ap stars	4.5h	2005	600B
074.C-0442	Bagnulo	Herbig stars	3N	2004	600B
074.C-0463	Yudin	Vega-like stars	8h	2005	1200g
074.D-0488	Bagnulo	Open cluster Ap stars	4h+2N	2005	600B
075.D-0289	Jordan	Planetary nebulae	3N	2005	600B
075.D-0295	Briquet	Pulsating B-type stars	30h	2005	1200g
075.D-0352	O'Toole	Hot subdwarfs	19h	2005	600B
075.D-0432	Schnerr	O-type stars	17h	2005	600B
075.D-0507	Yudin	Be-type stars	12h	2005	1200g
076.D-0435	Berdugina	White dwarfs	1N	2005	600B
077.D-0406	Yudin	Be-type stars	10h	2006	600B
077.D-0556	Schmitt	X-ray A-type stars	1N	2006	600B
277.D-5034	Greiner	Cataclysmic variable V504 Cen	2h	2006	600B
078.D-0140	Briquet	Pulsating B-type stars	16h	2007	600B
078.D-0330	Hubrig	Hanle effects in high-mass stars	18h	2007	600R
278.D-5056	Briquet	θ Car	1h	2007	1200B
079.D-0240	Mathys	roAp stars	28h	2007	600B
079.D-0241	Briquet	B-type stars	2N	2007	600B
079.D-0549	Karitskaya	Cyg X-1/HDE226868	7h	2007	1200B
079.D-0697	Jeffers	II Peg & V426 Oph	2N	2007	1200B
279.D-5042	Hubrig	v Sgr	2.5h	2007	1200B
080.D-0170	Mathys	HD75049	6.2h	2008	600B
080.D-0383	McSwain	Be-type stars	2N	2008	600B
080.D-0521	Kawka	White dwarfs	74h	2008	600B
081.D-2005	Barrera	HD 182180	2h	2008	1200B
280.D-5075	Korhonen	G-type giant star FK Comae	7.5h	2008	600B
380.D-0480	Yudin	Be-type star λ Eri	2H	2007	1200B
081.C-0410	Cure	Herbig stars	2N	2008	600B
081.D-0670	Jeffers	II Peg & V426 Oph	2N	2008	1200B
381.D-0138	Karitskaya	Cyg X-1/HDE226868	10h	2008	1200B
082.D-0342	Kolenberg	RR Lyrae stars	2.5N	2008	1200B
082.D-0695	Reinsch	Accreting white dwarfs	3N	2008	300V
082.D-0736	Vornanen	White dwarfs	2N	2008	600B
282.C-5041	Hubrig	Z CMa	2.7h	2008	1200B

- 18) The spectral resolution measured on the arc lamp in a spectral line situated approximately in the spectrum centre.
- 19–20) The wavelength spectral range (blue and red ends, in Å).
- 21) The S/N ratio per Å calculated as the median of the 100 highest pixels of the spectrum (but excluding emission lines).
- 22) The centre of the wavelength interval where the S/N ratio peaks.
- 23–25) The mean longitudinal field measurement $\langle B_z \rangle$ from Balmer lines with its error bar, and the corresponding reduced χ^2 ; if H Balmer lines are absent in the spectrum, the field value and its error bar are set to zero.
- 26–28) Same as 23–25) for the field measured from the null profiles, $\langle N_z \rangle$. For the observing series including only one pair of exposures, null fields values and their error bars are set to zero.
- 29–34) Same as 23–28) for metal lines; if metal lines are absent in the spectrum, all these columns contain zero values.
- 35–40) Same as 23–28) for both H Balmer and metal lines; if H Balmer lines are absent in the spectrum, these columns contain the same values as cols. 29–34). Conversely, if metal lines are absent from the spectrum, these columns contain the same values as cols. 23–28).
- 41) The name of a downloadable gzipped tar file that contains the intensity spectra described in Sect. 6.4.

There exist catalogue entries that do not include magnetic field determinations at all, which correspond to cases where the field is unmeasurable either because the spectrum has only (non-photospheric) emission lines, or because the spectrum is featureless, or because it is formed outside of the Zeeman regime, and Eq. (2) does not provide its estimate. These entries are still kept in the catalogue because it is still useful to know that a certain observing series has not been overlooked at. Furthermore the intensity spectrum is still potentially useful and available in the archive of reduced data, and a catalogue entry helps to identify the essential information about the observations.

6.3. Abridged printed version of the catalogue

Table 5 is an abridged version of the catalogue of the FORS magnetic field measurements and includes only the star name, the stellar classification, the MJD of the mid of the observation, the grism used, the $\langle B_z \rangle$ and $\langle N_z \rangle$ values in G with their error bars and corresponding reduced χ^2 . When no magnetic field measurement is available, a blank is left in the corresponding columns.

The last column of this Table is a three-character flag that helps to identify possible field detection. Each character reflects the results of the analysis carried out on the H Balmer lines, on the metal lines, and on the combination of the two sets of lines, respectively. An “n” means that the absolute field values was $< 3\sigma_{\langle B_z \rangle}$, a “d” corresponds to the cases where $3 \leq |\langle B_z \rangle|/\sigma_{\langle B_z \rangle} \leq 5$, and a “D” when the field was detected at more than 5σ level. The reason we assign a weaker detection certainty (d) to detections at the 3 to 5σ level than we do to detections at higher significance (D) is because of the problem of “occasional outlier” detections that has been clearly identified in FORS1 data (Bagnulo et al. 2012).

Our final assessment whether the star is really magnetic or not is given by the “M” flag in the classification. Since this assessment is often also based on measurements obtained with other instruments and on other observing dates, it is quite possible that a star classified as magnetic in col. 2 has a flag “nnn” in

the last column. Conversely, “d” flags (or even “D” flags) may be associated with stars that have not received the classification of magnetic stars in col. 2. This may happen for three reasons: either we think that the detection might be real, but that it needs be supported by further data (e.g. the case of the M giant star HD 298045), or we believe that the signal we measure is spurious, and/or the field detection has not been confirmed by further observations obtained with FORS1 itself or other instruments. Most of these spurious or dubious cases have been discussed by Bagnulo et al. (2012).

Finally, a dash (“-”) in the last column means that the corresponding part of the spectrum was not used to measure the field (in fact, there are cases where no field measurement was attempted, as explained in Sect.6.2).

6.4. The archive of intensity spectra

In the course of measuring the magnetic field strength from the circularly polarised spectra of FORS1, we have obtained the (uncalibrated) intensity (I) spectra. Since FORS is a single order spectrograph, these I spectra, even without flux calibration, provide potentially useful profiles of broad spectral lines such as those of H and He that are difficult to recover with accuracy from high-dispersion spectra derived from cross-dispersed instruments. The I spectra also illustrate clearly the overall shape of the detected spectral flux (convolved with the instrument+telescope transmission function) of each star observed. Because these I spectra could potentially be useful for a wide range of projects, we have made them available at CDS, and, temporarily, at <http://star.arm.ac.uk/FORS/>

In the ESO archive, each frame is identified by a name that refers to the instrument and the instant when an exposure was started. In case of FORS1 data:

`FORS1.YYYY-MM-DDThh-mm_ss.xxx.fits`

where YYYY-MM-DD refers to the year, month and day of the observation, and hh-mm_ss.xxx the hour, minute and second (with millisecond precision) when shutter was open for the observation (UT). We note that files produced until the end of period 67 were called `FORS.YYYY-MM-DDThh-mm_ss.xxx.fits`.

In our context it is useful to group all together the frames of the observing series that have been used to obtain a certain magnetic field measurement. Therefore, for each entry of our catalogue, we have produced a tarball named `STARNAME_PID_III.X-JJJJ_MJD_nnnnn.mmm.tar` where STARNAME is the star name, III.X-JJJJ is the programme ID and nnnnn.mmm is the Modified Julian Date of the observation. Very few objects observed in multi-object mode could not be identified (see Bagnulo et al. 2006). In these cases, for the instead of STARNAME we used RAhh_mm_ss.s where hh:mm:ss.s is the RA of the centre of the slit read in the fits-headers. This way, each tarball is unambiguously associated with each entry of the catalogue and Table 5.

Each tarball includes an ASCII file with the same name as the tarball itself (without the extension .tar) which contains the list of original frames used for the field determination. In this file, each filename is followed by: the exposure time in seconds of each individual frame (fits-header keyword EXPTIME); the position angle of the retarder waveplate with respect to the parallel beam of the Wollaston prism (fits-header keyword INS.RETA4.ROT)³; the exposure number, and the total number of exposures in each

³ Older FORS1 data did not include this keyword, in which case it was calculated as the difference between the fits-header keywords ADA.POSANG and INS.RETA4.POSANG which give the position angles

Table 4. Example of the content of the input file STARNAME_PID_III.X-JJJJ_MJD_nnnnn.mmm: here we consider HD190073_PID_081.C-0410_MJD_54609.411 (the file structure is explained in the text). From the file list one can infer that last two exposures of the observing series have been dropped (either because the observing series was interrupted, or because the frames were discarded due to some problem, e.g. saturation).

FORS1.2008-05-23T09:36:34.552.fits	180	315.0	1/ 8	200176637
FORS1.2008-05-23T09:41:07.012.fits	200	45.0	2/ 8	200176637
FORS1.2008-05-23T09:45:27.830.fits	250	45.0	3/ 8	200176637
FORS1.2008-05-23T09:51:10.408.fits	250	315.0	4/ 8	200176637
FORS1.2008-05-23T09:56:21.302.fits	250	315.0	5/ 8	200176637
FORS1.2008-05-23T10:02:03.889.fits	250	45.0	6/ 8	200176637
GRIS_600B 0.40 1797				
Norma III 4136x4096 1x1 200Kps/low_gain				

OB template, and the OB number, given by fits-keywords NEXP EXP and OB, respectively. The file name list is followed by two lines with the grism name, the slit width, the spectral resolution, the detector name and the readout mode. An example of such file is given in Table 4.

The tarball includes an ASCII file for each frame of the observing series used to determine $\langle B_z \rangle$. This file is identified by the same name as the original frame archive name, having replaced the extension .fits with .prof. In case of observations obtained in multi-object mode, the name of the .prof file refers also to the slitlet number where the star was centred, e.g., FORS1.YYYY-MM-DDThh-mm-ss.xxx_Syy.fits, where yy may be 02, 04, ..., 18. Each of these .prof files have three columns: wavelength in Å (col. 1), flux and flux error in ADUs (cols. 2 and 3, respectively).

7. Comparison with previously published field values

It is of interest to compare the $\langle B_z \rangle$ values obtained from the current suite of reduction programs with results published in the literature and obtained from the same datasets.

7.1. Data on magnetic Ap/Bp stars

A first comparison may be made with the Ap star field strength values obtained for open cluster Ap/Bp candidates that are described by Bagnulo et al. (2006). These measurements were made using a combination of Balmer and metallic line in order to maximise sensitivity to weak fields in these often faint stars. Field measurements made for this observing programme are found to have uncertainties that are rather similar to those in the present catalogue. For stars in which no field was detected, in general the result is still a null detection, although the actual value reported has often changed by an amount of the order of 1σ or even more, while still remaining a null detection. For stars with easily detectable fields, the values of the uncertainties are not greatly different from the present data, but the actual $\langle B_z \rangle$ values reported may differ from the current ones by 10 or even 20 %.

Another comparison may be made with the data used by Kochukhov & Bagnulo (2006) to study the evolution of magnetic field strength with age among bright field Ap/Bp stars. These data differ from the open cluster field strengths in that the stars observed are generally a few magnitudes brighter, and so the S/N ratio of the measurements are higher. Field strengths

of the instrument and of the retarder waveplate, respectively, with respect to the north celestial meridian.

were measured using only the Balmer lines, as this provided adequate precision for their project. Because the printed version of the catalogue presented here has field values derived from both metal and H lines, the catalogue uncertainties may be as much as two times smaller than those of Kochukhov & Bagnulo (2006), and range up to similar or slightly larger values in stars in which the metallic spectrum contributed little useful information. Again, the actual values of $\langle B_z \rangle$ in the present catalogue for stars in which the field is easily detected may differ from the earlier values by 10 or 20 %, in this case at least mainly because the field is not determined using the same lines in the two datasets.

7.2. White dwarfs

We have also compared the catalogue to the field measurements of DA white dwarfs described by Landstreet et al. (2012a). Since this publication was based on a method very similar to that adopted for this catalogue, the field values and uncertainties are generally very similar in the two places. The main exception concerns the two (null) field measurement of the white dwarf WD 1334–678 that were included (by mistake) in their online Table 3 of all FORS measurements of potential kG field DA white dwarfs. We discovered that the actual target of that measurement is in fact an anonymous G star rather than the white dwarf, and that the white dwarf is actually more than 1 arcmin away from the fits-header coordinates. In this catalogue, the observations have been assigned to the correct star (identified by the fits-header coordinates), and no field value is included in the catalogue, although the I spectrum is being made available.

For all the remaining stars, small field value differences are present, and due to the slightly different version of the algorithm that we have adopted for this catalogue.

7.3. Other stars

A thorough comparison of the results in the catalogue with reported magnetic field discoveries in non-Ap/Bp stars made by other groups from FORS1 observations has been carried out by Bagnulo et al. (2012). The general result of this comparison was that many of the reported discoveries are erroneous or at least unsupported by a revision of the original FORS1 data.

In Sect. 5 of Bagnulo et al. (2012) we highlighted a number of cases where our pipeline-based data reduction was unsatisfactory. We have re-addressed these cases, sometimes using a “hand-made” data reduction, and found the conclusions described in the remaining part of this Sect., which addresses a dozen very specific cases.

Table 5 of Bagnulo et al. (2012) reported no detection but very large error bars for the observations of Be star HD 148184 on MJD=53532.224 and 53862.380. Our new reduction produces much smaller error bars, and still does not confirm the detection previously reported in the literature.

Section 5.2 of Bagnulo et al. (2012) reported apparently significant but very suspicious field detections for four classical Be stars: an observation of HD 181615=HD 181616, one observation of HD 56014, two observations of HD 209409 (in which the original observers did not report any significant fields), and one observation of HD 224686. Our new data reduction has fixed all these problems and no detection is reported, fully confirming the claim by Bagnulo et al. (2012) that from FORS data there is no evidence for magnetic fields in any classical Be star.

Similar problems affected three slowly pulsating B (SPB) stars (see comments in Sect. 5.4 of Bagnulo et al. 2012).

For the $\langle B_z \rangle$ measurement of the SPB star HD 53921 obtained on MJD=52999.137, Bagnulo et al. (2012) reported a field detection with the opposite sign to that measured by Hubrig et al. (2006), and for the measurements obtained at MJD=53630.401 and 53631.408, Bagnulo et al. (2012) reported error bars five times higher than previously reported by Hubrig et al. (2006), with no significant detection in these two datasets (however, Bagnulo et al. 2012 confirmed that the star is magnetic based on HARPSpol measurements). With our new reduction we are able to confirm the field detection on MJD=52999.137 with a positive sign, and we have gotten rid of additional noise in the remaining two measurements, confirming the 5σ detections reported by Hubrig et al. (2006).

Bagnulo et al. (2012) reported an unsatisfactory reduction for the SPB star HD 152511 on MJD=54609.433 due to seeing conditions. Our revision of this dataset lead to much better results, which are consistent with those of Hubrig et al. (2009). Therefore we confirm all three detections reported by Hubrig et al. (2009) instead of only two as reported by Bagnulo et al. (2012).

For the observations of the SPB star HD 28114 obtained on MJD=54106.091 Bagnulo et al. (2012) obtained a larger noise than was previously published by Hubrig et al. (2009), and a field detection based only on a signal that appears in the highest-order H Balmer lines. Our new reduction has a higher S/N ratio, but we still get the same suspicious signal only on the highest-order H Balmer lines, and no credible field detection.

Section 5.4 of Bagnulo et al. (2012) conclude that six reported detections of a field in the β Cep star HD 16582 had decreased below the 3σ significance limit, although one measurement not originally claimed as detection, on MJD=54343.259, has risen to become an apparently significant detection. This detection has disappeared in our new reduction, highlighting once again how the reliability of marginal discoveries may crucially depend on data-reduction.

8. FORS detections of stellar magnetic fields

With the complete dataset of magnetic measurements obtained with FORS1, we can take stock of the achievements of this instrument, and assess its strengths and weaknesses.

We consider first FORS1 measurements of Ap/Bp stars. A large number of such stars have been observed, both in open clusters and in the field, and in the context of wide-ranging surveys as well as for studies of single objects. For such stars, the detection rate is reasonably high: if the star is securely identified as an Ap/Bp star (by specific chemical peculiarities, or by appropriate values of the photometric Maitzen Δa or Geneva Z peculiarity parameters), then the likelihood of clear detection of

a longitudinal field is around 50 %. This result occurs because in practice the main surveys have been able to achieve measurement uncertainties of the order of 50–100 G, while the fields to be detected are typically several hundred G. Thus a measurement with $\langle B_z \rangle / \sigma_{\langle B_z \rangle}$ ratio of order ten is often obtained, a value large enough to clearly establish the presence and amplitude of a field in spite of the excess noise that can sometimes trouble FORS1 measurements. It is clear that FORS is extremely powerful as a tool to search for fields in such stars, down to magnitudes fainter than $V \sim 10$, and is perfectly capable of detecting kG fields in stars as faint as $V = 13$ or 14.

The FORS1 Ap stars data have recently been discussed by Landstreet et al. (2014), who studied the general usefulness of FORS for systematic studies of individual Ap stars, and concluded that (apart from occasional outliers) the instrument furnishes data of high quality and consistency. However, only a few of the observing programmes carried out on FORS1 have focused on this kind of problem.

With the discovery that WD 446-789, WD 2105-820, WD 2359-434 (and perhaps also WD 1105-048) host a magnetic field, the FORS1 surveys of white dwarfs have opened a new stream of research, i.e. systematic investigations of weak field (10 kG or less) in degenerate stars (Aznar Cuadrado et al. 2004; Landstreet et al. 2012a), which definitely justify the use of a telescope with an 8 m size mirror. FORS1 has played also an important role in the study of faint but stronger magnetic white dwarfs (Kawka & Vennes 2012) and was used for the discovery of circular polarisation in the continuum and in the molecular bands of a DQ white dwarf (Vornanen et al. 2010).

When we look at the large number of observations of stars other than magnetic Ap/Bp stars, and the very small number of secure field detections, it is clear that most of the stellar magnetism programmes carried out on FORS1 of non-Ap/Bp stars were searches for fields in individual objects, or surveys of various classes of stars for detectable fields. The projects carried out have included large surveys of such star classes as Herbig Ae/Be stars, O stars, slowly pulsating B stars, β Cep B star pulsators, classical Be stars, normal B stars, and white dwarfs. A number of individual objects have also been studied.

However, from the ~ 1000 measurements carried out on stars other than Ap stars and white dwarfs, we have only a few clear field detections, namely the pre-main-sequence star HD 101412, the β Cep variable HD 46328, the SPB stars HD 53921 and HD 152511, and the rapidly rotating star FK Com. In addition, a number of $3\text{--}6\sigma$ FORS1 detections have been reported in the literature (some of which still present in this catalogue). As thoroughly discussed by (Bagnulo et al. 2012), some of these detections have been proved by subsequent monitoring with FORS2 and ESPaDOnS to be real (e.g. the Of?p star HD 148937), but many of them have not been confirmed by our reduction, or by observations with other instruments, and are probably spurious. A small number of cases would deserve further investigations (e.g. the SPB star HD 138769, and the M giant star HD 298045).

The null results obtained in the various surveys of stars other than Ap stars are certainly valuable for setting upper limits on possible fields, e.g. on RR Lyrae stars (Kolenberg & Bagnulo 2009), on hot subdwarfs (see Landstreet et al. 2012b, and references therein), and on the central stars of planetary nebulae (Leone et al. 2011; Jordan et al. 2012). These results are often useful for constraining possible theoretical models of various kinds. The extremely low detection rate is mainly a consequence of the rarity in hot stars of fields that are large enough to be clearly detectable with FORS1 spectropolarimetry; such stars have a frequency of occurrence of 10 % or less. It may also be

a consequence of a tendency of both proposers and the OPC to prefer the 8 m telescope for exploration of new fields rather than systematic study of individual fields found. In any case, the low yield suggests that surveys with FORS need to be Large Projects, and that otherwise the instrument should focus more on systematic study of single objects in which the field is known to be large enough to be studied at useful S/N ratio with FORS.

9. Conclusions

This paper is the concluding work in a series that started with the first demonstration that FORS1 could be used effectively for magnetic field measurements of main sequence stars (Bagnulo et al. 2002). This was followed by several years during which FORS1 (and, later, the twin instrument FORS2) was widely used for observations of many classes of stars. After some years it became apparent that a general discussion of the analysis of data obtained with dual-beam spectropolarimeters similar to that of FORS1 would be of considerable value to the community. This led to a paper presenting the fundamental ideas of the beam-swapping technique, and its application to night time astronomy (Bagnulo et al. 2009).

Further use of FORS1 led to announcements of numerous field discoveries at the 3 to 5σ level. When these results were not confirmed by our own reduction of the data and/or were contradicted by observations with other spectropolarimeters such as ESPaDOnS, it became apparent (1) that correct treatment of FORS1 data is less obvious than it appears at first sight, especially in the regime of small uncertainties and marginal field detections, and (2) that the instrument itself may be subject to small drifts and flexures that lead to erroneous data in a small fraction of cases. These issues were discussed in considerable detail by Bagnulo et al. (2012), who developed a suite of programs allowing the entire dataset of all magnetic observations obtained with FORS1 to be reduced together, with a variety of options. This tool made it possible to show that modest and reasonable improvements to the data reduction process (for example, optimal choice of a clipping algorithm to deal with cosmic ray events) could change field detections into non-detections (and occasionally vice versa).

Bagnulo et al. (2012) also clearly identified the occurrence of occasional outliers in FORS1 data, in which a single observation inconsistent with others obtained with FORS1/2, could occur. An important source of such occasional outliers, and more generally of excess noise in FORS1/2 field measurements, was identified by Bagnulo et al. (2013), who showed that small shifts in line position may occur in FORS data, probably as a result of small flexures (including spectral shifts following the rotation of the retarder waveplate) and of seeing, and that these shifts can lead to spurious field detections.

The present paper builds on the accumulated experience and experiments represented by these earlier works, also including the detailed discussion of the large body of field measurements of AP/Bp stars by Landstreet et al. (2014). It does not, of course present the definitive reduction of the FORS1 magnetic dataset; as discussed in the earlier papers, several different choices made during data reduction are equally reasonable, but lead to somewhat different results. However, the reductions leading to the present catalogue are based on reasonable choices, applied in a consistent way to all the FORS1 field measurements, and they do rest on an understanding of, and correction of, small errors or poor choices made to treat data in the past.

The results compiled in this catalogue show that FORS is a very powerful instrument for (longitudinal) field measurement

of both non-degenerate and degenerate stars. In the very best cases (for stars with rich spectra of deep lines), uncertainties of as low as 20 G or so can be achieved. Because of the outlier problem, new field detections should be repeated multiple times and/or made at the significance level of at least 5 or 6σ . More typically, FORS can achieve realistic uncertainties of the order of 50 – 100 G for a wide range of stars down to V magnitude of 10 to 12 , and $\sim 500\text{ G}$ uncertainties for white dwarfs of magnitude 12 or 13 . The instrument is particularly well-suited to measurement of fields that can be detected at several σ level.

It should be borne in mind, however, that FORS makes very inefficient use of telescope time in observations of stars brighter than $V \sim 7$, for which the readout time of the CCD is larger than the integration time of each subexposure. This is the origin of the striking difference between shutter time and allocated time mentioned at the beginning of Sect. 6. There may be times when FORS may still be the best instrument for the job, but it is used most efficiently on stars for which subexposure times of some or many minutes are needed.

The relevance of most of the considerations made in this series of papers are not limited to the FORS1 instrument, but should be taken into account when using/designing other spectro-polarimeters.

Acknowledgements. This paper is based on observations made with ESO telescopes at the La Silla Paranal Observatory under the programme IDs listed in Table 3, and made available through the ESO archive. LF acknowledges support from the Alexander von Humboldt Foundation. Work on this project by JDL has been supported by the Natural Sciences and Engineering Research Council of Canada. We thank the referee P. Petit, for a careful review of the manuscript.

References

- Appenzeller, I. 1967, PASP, 79, 136
- Appenzeller, I., Fricke, K., Furtig, W., et al. 1998, The Messenger, 94, 1
- Appenzeller, I., & Rupprecht, G. 1992, The Messenger, 67, 18
- Avila, G., Rupprecht, G., & Beckers, J.M. 1997, SPIE, 2871, 1135
- Aznar Cuadrado, R., Jordan, S., Napiwotzki, R. et al. 2004, A&A, 423, 1081
- Bagnulo, S., Szeifert, T., Wade, G.A., Landstreet, J.D., & Mathys, G. 2002, A&A, 389, 191
- Bagnulo, S., Landstreet, J. D., Mason, E., et al. 2006, A&A, 450, 777
- Bagnulo, S., Landolfi, M., Landstreet, J.D., Landi Degl'Innocenti, E., Fossati, L., & Sterzik, M. 2009, PASP, 121, 993
- Bagnulo, S., Landstreet, J.D., Fossati, L., & Kochukhov, O. 2012, A&A, 538, 129
- Bagnulo, S., Fossati, L., Landstreet, J.D., & Kochukhov, O. 2013, A&A, 559, 103
- Donati, J.-F., Semel, M., Carter, B.D., Rees, D.E., & Collier Cameron, A. 1997, MNRAS, 291, 658
- Fossati, L., Bagnulo, S., Landstreet, J. D. & Kochukhov, O. 2015. In: Y. Y. Balega, I. I. Romanyuk, & D. O. Kudryavtsev (eds.) Physics and evolution of magnetic and related stars, (San Francisco: ASP), ASP Conf. Ser., 494, 63
- Houk, N., Swift, C. 1999, "Michigan catalogue of two-dimensional spectral types for the HD Stars; vol. 5", Ann Arbor, Michigan : Department of Astronomy, University of Michigan
- Hubrig, S., Briquet, M., Schöller, M., et al. 2006, MNRAS, 369, 61
- Hubrig, S., Briquet, M., De Cat, P., et al. 2009a, AN, 330, 317
- Izzo, C., de Bilbao, L., Larsen, J., Bagnulo, S., Freudling, W., Moehler, S., & Ballester, P. 2010, SPIE, 7737, 773729
- Jordan, S., Bagnulo, S., Werner, K., & O'Toole, S. J. 2012, A&A, 542, 64
- Kawka, A., & Vennes, S. 2012, MNRAS, 425, 1394
- Kochukhov, O., & Bagnulo, S. 2006, A&A, 450, 763
- Kolenberg, K., & Bagnulo, S. 2012, A&A, 498, 543
- Landstreet, J.D., Bagnulo, S., Fossati, L., Jordan, S., & O'Toole, S.J.O. 2012a, A&A 541, A100
- Landstreet, J.D., Bagnulo, S., Valyavin, G.G., Fossati, L., Jordan, S., Monin, D., & Wade, G. A. 2012b, A&A, 545, 30
- Landstreet, J.D., Bagnulo, S., & Fossati, L. 2014, A&A, 572, A113
- Leone, F., Martínez González, M.J., Corradi, R.L. M., Privitera, G.; & Manso Sainz, R. 2011, ApJL, 731, 33
- McCook, G.P., & Sion, E.M. 1999, ApJS, 121, 1

- Scarrott, S.M., Warren-Smith, R.F., Pallister, W.S., Axon, D.J., & Bingham, R.G.
1983, MNRAS, 204, 1163
- Sion, E.M., Greenstein, J.L., Landstreet, J.D., Liebert, J., Shipman, H.L., &
Wegner, G.A. 1983, ApJ, 269, 253.
- Szeifert, Th., Reiss, R., Baksai, P., et al. 2007, The Messenger, 128, 9
- Vornanen, T., Berdyugina, S.V., Berdyugin, A.V., & Piironen, V. 2010, ApJ, 720,
L52
- Wade, G.A., Bagnulo, S., Drouin, D., Landstreet, J.D., & Monin, D. 2007, MN-
RAS, 376, 1145

Table 5. Magnetic field and null field are calculated from the combination of H Balmer and metal lines.

Star	Classification	Prog. ID	MJD	grism	$\langle B_z \rangle$ (G)	χ^2/ν	$\langle N_z \rangle$ (G)	χ^2/ν	HmT
WD 2359-434	WD:DA5:M	070.D-0259	52583.025	600B	3692 ± 842	1.02	496 ± 853	1.07	d-d
WD 2359-434	WD:DA5:M	070.D-0259	52608.056	600B	3144 ± 528	1.02	663 ± 483	0.86	D-D
HD 225041	MS:A:RR	082.D-0342	54781.102	1200B	4 ± 32	1.49	12 ± 25	0.96	nnn
HD 225264	MS:A1:AP	073.D-0498	53217.409	600B	-26 ± 34	0.90	-22 ± 31	0.79	nnn
HD 358	MS:B9:HGMN	071.D-0308	52910.092	600B	-304 ± 123	1.08	31 ± 120	1.02	nnn
HD 358	MS:B9:HGMN	072.D-0377	52963.020	600B	139 ± 101	1.00	-150 ± 102	1.01	nnn
HD 358	MS:B9:HGMN	075.D-0295	53519.448	1200g	-88 ± 97	2.23	194 ± 107	2.23	nnn
HD 358	MS:B9:HGMN	075.D-0295	53629.286	1200g	23 ± 30	1.21	23 ± 29	0.95	nnn
HD 358	MS:B9:HGMN	075.D-0295	53630.208	1200g	5 ± 34	1.08	-15 ± 31	0.94	nnn
HD 358	MS:B9:HGMN	075.D-0295	53638.205	1200g	-17 ± 35	0.99	-16 ± 35	0.96	nnn
HD 358	MS:B9:HGMN	380.D-0480	54432.045	1200B	-25 ± 25	0.89	48 ± 24	0.80	nnn
HD 358	MS:B9:HGMN	380.D-0480	54433.023	1200B	-25 ± 23	1.87	-27 ± 20	1.38	nnn
HD 1048	MS:A1:AP	071.D-0308	52910.103	600B	219 ± 83	0.92	-203 ± 84	0.95	dnn
HD 1048	MS:A1:AP	073.D-0464	53199.406	600B	-46 ± 38	0.91	-44 ± 37	0.88	nnn
HD 1048	MS:A1:AP	073.D-0464	53215.382	600B	57 ± 44	1.16	-26 ± 42	1.10	nnn
NLTT 888	WD:DAZ9:HPM	080.D-0521	54419.126	600B					—
NLTT 888	WD:DAZ9:HPM	080.D-0521	54446.049	600B					—
RX Cet	MS:A:RR	082.D-0342	54782.153	1200B	9 ± 48	1.45	107 ± 47	1.42	nnn
HD 3326	MS:A5:AP	072.D-0377	52908.190	600B	-3 ± 35	0.92	-100 ± 35	0.92	nnn
HD 3379	MS:B2:SPB	073.D-0466	53244.402	600B	93 ± 46	0.99	-53 ± 46	1.03	nnn
HD 3379	MS:B2:SPB	073.D-0466	53245.214	600B	-47 ± 34	0.87	-24 ± 35	0.97	nnn
HD 3379	MS:B2:SPB	075.D-0295	53629.305	1200g	-8 ± 27	0.99	18 ± 25	0.87	nnn
HD 3379	MS:B2:SPB	075.D-0295	53630.195	1200g	-22 ± 31	1.05	8 ± 30	1.03	nnn
HD 3379	MS:B2:SPB	078.D-0140	54109.051	600B	9 ± 57	0.77	20 ± 41	0.75	nnn
HD 3379	MS:B2:SPB	078.D-0140	54112.025	600B	18 ± 45	1.13	-27 ± 42	0.96	nnn
HD 3379	MS:B2:SPB	079.D-0241	54344.233	600B	66 ± 35	0.73	-126 ± 43	0.76	nnn
HD 3379	MS:B2:SPB	079.D-0241	54345.190	600B	-16 ± 40	0.85	-37 ± 45	0.73	nnn
NLTT 2219	WD:DA8:HPM	080.D-0521	54448.083	600B					—
HD 3980	MS:A7:M.AP	075.D-0295	53624.076	1200g	463 ± 31	4.11	15 ± 15	0.97	dDD
HD 3980	MS:A7:M.AP	075.D-0295	53630.232	1200g	408 ± 30	9.75	29 ± 10	0.99	DDD
HD 3980	MS:A7:M.AP	380.D-0480	54432.010	1200B	-866 ± 24	7.47	30 ± 11	1.45	DDD
HD 3980	MS:A7:M.AP	380.D-0480	54433.039	1200B	1688 ± 29	12.39	-12 ± 11	1.02	DDD
HD 3980	MS:A:M.AP	075.D-0295	53559.410	1200g	1147 ± 30	4.61	6 ± 12	0.75	DDD
CD-38 222	SD:B	075.D-0352	53574.364	600B	54 ± 148	0.90	56 ± 156	1.00	nnn
CD-38 222	SD:B	075.D-0352	53624.097	600B	-234 ± 201	0.93	217 ± 284	1.06	nnn
HD 4539	SD:B	075.D-0352	53593.218	600B	552 ± 180	1.00	87 ± 216	0.92	nnd
PHL 932	SD:B	075.D-0352	53593.256	600B	-87 ± 291	0.90	-155 ± 365	0.95	nnn
HD 6532	MS:A5:M.AP	069.D-0210	52531.392	600R	267 ± 73	2.13	-97 ± 52	1.05	ndd
CD-53 251	PM:F2	074.C-0442	53330.057	600B	174 ± 62	0.97	-2 ± 60	0.89	nnn
CD-53 251	PM:F2	074.C-0442	53330.085	1200g	109 ± 33	0.88	8 ± 32	0.81	ndd
CD-53 251	PM:F2	081.C-0410	54610.400	600B	10 ± 32	0.77	-67 ± 41	0.76	nnn
WD 0115+159	WD:DQ6	082.D-0736	54786.159	600B					—
HD 8783	MS:A2:AP	071.D-0308	52852.358	600B	57 ± 74	0.91	-143 ± 75	0.93	nnn
HD 9289	MS:A3:M.AP.ROAP	269.D-5044	52519.252	600B	760 ± 56	1.29	13 ± 47	0.92	DDD
HD 9672	MS:A1	081.C-0410	54610.437	600B	-100 ± 32	0.86	22 ± 33	0.78	dnd
PG 0133+114	SD:B	075.D-0352	53638.250	600B	-778 ± 376	0.97	290 ± 437	0.90	dnn
WD 0135-052	WD:DA7	070.D-0295	52608.097	600B	-318 ± 416	1.13	244 ± 388	0.98	n-n
WD 0136-340	WD:DA8:HPM	080.D-0521	54381.205	600B	-1016 ± 2542	0.79	-1617 ± 2643	0.85	n-n
CD-24 731	SD:B	075.D-0352	53629.135	600B	536 ± 373	1.07	601 ± 487	1.14	n-n
HD 10840	MS:B9:M.AP	073.D-0464	53184.331	600B	-174 ± 42	0.77	107 ± 42	0.75	dnd
NLTT 6004	WD:DA8:HPM	080.D-0521	54407.220	600B	-12297 ± 3823	0.60			d-d
HD 11462	MS:B8:SPB	079.D-0241	54344.248	600B	21 ± 45	0.78	103 ± 55	0.76	nnn
NLTT 6390	WD:DAZ8:HPM	080.D-0521	54405.182	600B	-2845 ± 5635	0.95			n-n
CD-28 595	MS:G:HPM	082.D-0695	54829.015	300V	1886 ± 1164	0.83			nnn
CD-28 595	MS:G:HPM	082.D-0695	54830.035	300V	-1048 ± 1023	0.75			nnn
CD-28 595	MS:G:HPM	082.D-0695	54831.032	300V	-1513 ± 1357	0.73			nnn
HD 12932	MS:A5:M.AP.ROAP	269.D-5044	52517.383	600B	915 ± 67	1.20	8 ± 60	0.97	ddd
SS For	MS:A:RR	082.D-0342	54781.050	1200B	34 ± 35	1.15	-37 ± 34	1.10	nnn
SS For	MS:A:RR	082.D-0342	54782.279	1200B	-43 ± 45	1.44	-37 ± 40	1.18	nnn
SS For	MS:A:RR	082.D-0342	54783.177	1200B	42 ± 56	1.13	126 ± 61	1.34	nnn
HD 13588	MS:A1:AM	060.A-9203	53717.023	300V	778 ± 449	0.85	170 ± 443	0.85	nnn
HD 13588	MS:A1:AM	076.D-0435	53715.018	300V	-92 ± 367	0.86	-541 ± 363	0.84	nnn
HD 13588	MS:A1:AM	076.D-0435	53715.022	600B	42 ± 130	0.87	143 ± 130	0.87	nnn
HD 13588	MS:A1:AM	082.D-0695	54829.031	300V	-1107 ± 503	0.90	1490 ± 466	0.77	nnn
RV Cet	MS:A:RR	082.D-0342	54781.252	1200B	-21 ± 34	1.51	57 ± 30	1.24	nnn
NLTT 7547	WD:DAZ9:HPM	080.D-0521	54447.136	600B					—
NLTT 7547	WD:DAZ9:HPM	080.D-0521	54447.172	600B					—

Table 5. continued.

Star	Classification	Prog. ID	MJD	grism	$\langle B_z \rangle$ (G)	χ^2/ν	$\langle N_z \rangle$ (G)	χ^2/ν	HmT
WD 0227+050	WD:DA3	070.D-0259	52637.120	600B	693 ± 584	1.01	-396 ± 695	0.95	n-n
WD 0227+050	WD:DA3	070.D-0259	52669.062	600B	-507 ± 588	1.02	986 ± 677	0.91	n-n
HD 16456	MS:A:RR	082.D-0342	54782.108	1200B	-9 ± 43	1.40	32 ± 35	1.06	nnn
HD 16456	MS:A:RR	082.D-0342	54783.257	1200B	119 ± 43	1.24	15 ± 35	0.93	nnn
NLTT 8525	WD:DC:HPM	080.D-0521	54397.126	600B					—
HD 16582	MS:B2:BCEP	078.D-0140	54047.129	600B	45 ± 95	0.96	142 ± 91	0.89	nnn
HD 16582	MS:B2:BCEP	078.D-0140	54040.170	600B	96 ± 37	0.93	11 ± 39	0.90	nnn
HD 16582	MS:B2:BCEP	078.D-0330	54109.071	600R	-190 ± 79	1.06	-76 ± 83	0.97	nnn
HD 16582	MS:B2:BCEP	079.D-0241	54343.259	1200B	-59 ± 16	1.38	-11 ± 13	0.97	dnd
HD 16582	MS:B2:BCEP	079.D-0241	54344.200	1200B	6 ± 18	1.42	23 ± 14	0.88	nnn
HD 16582	MS:B2:BCEP	079.D-0241	54344.264	1200B	2 ± 15	1.08	-40 ± 14	0.66	nnn
HD 16582	MS:B2:BCEP	079.D-0241	54345.246	1200B	-3 ± 18	1.17	-66 ± 18	1.13	nnn
HD 16582	MS:B2:BCEP	079.D-0241	54345.293	1200B	0 ± 15	1.09	-11 ± 12	0.73	nnn
HD 16582	MS:B2:BCEP	078.D-0330	54014.211	600R	-130 ± 66	1.06	-144 ± 60	0.96	nnn
NLTT 8733	WD:DQ:HPM	080.D-0521	54397.164	600B					—
HD 17081	PM:B7	074.C-0442	53331.053	600B	139 ± 59	1.01	-129 ± 56	0.90	nnn
HD 17081	PM:B7	074.C-0442	53331.062	1200g	53 ± 45	0.98	75 ± 42	0.85	nnn
HD 19918	MS:A5:M.AP	072.D-0377	52908.210	600B	-751 ± 63	1.05	21 ± 56	0.86	DDD
HD 19400	MS:B8	071.D-0308	52852.371	600B	170 ± 85	1.12	-162 ± 77	0.91	nnn
HD 21190	G:F2:V	079.D-0241	54343.280	600B	14 ± 16	0.82	42 ± 19	0.74	nnn
HD 19712	MS:A0:M.AP	072.D-0377	52905.384	600B	-1187 ± 87	1.02	-61 ± 99	0.88	DDD
HD 19712	MS:A0:M.AP	072.D-0377	52999.025	600B	903 ± 59	1.41	38 ± 46	0.85	DDD
WD 0310-688	WD:DA3	070.D-0259	52695.054	600B	197 ± 414	0.97	-358 ± 441	0.93	n-n
WD 0310-688	WD:DA3	080.D-0521	54405.249	600B	3773 ± 3493	0.87			n-n
RX For	MS:A:RR	082.D-0342	54783.220	1200B	9 ± 55	1.17	75 ± 59	1.32	nnn
NLTT 10480	WD:DAZ9:HPM	080.D-0521	54405.224	600B					—
NLTT 10884	WD:DA7:HPM	080.D-0521	54400.144	600B	-4756 ± 6009	0.92			n-n
X Ret	MS:A:RR	082.D-0342	54782.219	1200B	-45 ± 47	1.18	-21 ± 45	1.08	nnn
NLTT 11051	WD:DC:HPM	080.D-0521	54407.269	600B					—
HD 22488	MS:A3:AP	073.D-0464	53087.014	600B	17 ± 26	0.91	27 ± 26	0.94	nnn
CD-26 1339	CP	072.D-0089	52946.291	600B	207 ± 318	0.94	359 ± 333	1.05	nnn
CD-26 1339	CP	072.D-0089	52988.235	600B	265 ± 269	0.91	-36 ± 262	0.83	nnn
CD-26 1339	CP	072.D-0089	52989.060	600B	354 ± 364	1.08	105 ± 370	1.10	nnn
CD-26 1339	CP	072.D-0089	52990.081	600B	86 ± 313	0.90	56 ± 290	0.77	nnn
NLTT 11393	WD:DAZ8:HPM	080.D-0521	54407.322	600B	5497 ± 6080	0.86			n-n
HD 22374	MS:A1:AP	072.D-0377	52999.039	600B	-135 ± 50	1.02	-57 ± 50	1.02	nnn
HD 22374	MS:A1:AP	073.D-0464	53216.380	600B	28 ± 38	1.80	-137 ± 52	2.29	nnn
HD 278937	PM:A3	074.C-0442	53330.181	600B	20 ± 90	0.94	-4 ± 84	0.82	nnn
HD 23207	MS:A2:M.AP	073.D-0464	53215.361	600B	159 ± 44	1.44	27 ± 40	1.18	nnd
HD 23207	MS:A2:M.AP	073.D-0464	53218.336	600B	614 ± 47	4.68	-7 ± 33	2.21	dDD
WD 0341+182	WD:DQ8	082.D-0736	54787.175	600B					—
HD 24188	MS:A0:M.AP	073.D-0464	53087.032	600B	538 ± 44	1.09	-58 ± 41	0.93	DDD
PG 0342+026	SD:B	075.D-0352	53593.377	600B	-121 ± 174	0.99	258 ± 204	0.92	nnn
HD 23408	MS:B7:HEW	072.D-0377	52963.155	600B	-80 ± 64	0.94	-78 ± 81	0.98	nnn
HD 23598	MS:B8:SPB	079.D-0241	54344.397	600B	-20 ± 44	0.73	-45 ± 55	0.78	nnn
WD 0346-011	WD:DA1	070.D-0259	52637.176	600B	2009 ± 3239	1.03	767 ± 3350	1.10	n-n
WD 0346-011	WD:DA1	070.D-0259	52674.078	600B	2753 ± 3111	1.26	2645 ± 3242	1.36	n-n
HD 275877	PM:A2:V	074.C-0442	53330.222	600B	-159 ± 57	0.92	-27 ± 57	0.92	nnn
HD 23950	MS:B9:HGMM	073.D-0464	53216.419	600B	60 ± 41	0.95	99 ± 38	0.86	nnn
HD 24626	MS:B6	078.D-0140	54086.134	600B	39 ± 70	1.02	44 ± 66	0.90	nnn
HD 24587	MS:B5:SPB	072.D-0377	52971.071	600B	-37 ± 80	1.01	-11 ± 70	0.78	nnn
HD 24587	MS:B5:SPB	075.D-0295	53574.415	1200g	-12 ± 50	1.16	38 ± 48	1.05	nnn
HD 24587	MS:B5:SPB	075.D-0295	53630.252	1200g	18 ± 41	1.12	0 ± 36	0.88	nnn
HD 24587	MS:B5:SPB	078.D-0140	54086.174	600B	-107 ± 69	0.83	-64 ± 69	0.84	nnn
HD 24587	MS:B5:SPB	079.D-0241	54343.301	600B	-30 ± 63	0.80	-84 ± 61	0.74	nnn
HD 25558	MS:B3:SPB	078.D-0140	54086.244	600B	-78 ± 65	0.92	-60 ± 64	0.90	nnn
HD 25558	MS:B3:SPB	079.D-0241	54345.264	600B	43 ± 41	0.84	-37 ± 40	0.79	nnn
HD 26326	MS:B5:SPB	072.D-0377	52909.389	600B	-30 ± 80	1.05	-69 ± 74	0.91	nnn
HD 26326	MS:B5:SPB	073.D-0466	53218.357	600B	-8 ± 57	0.88	83 ± 57	0.88	nnn
HD 26326	MS:B5:SPB	075.D-0295	53630.370	1200g	-32 ± 29	1.16	19 ± 25	0.92	nnn
HD 26326	MS:B5:SPB	078.D-0140	54086.262	600B	-71 ± 64	0.77	-7 ± 69	0.89	nnn
HD 26739	MS:B5:SPB	079.D-0241	54344.283	600B	-20 ± 38	0.77	126 ± 37	0.75	nnn
HD 26676	MS:B8	074.C-0463	53277.345	1200g	36 ± 112	0.98	240 ± 129	0.99	nnn
HD 27742	MS:B8:SPB	079.D-0241	54345.355	600B	-29 ± 60	0.97	75 ± 52	0.73	nnn
HD 28114	MS:B6:SPB	073.D-0466	53223.413	600B	-37 ± 89	0.93			nnn
HD 28114	MS:B6:SPB	075.D-0295	53638.395	1200g	-29 ± 47	0.95	32 ± 48	0.99	nnn
HD 28114	MS:B6:SPB	078.D-0140	54106.091	600B	-128 ± 52	1.22	148 ± 43	0.96	dnn

Table 5. continued.

Star	Classification	Prog. ID	MJD	grism	$\langle B_z \rangle$ (G)	χ^2/ν	$\langle N_z \rangle$ (G)	χ^2/ν	HmT
HD 28475	MS:B5:SPB	078.D-0140	54107.129	600B	101 ± 50	0.99	41 ± 50	0.99	nnn
HD 28475	MS:B5:SPB	079.D-0241	54345.312	600B	5 ± 40	0.77	89 ± 53	0.80	nnn
LSR J04356-6105	WD:DC:HPM	080.D-0521	54404.321	600B					—
HD 29248	GS:B2:BCEP	075.D-0295	53629.322	1200g	-84 ± 38	1.01	0 ± 35	0.87	nnn
HD 29248	GS:B2:BCEP	075.D-0295	53630.347	1200g	-45 ± 24	1.37	-69 ± 26	1.18	nnn
HD 29248	GS:B2:BCEP	078.D-0140	54086.286	600B	75 ± 67	0.96	-11 ± 65	0.91	nnn
WD 0435-088	WD:DQ7	082.D-0736	54787.274	600B					—
HD 29376	MS:B3:SPB.SB	079.D-0241	54345.279	600B	48 ± 51	0.75	25 ± 53	0.81	nnn
HD 30612	MS:B9:AP	073.D-0464	53087.046	600B	34 ± 43	0.95	-10 ± 43	0.93	nnn
WD 0446-789	WD:DA3:M	070.D-0259	52609.229	600B	-2618 ± 805	1.12	1200 ± 787	1.09	d-d
WD 0446-789	WD:DA3:M	070.D-0259	52668.087	600B	-5235 ± 974	1.21	-915 ± 953	1.16	D-D
HD 30598	MS:A1:AP	073.D-0498	53249.321	600B	-5 ± 114	1.19	252 ± 114	1.20	nnn
HD 30598	MS:A1:AP	074.D-0488	53399.080	600B	125 ± 53	0.89	-117 ± 55	0.92	nnn
HD 31293	PM:A0:P.E	074.C-0442	53331.178	600B	-107 ± 108	0.92	-10 ± 108	0.91	nnn
U Lep	MS:A:RR	082.D-0342	54781.213	1200B	-58 ± 45	1.34	143 ± 38	1.08	nnn
HD 31648	PM:A3:P.E.SH	074.C-0442	53331.194	600B	102 ± 66	0.98	21 ± 61	0.84	ndn
HD 31648	PM:A3:P.E.SH	074.C-0463	53296.355	1200g	-32 ± 45	1.14	-85 ± 42	1.02	nnn
HD 293782	PM:A3:E	074.C-0442	53330.114	600B	-78 ± 68	0.85	60 ± 72	0.93	nnn
HD 33331	GS:B5:SPB	079.D-0241	54344.425	600B	-6 ± 37	0.78	-31 ± 43	0.70	nnn
NLTT 14553	WD:DQ:HPM	080.D-0521	54501.128	600B					—
NLTT 14558	WD:DA9:HPM	080.D-0521	54496.106	600B					—
HD 33328	MS:B2:E	077.D-0406	53955.400	600B	-86 ± 35	1.00	7 ± 33	0.89	nnn
HD 33328	MS:B2:E	380.D-0480	54432.114	1200B	46 ± 18	1.20	1 ± 14	0.68	nnn
HD 33328	MS:B2:E	380.D-0480	54433.114	1200B	33 ± 22	1.77	77 ± 16	0.88	nnn
HD 33904	MS:B9:HGMN	380.D-0480	54432.179	1200B	-54 ± 36	1.17	65 ± 43	1.00	nnn
TD1 32702	SD:B	072.D-0290	53058.025	600B	158 ± 143	1.01	128 ± 177	1.04	nnn
HD 273211	MS:A:RR	082.D-0342	54781.162	1200B	4 ± 41	1.43	67 ± 41	1.39	nnn
HD 34282	PM:A0:SH.E	074.C-0442	53330.146	600B	1 ± 76	0.96	0 ± 73	0.91	nnn
HD 34798	MS:B3:SPB	073.D-0466	53218.407	600B	-106 ± 45	0.88	115 ± 52	0.84	nnn
HD 34798	MS:B5:SPB	072.D-0377	52999.055	600B	79 ± 76	1.10	-39 ± 73	1.01	nnn
HD 34798	MS:B5:SPB	075.D-0295	53638.366	1200g	-35 ± 24	0.96	-30 ± 24	0.87	nnn
HD 34798	MS:B5:SPB	078.D-0140	54100.150	600B	45 ± 70	1.05	-162 ± 68	1.12	nnn
HD 34797	MS:B8:M.HEW	072.D-0377	52999.066	600B	1229 ± 75	0.89	37 ± 72	0.84	DDD
HD 35008	MS:B9:M.AP	074.D-0488	53399.015	600B	-321 ± 66	0.86	-75 ± 70	0.96	dnd
HD 35187	PM:A2:E	074.C-0442	53331.231	600B	-18 ± 59	0.88	17 ± 58	0.87	nnn
HD 35187	PM:A2:E	074.C-0442	53331.251	600B	121 ± 58	0.97	-114 ± 55	0.89	nnn
HD 287841	PM:A5:E	074.C-0442	53330.299	600B	-8 ± 69	0.90	-46 ± 68	0.89	nnn
HD 35929	PM:A3:E	074.C-0442	53331.094	600B	63 ± 40	0.92	45 ± 40	0.90	nnn
HD 35929	PM:A3:E	074.C-0463	53297.365	1200g	-1 ± 16	1.65	-11 ± 12	1.02	nnn
HD 36046	MS:B8:HEW	074.D-0488	53400.056	600B	-9 ± 74	0.84	50 ± 78	0.92	nnn
HD 36112	PM:A8:E	074.C-0442	53331.210	600B	-92 ± 67	0.85	119 ± 69	0.92	nnn
HD 244604	PM:A3	074.C-0442	53331.123	600B	-12 ± 59	0.88	-71 ± 57	0.84	nnn
GJ 206	MS:M3:FLS	082.D-0695	54831.042	300V	38 ± 394	1.41			-nn
HD 36540	MS:B7:M.AP	070.D-0352	52678.070	600B	312 ± 51	0.74	89 ± 49	0.66	DnD
HD 36559	MS:B9	070.D-0352	52678.070	600B	48 ± 61	0.69	51 ± 59	0.68	nnn
HD 36549	MS:B7:HEW	074.D-0488	53400.085	600B	-27 ± 71	0.87	-122 ± 71	0.88	nnn
NSV 2123	MS:G5:V	070.D-0352	52678.089	600B	129 ± 99	0.77	187 ± 92	0.68	nnn
HD 36629	MS:B2:V	070.D-0352	52678.089	600B	27 ± 47	0.70	-4 ± 46	0.65	nnn
HD 36671	MS:B9	070.D-0352	52678.089	600B	55 ± 57	0.71	-4 ± 53	0.64	nnn
HD 36918	MS:B9	070.D-0352	52679.090	600B	84 ± 51	0.82	-11 ± 56	0.94	nnn
HD 36916	MS:B8:M.HEW	070.D-0352	52679.042	600B	-582 ± 48	0.81	79 ± 50	0.94	DnD
HD 36960	MS:B0	070.D-0352	52679.071	600B	-47 ± 43	0.87	-18 ± 45	0.91	nnn
HD 245185	PM:A5	074.C-0442	53331.154	600B	94 ± 87	0.91	-197 ± 86	0.90	nnn
HD 36982	MS:B2:P	070.D-0352	52678.049	600B	96 ± 178	0.66	49 ± 177	0.65	nnn
HD 290665	MS:A0:M.AP	074.D-0488	53399.056	600B	-1828 ± 58	1.43	-112 ± 45	0.86	DDD
HD 37022	MS:O6:M.P.E	078.D-0330	54114.150	600R	-122 ± 142	1.17	117 ± 137	0.98	-nn
HD 37022	MS:O6:M.P.E	078.D-0330	54116.057	600R	-381 ± 95	1.14	-18 ± 89	0.95	-dd
HD 37022	MS:O5:M.P.E	070.D-0352	52678.049	600B	141 ± 58	0.72	-64 ± 57	0.73	ndn
HD 37022	MS:O6:M.P.E	078.D-0330	54107.220	600R	418 ± 81	1.15	140 ± 85	1.05	-DD
HD 37022	MS:O6:M.P.E	078.D-0330	54108.271	600R	506 ± 133	1.11	-102 ± 113	0.97	-dd
HD 37022	MS:O6:M.P.E	078.D-0330	54112.174	600R	304 ± 101	1.10	-220 ± 102	0.89	-dd
HD 37022	MS:O6:M.P.E	078.D-0330	54155.062	600R	439 ± 104	1.43	-202 ± 89	1.05	-dd
HD 37022	MS:O6:M.P.E	078.D-0330	54156.072	600R	510 ± 76	1.43	2 ± 67	1.10	-DD
HD 37022	MS:O6:M.P.E	078.D-0330	54157.051	600R	369 ± 78	1.51	47 ± 69	0.99	-dd
HD 37022	MS:O6:M.P.E	078.D-0330	54158.085	600R	118 ± 84	1.23	-46 ± 90	1.14	-nn
HD 37022	MS:O6:M.P.E	078.D-0330	54177.063	600R	-55 ± 92	0.99	113 ± 96	1.10	-nn
HD 37022	MS:O6:M.P.E	078.D-0330	54182.048	600R	230 ± 73	1.25	-12 ± 68	0.83	-dd

Table 5. continued.

Star	Classification	Prog. ID	MJD	grism	$\langle B_z \rangle$ (G)	χ^2/ν	$\langle N_z \rangle$ (G)	χ^2/ν	HmT
HD 37041	MS:B1	070.D-0352	52678.049	600B	73 ± 55	0.67	63 ± 55	0.68	nnn
HD 37058	MS:B3:M.HEW	070.D-0352	52679.029	600B	-965 ± 58	0.86	20 ± 59	0.86	DDD
HD 36879	GS:O7	079.D-0241	54345.389	600B	83 ± 51	0.74	-29 ± 51	0.75	nnn
T Ori	PM:A3	074.C-0442	53332.111	600B	-67 ± 83	0.93	-72 ± 87	1.05	nnn
HD 37151	MS:B8:SPB	078.D-0140	54107.154	600B	-54 ± 49	0.97	-70 ± 47	0.90	nnn
V380 Ori	PM:A0:M.E	074.C-0442	53330.258	600B					—
HD 37210	MS:B8:HEW	070.D-0352	52679.057	600B	-62 ± 60	0.92	137 ± 58	0.83	nnn
HD 37258	PM:A2	074.C-0442	53332.138	600B	-99 ± 77	0.92	3 ± 74	0.87	nnn
BF Ori	PM:A5:E.V	074.C-0442	53330.277	600B	-115 ± 38	0.91	58 ± 36	0.86	nnd
HD 37333	MS:A0:AP	074.D-0488	53399.033	600B	97 ± 60	1.09	291 ± 53	0.87	nnn
HD 37357	PM:A0:E	074.C-0442	53332.157	600B	-13 ± 66	0.83	-123 ± 64	0.77	nnn
HD 37411	PM:B9	074.C-0442	53330.320	600B	-69 ± 68	0.88	-39 ± 66	0.86	nnn
HD 37428	MS:A0	070.D-0352	52678.117	600B	-165 ± 66	0.68	-123 ± 65	0.67	nnn
HD 37470	MS:B8:AP	070.D-0352	52678.117	600B	-95 ± 53	0.68	211 ± 52	0.69	nnn
HD 37490	PM:B3:E	074.C-0442	53332.171	600B	-77 ± 119	1.00	127 ± 114	0.93	nnn
HD 37490	PM:B3:E	074.C-0442	53332.179	1200g	-13 ± 96	0.83	-214 ± 98	0.94	nnn
HD 37633	MS:B9:M.AP	074.D-0488	53400.071	600B	470 ± 66	0.91	-60 ± 65	0.84	ddD
HD 37776	MS:B2:M.HES	072.D-0119	52940.368	300V	-476 ± 928	1.00	-234 ± 1056	0.87	nnn
HD 37806	PM:A0	074.C-0442	53332.193	600B	53 ± 61	0.94	-28 ± 58	0.84	nnn
HD 37806	PM:A0	074.C-0442	53332.202	1200g	-121 ± 56	0.91	163 ± 54	0.83	nnn
NGC 2024 1	MS:B0	060.A-9800	54832.205	300V	-2002 ± 1792	0.84	113 ± 1614	0.66	nnn
NGC 2024 1	MS:B0	060.A-9203	54086.226	600B	-843 ± 912	0.94			nnn
NGC 2024 1	MS:B0	060.A-9800	54815.199	300V	-90 ± 801	1.04	-254 ± 733	0.87	nnn
NGC 2024 1	MS:B0	060.A-9800	54815.219	300V	-204 ± 306	0.87	513 ± 430	1.67	nnn
NGC 2024 1	MS:B0	060.A-9800	54820.182	300V	-661 ± 1393	0.60	-704 ± 1532	0.73	nnn
NGC 2024 1	MS:B0	060.A-9800	54832.178	300V	2120 ± 1540	0.80	-288 ± 1524	0.79	nnn
NGC 2024 1	MS:B0	082.D-0695	54829.024	300V	-262 ± 1319	0.77			nnn
NGC 2024 1	MS:B0	060.A-9800	54820.167	300V	794 ± 1158	0.81	1263 ± 1094	0.72	nnn
HD 38238	MS:A7:DSCT	073.D-0464	53249.367	600B	37 ± 44	1.34	-136 ± 40	1.16	nnn
HD 38238	MS:A7:DSCT	075.D-0295	53629.377	1200g	-2 ± 30	1.01	20 ± 29	0.91	nnn
HD 39060	MS:A6:CSD	081.C-0410	54609.954	600B	-12 ± 23	0.76	-85 ± 25	0.87	nnn
HD 39060	MS:A6:CSD	074.C-0463	53296.272	1200g	-148 ± 58	1.27	98 ± 66	1.29	nnn
CPD-64 481	SD:B	072.D-0290	53058.069	600B	87 ± 214	1.03	-536 ± 269	0.99	nnn
HD 39844	MS:B6:SPB	079.D-0241	54344.411	600B	-117 ± 34	0.84	-28 ± 42	0.77	nnd
WD 0548-001	WD:DQP8	082.D-0736	54787.330	600B					—
HD 40494	MS:B2:SPB	079.D-0241	54343.427	600B	34 ± 30	0.86	41 ± 29	0.78	nnn
HD 250550	PM:B7:E	074.C-0442	53332.220	600B	186 ± 122	1.14	-39 ± 104	0.79	nnn
HD 41335	MS:B2:E	080.D-0383	54549.982	600B	-194 ± 113	0.96	111 ± 103	0.79	nnn
HD 271924	MS:A:RR	082.D-0342	54782.316	1200B	-105 ± 44	1.07	77 ± 45	1.15	nnn
HD 252214	MS:B2	070.D-0352	52678.153	600B	24 ± 40	2.05	172 ± 47	2.44	nnn
HD 41909	GS:G0	070.D-0352	52678.153	600B	49 ± 27	1.24	-14 ± 21	0.72	nnn
NGC 2169 12	MS:A0:M.AP	070.D-0352	52678.153	600B	-2914 ± 114	0.90	-172 ± 111	0.85	DDD
HD 252248	MS:B3	070.D-0352	52678.153	600B	-98 ± 67	0.73	-69 ± 67	0.67	nnn
HD 252266	MS:B3	070.D-0352	52678.153	600B	-17 ± 55	0.70	32 ± 55	0.69	nnn
HD 42659	MS:A3:M.AP	072.D-0377	52999.119	600B	382 ± 48	1.17	-39 ± 42	0.90	DDD
RX Col	MS:A:RR	082.D-0342	54781.308	1200B	41 ± 77	1.16	-6 ± 75	1.12	nnn
WD 0612+177	WD:DA2	070.D-0259	52609.274	600B	-1282 ± 754	0.93	980 ± 755	0.93	n-n
WD 0612+177	WD:DA2	070.D-0259	52672.079	600B	-424 ± 733	0.86	-1431 ± 747	0.89	n-n
HD 44743	GS:B1:BCEP	075.D-0295	53475.031	1200g	-96 ± 66	1.24	-18 ± 65	1.21	nnn
HD 44743	GS:B1:BCEP	075.D-0295	53629.343	1200g	-32 ± 20	0.74	-1 ± 20	0.76	nnn
HD 44743	GS:B1:BCEP	078.D-0140	54046.360	600B	158 ± 75	0.88	97 ± 75	0.87	nnn
HD 45284	MS:B8:SPB.SB	073.D-0466	53252.367	600B	56 ± 47	1.00	-9 ± 56	0.93	nnn
HD 45284	MS:B8:SPB.SB	078.D-0140	54107.242	600B	-46 ± 57	0.85	-111 ± 58	0.89	nnn
HD 45284	MS:B8:SPB.SB	078.D-0140	54107.282	600B	114 ± 108	0.84	-15 ± 111	0.88	nnn
HD 45583	MS:B9:M.AP	070.D-0352	52679.237	600B	-1545 ± 61	1.49	-41 ± 47	0.91	DDD
HD 46005	MS:B8:EB	073.D-0466	53259.399	600B	-27 ± 68	0.99	-2 ± 65	0.98	nnn
HD 46328	GS:B1:M.BCEP	075.D-0295	53475.046	1200g	317 ± 22	0.56	6 ± 19	0.44	DDD
HD 46328	GS:B1:M.BCEP	075.D-0295	53506.971	1200g	325 ± 34	1.09	-95 ± 33	0.99	DDD
HD 46328	GS:B1:M.BCEP	078.D-0140	54061.325	600B	434 ± 59	1.01	30 ± 56	0.91	DdD
HD 46328	GS:B1:M.BCEP	078.D-0140	54107.266	600B	423 ± 61	1.18	60 ± 60	1.01	DdD
HD 46328	GS:B1:M.BCEP	078.D-0140	54114.030	600B	307 ± 57	1.08	-150 ± 62	1.04	ndD
HD 46328	GS:B1:M.BCEP	078.D-0140	54114.178	600B	457 ± 44	1.00	-27 ± 47	0.99	DDD
HD 46328	GS:B1:M.BCEP	078.D-0140	54116.109	600B	169 ± 63	1.08	189 ± 56	0.92	ndn
HD 46328	GS:B1:M.BCEP	078.D-0140	54155.083	600B	299 ± 33	1.03	-9 ± 33	0.87	DDD
HD 46328	GS:B1:M.BCEP	079.D-0241	54343.372	1200B	378 ± 16	1.33	-38 ± 17	0.99	DDD
HD 46328	GS:B1:M.BCEP	079.D-0241	54345.376	1200B	414 ± 13	1.54	-6 ± 11	0.95	DDD
HD 46328	GS:B1:M.BCEP	080.D-0383	54548.976	600B	278 ± 50	0.75			nDD

Table 5. continued.

Star	Classification	Prog. ID	MJD	grism	$\langle B_z \rangle$ (G)	χ^2/ν	$\langle N_z \rangle$ (G)	χ^2/ν	HmT
HD 46328	GS:B1:M.BCEP	080.D-0383	54549.995	600B	472 ± 43	0.77	-61 ± 51	0.73	DDD
NGC 2244 330	?:K7	070.D-0352	52679.162	600B	54 ± 22	1.28	-91 ± 19	0.97	-nn
NGC 2244 331	MS:B7	070.D-0352	52679.162	600B	-2024 ± 402	1.22	-1161 ± 387	1.02	DnD
NGC 2244 336	MS:A5	070.D-0352	52679.162	600B	113 ± 86	1.14	-127 ± 86	1.16	nnn
NGC 2244 334	MS:B5:M.AP	070.D-0352	52679.162	600B	-7431 ± 154	1.72	159 ± 123	1.20	DDD
NGC 2244 365	?:G5	070.D-0352	52679.162	600B	-22 ± 56	1.07	-201 ± 52	0.93	nnn
NGC 2244 364	?:K5	070.D-0352	52679.162	600B	119 ± 39	0.89	-1 ± 37	0.78	-dd
HD 259431	PM:B6:P.E	074.C-0442	53332.238	600B	-294 ± 247	1.12	-3 ± 215	0.85	nnn
WD 0631+107	WD:DA2	070.D-0259	52700.130	600B	-1838 ± 1092	1.10	1885 ± 1172	1.29	n-n
WD 0631+107	WD:DA2	070.D-0259	52702.125	600B	1267 ± 1108	1.19	323 ± 1069	1.10	n-n
R Mon	MS:B0:V	074.C-0442	53332.257	600B					—
HD 47839	PM:O7:E	081.C-0410	54609.967	600B	-36 ± 58	0.87	-31 ± 58	0.87	nnn
HD 289002	SD:B3	072.D-0119	52940.376	300V	3285 ± 2579	0.80			nnn
HD 49023	MS:B9:AP	074.D-0488	53400.098	600B	27 ± 70	1.00	24 ± 65	0.84	nnn
CPD-20 1637	MS:A1	073.D-0498	53276.352	600B	54 ± 58	0.70	16 ± 61	0.77	nnn
CPD-20 1637	MS:A1	074.D-0488	53400.119	600B	-89 ± 192	0.70	-152 ± 190	0.68	nnn
CPD-20 1640	MS:A5:AP	074.D-0488	53400.150	600B	110 ± 58	0.73	91 ± 60	0.76	nnn
BD-20 1571	MS:A3	073.D-0498	53276.352	600B	-81 ± 68	0.79	55 ± 68	0.79	nnn
BD-20 1571	MS:A3	074.D-0488	53400.119	600B	200 ± 74	0.69	-57 ± 73	0.68	nnn
06:46:52 -20:57:06	?:F	074.D-0488	53400.150	600B	-91 ± 90	0.66	-217 ± 96	0.75	nnn
NGC 2287 AR157	MS:A6:AM	074.D-0488	53400.150	600B	-139 ± 94	0.66	-104 ± 102	0.77	nnn
CPD-20 1645	MS:A2	074.D-0488	53400.150	600B	-37 ± 67	0.76	53 ± 66	0.73	nnn
HD 49299	MS:A0:M.AP	073.D-0498	53276.352	600B	-543 ± 38	0.85	99 ± 36	0.75	DDD
HD 49299	MS:A0:M.AP	074.D-0488	53400.119	600B	-2728 ± 58	1.55	145 ± 40	0.74	DDD
HD 49606	GS:B8:HEW	072.D-0377	52946.354	600B	-8 ± 79	0.84	49 ± 82	0.92	nnn
HD 49606	GS:B8:HEW	380.D-0480	54432.192	1200B	145 ± 31	1.15	61 ± 36	0.94	dnd
HD 50707	SG:B1:BCEP	078.D-0140	54107.319	600B	44 ± 70	0.91	4 ± 68	0.89	nnn
HD 50707	SG:B1:BCEP	079.D-0241	54345.372	600B	54 ± 27	0.86	2 ± 26	0.77	nnn
HD 51088	MS:B8:AP	073.D-0498	53269.384	600B	-143 ± 51	0.86	58 ± 50	0.86	nnn
HD 51088	MS:B8:AP	074.D-0488	53400.224	600B	108 ± 64	0.89	-22 ± 64	0.90	nnn
HD 52089	SG:B2	079.D-0241	54343.388	600B	-195 ± 37	0.86	90 ± 35	0.79	dnd
HD 52089	SG:B2	078.D-0140	54046.339	600B	-112 ± 60	0.97	93 ± 61	1.02	nnn
HD 52721	PM:B2:E	074.C-0442	53331.296	600B	202 ± 157	1.04	-156 ± 144	0.87	nnn
HD 52965	MS:B8	074.D-0488	53400.211	600B	-74 ± 69	0.66	-87 ± 70	0.68	nnn
HD 52980	GS:B9	074.D-0488	53400.211	600B	-149 ± 47	0.74	68 ± 46	0.70	nnd
BD-08 1708	MS:B6	074.D-0488	53400.211	600B	-42 ± 110	0.68	180 ± 110	0.67	nnn
HD 53921	MS:B9:M.SP.B.SB	075.D-0295	53630.401	1200g	144 ± 25	0.80	7 ± 25	0.80	DnD
HD 53921	MS:B9:M.SP.B.SB	075.D-0295	53631.408	1200g	170 ± 20	0.95	-9 ± 19	0.87	DDD
HD 53921	MS:B9:M.SP.B.SB	078.D-0140	54061.304	600B	-16 ± 133	0.83	-86 ± 137	0.88	nnn
HD 53921A	MS:B9:M.SP.B.SB	072.D-0377	52999.137	600B	511 ± 83	0.86	-77 ± 80	0.79	DdD
HD 53921B	MS:B8:SB	072.D-0377	52999.137	600B	257 ± 133	0.81	-326 ± 133	0.83	nnn
HD 53179	PM:B:P.E	081.C-0410	54608.975	600B	-250 ± 42	1.01	29 ± 48	0.93	DdD
HD 53179	PM:B:P.E	282.C-5041	54826.242	600B					—
HD 53179	PM:B:P.E	282.C-5041	54826.307	1200B					—
HD 53179	PM:B:PE	074.C-0442	53331.312	600B	-308 ± 171	0.98	116 ± 180	1.06	n-n
HD 53244	GS:B8	072.D-0377	52999.155	600B	15 ± 60	0.89	174 ± 71	1.10	nnn
HD 53367	PM:B0:E	075.D-0507	53475.064	1200g	38 ± 252	1.26	-83 ± 242	1.17	nnn
HD 53367	PM:B0:E	075.D-0507	53503.002	1200g	27 ± 50	1.11	-77 ± 59	1.11	nnn
HD 53367A	PM:B0:E	074.C-0442	53330.338	600B	72 ± 81	0.84	101 ± 83	0.89	nnn
HD 53367B	PM:B0:E	074.C-0442	53330.351	600B	-103 ± 91	0.96	-231 ± 84	0.82	nnn
HD 53929	GS:B9	072.D-0377	52992.306	600B	58 ± 212	1.07	-242 ± 215	1.10	nnn
HD 53929	GS:B9	072.D-0377	53004.210	600B	36 ± 83	0.85	102 ± 86	0.93	nnn
TYC5385-927-1	?:F	068.D-0403	52310.057	600R	14 ± 245	1.25	101 ± 250	1.29	nnn
NGC 2343 13	MS:B3	068.D-0403	52310.057	600R	-49 ± 101	0.86	-47 ± 98	0.83	nnn
07:07:23 -10:31:45	UNCLASSIFIED	068.D-0403	52310.057	600R	259 ± 115	0.97	-55 ± 120	1.08	nnn
BD-10 1875	?:A	068.D-0403	52310.057	600R	-194 ± 149	0.85	181 ± 140	0.74	nnn
NGC 2343 22	MS:A0	068.D-0403	52310.057	600R	55 ± 148	0.91	-208 ± 142	0.81	nnn
NGC 2343 40	MS:F1	068.D-0403	52310.125	600R	-18 ± 162	0.91	230 ± 160	0.89	nnn
NGC 2343 35	MS:A6	068.D-0403	52310.057	600R	262 ± 185	1.02	-617 ± 178	0.93	nnn
BD-10 1878	MS:B8	068.D-0403	52310.125	600R	139 ± 98	0.81	107 ± 95	0.78	nnn
07:07:47 -10:37:54	UNCLASSIFIED	068.D-0403	52310.125	600R					—
NGC 2343 25	MS:A3	068.D-0403	52310.125	600R	341 ± 152	0.75	-131 ± 158	0.82	nnn
NGC 2343 16	?:A8	068.D-0403	52310.125	600R	-233 ± 129	0.92	96 ± 121	0.84	nnn
BD-10 1879a	MS:A3	068.D-0403	52309.160	600R	-87 ± 124	0.72	334 ± 129	0.78	nnn
07:07:55 -10:36:11	UNCLASSIFIED	068.D-0403	52310.125	600R	38 ± 220	1.00	577 ± 214	0.94	nnn
NGC 2343 34	MS:A6	068.D-0403	52309.067	600R	60 ± 170	0.88	126 ± 171	0.89	nnn
NGC 2343 43	MS:F	068.D-0403	52309.210	600R	117 ± 212	0.98	7 ± 210	0.98	nnn

Table 5. continued.

Star	Classification	Prog. ID	MJD	grism	$\langle B_z \rangle$ (G)	χ^2/ν	$\langle N_z \rangle$ (G)	χ^2/ν	HmT
NGC 2343 15	GS:K4	068.D-0403	52309.067	600R	94 ± 46	0.97	-29 ± 44	0.87	nnn
NGC 2343 28	MS:A5	068.D-0403	52310.125	600R	294 ± 160	0.91	237 ± 161	0.94	nnn
NGC 2343 37	MS:A8	068.D-0403	52309.210	600R	47 ± 154	0.91	3 ± 163	1.02	nnn
HD 54304	MS:B5	068.D-0403	52309.123	600R	-72 ± 62	0.86	57 ± 56	0.65	nnn
07:08:00 – 10:48:17	UNCLASSIFIED	068.D-0403	52309.160	600R					—
07:08:01 – 10:41:25	UNCLASSIFIED	068.D-0403	52310.125	600R	101 ± 275	1.25	-274 ± 254	1.06	nnn
NGC 2343 27	MS:A5	068.D-0403	52309.210	600R	-108 ± 175	0.83	80 ± 175	0.90	nnn
07:08:03 – 10:33:48	UNCLASSIFIED	068.D-0403	52309.210	600R					—
NGC 2343 23	GS:F2	068.D-0403	52309.123	600R	-58 ± 76	0.80	-18 ± 73	0.73	nnn
07:08:05 – 10:34:48	UNCLASSIFIED	068.D-0403	52309.123	600R					—
NGC 2343 26	MS:A7	068.D-0403	52309.210	600R	73 ± 147	0.95	-194 ± 139	0.86	nnn
NGC 2343 36	MS:A7	068.D-0403	52309.067	600R	-21 ± 170	1.00	276 ± 166	0.95	nnn
NGC 2343 10	MS:B8	068.D-0403	52309.123	600R	38 ± 115	0.85	-113 ± 105	0.71	nnn
NGC 2343 17	MS:A2	068.D-0403	52309.067	600R	281 ± 131	0.93	295 ± 116	0.78	nnn
NGC 2343 6	MS:B8	068.D-0403	52309.123	600R	-8 ± 81	0.86	63 ± 74	0.73	nnn
TYC5385-2097-1	MS:A0	068.D-0403	52309.160	600R	-169 ± 318	0.83	-133 ± 310	0.79	nnn
BD-10 1883	MS:B9	068.D-0403	52309.067	600R	-75 ± 86	0.87	-124 ± 79	0.73	nnn
NGC 2343 18	MS:A4	068.D-0403	52309.067	600R	124 ± 105	0.92	-151 ± 99	0.81	nnn
NGC 2343 31	MS:A6	068.D-0403	52309.210	600R	-103 ± 194	0.97	172 ± 194	0.96	nnn
V931 Mon	MS:B9	068.D-0403	52309.123	600R	29 ± 147	0.89	284 ± 151	0.94	nnn
NGC 2343 38	MS:A7	068.D-0403	52309.123	600R	-24 ± 193	0.82	128 ± 198	0.87	nnn
HD 54360	MS:A0	068.D-0403	52309.067	600R	-27 ± 80	1.51	94 ± 61	0.86	nnn
NGC 2343 19	GS:K	068.D-0403	52309.067	600R	-137 ± 154	1.16	-108 ± 119	0.87	nnn
BD-10 1885B	MS:B9	068.D-0403	52309.210	600R	148 ± 99	1.02	-71 ± 91	0.86	nnn
07:08:16 – 10:33:50	UNCLASSIFIED	068.D-0403	52309.123	600R					—
HD 54387	??:G5	068.D-0403	52309.067	600R	103 ± 38	1.18	-33 ± 33	0.92	nnn
HD 54388	??:A3	068.D-0403	52309.160	600R	-60 ± 64	1.64	-68 ± 43	0.72	nnn
NGC 2343 30	MS:A	068.D-0403	52309.123	600R	201 ± 241	0.92	-293 ± 229	0.83	nnn
07:09:18 – 32:04:30	??:G	080.D-0521	54404.353	600B					—
HD 55522	MS:B2:M.AP	072.D-0377	52999.223	600B	148 ± 83	0.92	-19 ± 79	0.82	nnn
HD 55522	MS:B2:M.AP	072.D-0377	53000.053	600B	920 ± 61	0.93	-139 ± 62	0.95	DDD
HD 55522	MS:B2:M.AP	073.D-0466	53275.295	600B	806 ± 47	1.07	33 ± 44	0.96	DDD
HD 55718	MS:B3:SPB	079.D-0241	54343.401	600B	-6 ± 48	0.78	31 ± 59	0.78	nnn
HD 56350	MS:B:M.AP	072.D-0377	52999.239	600B	888 ± 75	0.96	-8 ± 69	0.80	DDD
HD 55958	MS:B2:BCEP	079.D-0241	54343.414	600B	-76 ± 39	0.74	-67 ± 51	0.82	nnn
HD 56014	GS:B3:E	075.D-0507	53511.976	1200g	-91 ± 44	0.96	41 ± 43	0.91	nnn
HD 56014	GS:B3:E	080.D-0383	54549.071	600B	-48 ± 52	0.82	-104 ± 62	0.77	nnn
HD 56014	GS:B3:E	380.D-0480	54432.163	1200B	54 ± 26	0.78	-33 ± 24	0.65	nnn
HD 56014	GS:B3:E	380.D-0480	54433.134	1200B	9 ± 26	1.26	-41 ± 21	0.83	nnn
HD 56455	MS:A0:AP	072.D-0377	52999.251	600B	160 ± 91	0.83	-120 ± 93	0.86	nnn
HD 56139	MS:B2:E	075.D-0507	53503.049	1200g	46 ± 54	1.10	19 ± 51	0.96	nnn
HD 56343	MS:B9:M.AP	073.D-0498	53269.356	600B	-3731 ± 78	1.34	83 ± 65	0.91	DDD
NX Pup	PM:A0	074.C-0442	53331.275	600B	-178 ± 53	1.02	138 ± 52	0.99	dnd
HD 58448	MS:B8:AP	072.D-0377	52999.265	600B	44 ± 89	0.83	34 ± 89	0.84	nnn
HD 58011	SG:B1:E.P	075.D-0507	53503.031	1200g	-6 ± 70	1.04	119 ± 68	0.98	nnn
HD 58011	SG:B1:E.P	080.D-0383	54549.082	600B	-145 ± 106	0.69	203 ± 148	0.86	nnn
HD 58050	MS:B2:E	075.D-0507	53630.417	1200g	-116 ± 51	0.93	-66 ± 51	0.91	nnn
HD 58978	GS:B1	080.D-0383	54548.996	600B	-148 ± 232	1.02	310 ± 262	0.87	nnn
HD 58715	MS:B8:E	080.D-0383	54549.060	600B	-38 ± 52	0.88	63 ± 61	0.88	nnn
HD 60435	MS:A3:M.AP	072.D-0377	53000.072	600B	-454 ± 54	0.95	-138 ± 52	0.89	dDD
HD 60855	MS:B2	080.D-0383	54549.049	600B	88 ± 93	0.81	14 ± 92	0.79	nnn
HD 60940	MS:B8	074.D-0488	53399.241	600B	9 ± 38	0.68	6 ± 38	0.66	nnn
BD-14 2015	MS:B9	074.D-0488	53399.241	600B	-42 ± 54	0.65	-97 ± 58	0.73	nnn
HD 60968	MS:G5	074.D-0488	53399.241	600B	-55 ± 22	0.77	-20 ± 21	0.70	-nn
CD-31 4800	SD:O	072.D-0290	53058.215	600B	-75 ± 129	0.93	-37 ± 151	0.87	nnn
HD 60996	MS:B9	074.D-0488	53399.241	600B	71 ± 43	0.67	-29 ± 43	0.67	nnn
HD 61068	GS:B2:BCEP	078.D-0140	54107.338	600B	-3 ± 52	0.97	-6 ± 47	0.85	nnn
NGC 2422 PMS921	MS:A6	070.D-0352	52678.186	600B	-184 ± 224	0.70	124 ± 227	0.72	nnn
NGC 2422 PMS119	MS:A8	070.D-0352	52678.186	600B	37 ± 200	0.68	123 ± 200	0.69	nnn
BD-14 2028	MS:A1:AP	272.D-5026	53063.180	600B	25 ± 93	0.92	-189 ± 91	0.89	nnn
BD-14 2028	MS:A1:AP	272.D-5026	53072.198	600B	-64 ± 110	0.93	263 ± 109	0.92	nnn
HD 61045	MS:B8:M.AP	070.D-0352	52678.186	600B	412 ± 45	0.67	46 ± 46	0.69	DDD
HD 61045	MS:B8:M.AP	074.D-0488	53399.258	600B	297 ± 59	0.80	95 ± 61	0.85	dnd
BD-14 2033	MS:A1	070.D-0352	52678.186	600B	614 ± 201	0.70	39 ± 193	0.64	nnd
BD-14 2040	MS:A1:AP	070.D-0352	52678.186	600B	26 ± 164	0.68	70 ± 164	0.68	nnn
BD-14 2040	MS:A1:AP	074.D-0488	53399.212	600B	-57 ± 58	0.95	12 ± 56	0.86	nnn
HD 61712	MS:B7:CSD	074.C-0463	53359.251	1200g	-102 ± 39	0.95	-66 ± 37	0.90	nnn

Table 5. continued.

Star	Classification	Prog. ID	MJD	grism	$\langle B_z \rangle$ (G)	χ^2/ν	$\langle N_z \rangle$ (G)	χ^2/ν	HmT
V547 Pup	WD:?:NOV	274.D-5025	53348.236	1200g					—
HD 62376	MS:B7	074.D-0488	53399.112	600B	88 ± 54	0.82	-214 ± 57	0.90	nnn
HD 62367	MS:B8:E	080.D-0383	54549.096	600B	31 ± 55	0.86	-117 ± 66	0.83	nnn
CD-37 3845	MS:A0:P	070.D-0352	52678.203	600B	-57 ± 87	0.75	-67 ± 87	0.72	ndn
HD 62974	MS:A3	070.D-0352	52678.203	600B	10 ± 80	0.71	56 ± 76	0.65	nnn
HD 62992	MS:A0:M.AP	070.D-0352	52678.203	600B	-189 ± 37	0.67	-33 ± 37	0.63	ddD
HD 63079	MS:B7:AP	074.D-0488	53399.098	600B	65 ± 59	0.86	67 ± 60	0.88	nnn
NLTT 18393	MS:M3:HPM	080.D-0521	54426.285	600B	-385 ± 341	0.75			—
HD 63401	MS:B8:M.AP	070.D-0352	52678.026	600B	-589 ± 53	0.88	-65 ± 52	0.84	DDD
HD 63401	MS:B8:M.AP	072.D-0377	53002.053	600B	153 ± 95	0.85	-55 ± 95	0.84	nnn
HD 63401	MS:B8:M.AP	072.D-0377	53004.228	600B	-414 ± 101	0.88	31 ± 101	0.87	dnd
HD 63401	MS:B8:M.AP	074.D-0488	53399.125	600B	322 ± 55	0.84	-21 ± 70	0.87	DnD
HD 64368	MS:A5	079.D-0241	54345.429	600B	13 ± 93	0.84			nnn
HD 63975	MS:B8:HGMN	072.D-0377	52992.278	600B	132 ± 90	0.93	52 ± 86	0.87	nnn
NGC 2489 59	MS:B9	074.D-0488	53400.258	600B	538 ± 136	0.99	27 ± 150	0.89	ddd
NGC 2489 58	MS:A0	074.D-0488	53400.258	600B	-6 ± 165	1.04	-370 ± 202	1.01	nnn
NGC 2489 40	MS:B8	074.D-0488	53400.258	600B	-312 ± 158	0.97	-84 ± 180	0.82	nnn
HD 65691	MS:B8	068.D-0403	52310.252	600R	-257 ± 130	0.83	-66 ± 131	0.82	nnn
NGC 2489 5	MS:A0	074.D-0488	53400.258	600B	478 ± 198	0.97	65 ± 232	0.89	nnn
HD 65712	MS:A0:M.AP	070.D-0352	52679.306	600B	-1296 ± 71	1.42	64 ± 61	1.03	DDD
HD 65712	MS:A0:M.AP	074.D-0488	53399.183	600B	-569 ± 49	1.08	33 ± 45	0.90	DDD
CPD-60 942	MS:A1	068.D-0403	52310.252	600R	210 ± 212	1.07	-62 ± 205	1.00	nnn
CPD-60 944A	MS:A0:AP	068.D-0403	52310.252	600R	53 ± 67	0.85	7 ± 64	0.76	nnn
CPD-60 944A	MS:A0:AP	074.D-0488	53399.142	600B	-61 ± 52	0.91	-99 ± 53	0.93	nnn
CD-60 1929	GS:B9	068.D-0403	52310.252	600R	29 ± 83	1.05	10 ± 79	0.92	nnn
CPD-60 944B	MS:B9:M.AP	068.D-0403	52310.288	600R	463 ± 72	0.84	67 ± 67	0.75	dDD
CPD-60 944B	MS:B9:M.AP	074.D-0488	53399.161	600B	240 ± 53	0.94	31 ± 51	0.88	dnd
CD-60 1932	MS:A0	068.D-0403	52310.252	600R	-244 ± 253	0.93	141 ± 246	0.88	nnn
CD-60 1932	MS:A0	068.D-0403	52310.288	600R	-48 ± 209	0.80	-272 ± 209	0.76	nnn
NGC 2516 DAC311	MS:A0	068.D-0403	52310.288	600R	351 ± 346	1.23	287 ± 320	1.06	nnn
NGC 2516 DAC313	?:G	068.D-0403	52310.288	600R	-389 ± 433	1.35	446 ± 465	1.53	dnn
NGC 2516 SBL333	MS:B8	068.D-0403	52310.288	600R					—
HD 65869	MS:B9	068.D-0403	52310.288	600R	179 ± 106	1.10	32 ± 94	0.87	nnn
HD 65896	MS:A0	068.D-0403	52309.330	600R	165 ± 78	0.84	-187 ± 74	0.77	nnn
HD 65950	MS:B9:HGMN	068.D-0403	52310.323	600R	-90 ± 45	0.90	-2 ± 40	0.73	nnn
HD 65950	MS:B9:HGMN	072.D-0377	53002.067	600B	48 ± 73	0.98	25 ± 69	0.88	nnn
NGC 2516 DAC515	?:F	068.D-0403	52310.323	600R	145 ± 189	1.21	-328 ± 178	1.06	nnn
V373 Car	MS:B	272.D-5026	53072.226	600B	-98 ± 48	0.80	150 ± 46	0.74	nnn
V373 Car	MS:B	068.D-0403	52310.180	600R	56 ± 39	0.86	22 ± 36	0.73	nnn
HD 65949	MS:B8:HGMN	072.D-0377	53002.082	600B	-45 ± 78	0.85	-80 ± 77	0.82	nnn
HD 65949	MS:B8:HGMN	078.D-0140	54108.300	600B	-59 ± 64	0.91	25 ± 61	0.84	nnn
HD 65949	MS:B8:HGMN	380.D-0480	54433.367	1200B	-105 ± 30	1.16	-253 ± 28	1.00	ndd
CPD-60 969	MS:B9	068.D-0403	52309.330	600R	47 ± 98	0.79	32 ± 87	0.62	nnn
HD 65949	MS:B8:HGMN	068.D-0403	52309.330	600R	48 ± 68	0.89	24 ± 61	0.74	nnn
NGC 2516 SBL559	UNCLASSIFIED	068.D-0403	52309.330	600R	-279 ± 229	1.02	593 ± 238	1.10	-nn
CPD-60 975	MS:A:V	068.D-0403	52309.160	600R	198 ± 93	0.71	-85 ± 97	0.76	ndn
CPD-60 975	MS:A:V	068.D-0403	52310.180	600R	38 ± 86	0.76	-87 ± 79	0.63	nnn
CPD-60 977	MS:F0	068.D-0403	52309.293	600R	32 ± 64	0.74	89 ± 64	0.75	nnn
HD 65987	MS:B9:M.AP	272.D-5026	53063.222	600B	-442 ± 62	0.96	-88 ± 59	0.89	DdD
V391 Car	MS:A0:AP	068.D-0403	52309.160	600R	5 ± 60	0.72	115 ± 56	0.65	nnn
V391 Car	MS:A0:AP	272.D-5026	53072.226	600B	-138 ± 78	0.74	-7 ± 78	0.74	nnn
HD 65987	MS:B9:M.AP	068.D-0403	52309.330	600R	738 ± 122	1.07	-327 ± 114	0.94	ddD
V391 Car	MS:A0:AP	068.D-0403	52310.180	600R	14 ± 58	0.81	-39 ± 51	0.69	nnn
V410 Car	MS:A7	068.D-0403	52309.293	600R	-93 ± 143	0.86	35 ± 139	0.81	nnn
V392 Car	MS:A2	068.D-0403	52310.180	600R	63 ± 69	0.98	125 ± 58	0.69	nnn
V392 Car	MS:A2	068.D-0403	52310.323	600R	147 ± 133	0.91	139 ± 135	0.93	nnn
V392 Car	MS:A2	272.D-5026	53072.226	600B	96 ± 80	0.70	143 ± 81	0.72	nnn
NGC 2516 SBL658	UNCLASSIFIED	068.D-0403	52309.293	600R	61 ± 370	1.07	133 ± 373	1.10	nnn
CD-60 1967	MS:B9	068.D-0403	52309.160	600R	60 ± 63	0.74	8 ± 64	0.79	-nn
CD-60 1971	MS:B8	068.D-0403	52309.160	600R	239 ± 134	0.86	16 ± 124	0.74	n-n
V417 Car	MS:A6	068.D-0403	52309.330	600R	-169 ± 87	0.77	89 ± 87	0.77	nnn
CPD-60 984	MS:A2	068.D-0403	52309.293	600R	216 ± 102	0.85	-80 ± 98	0.79	-nn
CPD-60 986	MS:A2	068.D-0403	52309.293	600R	0 ± 102	0.77	-196 ± 101	0.76	nnn
V418 Car	MS:A6	068.D-0403	52310.180	600R	69 ± 128	0.76	-46 ± 129	0.76	nnn
CPD-60 988AB	MS:B8	068.D-0403	52309.160	600R	110 ± 362	1.18	-601 ± 326	0.96	n-n
CD-60 1974	MS:A1	272.D-5026	53072.226	600B	-179 ± 105	0.76	-34 ± 103	0.74	nnn
CD-60 1974	MS:A1	068.D-0403	52310.180	600R	-251 ± 115	0.82	-242 ± 111	0.76	nnn

Table 5. continued.

Star	Classification	Prog. ID	MJD	grism	$\langle B_z \rangle$ (G)	χ^2/ν	$\langle N_z \rangle$ (G)	χ^2/ν	HmT
CD-60 1975	MS:B9	068.D-0403	52309.160	600R	73 ± 89	0.88	207 ± 89	0.88	nnn
CD-60 1976	MS:A0	068.D-0403	52309.293	600R	-135 ± 122	0.87	78 ± 112	0.77	nnn
CD-60 1978	MS:B8	068.D-0403	52309.293	600R	388 ± 171	0.98	-332 ± 157	0.80	nnn
CD-60 1979	MS:A3	068.D-0403	52310.323	600R	-233 ± 220	0.88	310 ± 240	1.06	nnn
CD-60 1981	MS:A1:AM	068.D-0403	52310.323	600R	171 ± 142	1.04	-64 ± 146	1.10	nnn
NGC 2516 DAC801	UNCLASSIFIED	068.D-0403	52309.160	600R	-62 ± 170	0.96	119 ± 165	0.90	nnn
V420 Car	MS:A3	068.D-0403	52310.180	600R	-169 ± 122	0.69	-8 ± 127	0.74	nnn
NGC 2516 SBL832	UNCLASSIFIED	068.D-0403	52309.293	600R					—
HD 66137	MS:B9	068.D-0403	52309.293	600R	-165 ± 142	1.00	-55 ± 120	0.71	nnn
HD 66194	MS:B2:P.E	068.D-0403	52309.160	600R					—
CD-60 1996	MS:A8	068.D-0403	52310.214	600R	528 ± 134	0.79	-120 ± 132	0.77	nnd
CD-60 1996	MS:A8	070.D-0352	52679.271	600R	203 ± 103	0.81	-148 ± 102	0.79	nnn
CD-60 1997	MS:F2	068.D-0403	52310.214	600R	41 ± 52	0.79	25 ± 49	0.69	nnn
CD-60 1997	MS:F2	070.D-0352	52679.271	600R	121 ± 43	0.92	-10 ± 41	0.82	nnn
CD-60 1999	MS:A2	068.D-0403	52310.214	600R	-106 ± 148	0.79	-432 ± 151	0.82	nnn
CD-60 1999	MS:A2	070.D-0352	52679.271	600R	-95 ± 155	0.81	183 ± 146	0.73	nnn
HD 66295	MS:B8:M.AP	068.D-0403	52310.214	600R	-635 ± 66	1.04	15 ± 53	0.67	DDD
HD 66295	MS:B8:M.AP	070.D-0352	52679.271	600R	492 ± 50	1.16	15 ± 42	0.86	dDD
HD 66318	MS:A0:M.AP	068.D-0403	52310.214	600R	6267 ± 89	3.65	-1 ± 38	0.78	DDD
HD 66318	MS:A0:M.AP	070.D-0352	52679.271	600R	6480 ± 91	5.87	12 ± 31	0.78	DDD
EGB5	CP	072.D-0089	52988.347	600B	-294 ± 776	1.00	-1278 ± 1017	1.13	nnn
NGC 2546 258	MS:A8:AP	073.D-0498	53275.331	600B	-164 ± 84	0.79	-92 ± 83	0.80	nnn
NGC 2546 258	MS:A8:AP	074.D-0488	53400.301	600B	3 ± 54	0.72	-148 ± 55	0.74	nnn
[N75] 195	MS:B5	074.D-0488	53400.301	600B	79 ± 57	0.77	-52 ± 53	0.66	nnn
CPD-37 1978	MS:B4	073.D-0498	53275.331	600B	82 ± 83	0.73	-55 ± 79	0.68	nnn
CPD-37 1978	MS:B4	074.D-0488	53400.301	600B	100 ± 72	0.70	-109 ± 73	0.72	nnn
[N75] 196	MS:B3	073.D-0498	53275.331	600B	268 ± 152	0.82	-292 ± 140	0.70	nnn
[N75] 196	MS:B3	074.D-0488	53400.301	600B	-28 ± 112	0.76	6 ± 108	0.70	nnn
CD-37 4353	MS:B7	074.D-0488	53399.286	600B	-132 ± 60	0.73	-64 ± 60	0.74	nnn
CD-37 4355	MS:B8.M	074.D-0488	53399.286	600B	363 ± 56	1.01	-68 ± 54	0.96	DdD
HD 68695	PM:A0	074.C-0442	53332.277	600B	-84 ± 100	0.95	30 ± 103	1.02	nnn
CPD-37 1989	MS:A2	074.D-0488	53399.286	600B	-49 ± 73	0.80	-105 ± 71	0.77	nnn
HD 68826	GS:B9:EB	075.D-0295	53454.077	1200g	106 ± 68	0.93	246 ± 68	0.93	nnn
GJ 299	MS:M4:HPM	082.D-0695	54831.374	300V	213 ± 390	0.99			-nn
HD 69003	MS:A0	073.D-0498	53275.370	600B	-38 ± 44	0.64	-23 ± 42	0.59	nnn
HD 69004	MS:B9:AP	073.D-0498	53275.370	600B	-59 ± 44	0.66	-53 ± 43	0.66	nnn
HD 69144	MS:B2:SPB	072.D-0377	52989.350	600B	83 ± 63	0.90	-19 ± 59	0.78	nnn
HD 69144	MS:B2:SPB	078.D-0140	54061.342	600B	-1 ± 65	0.98	18 ± 63	0.92	nnn
HD 69067	MS:B8:M.AP	073.D-0498	53115.979	600B	708 ± 58	1.03	-61 ± 55	0.90	DDD
HD 69067	MS:B8:M.AP	073.D-0498	53277.369	600B	453 ± 54	0.93	54 ± 53	0.90	DDD
HD 71066	MS:A0:AP?	072.D-0377	53002.097	600B	56 ± 55	0.90	45 ± 59	0.87	nnn
HD 72106A	PM:A0:M	074.C-0442	53332.296	600B	196 ± 58	0.86	-124 ± 56	0.82	nnd
HD 72106B	PM:A0:E	074.C-0442	53332.314	600B	147 ± 75	0.95	67 ± 71	0.85	nnn
HD 74169	MS:A1:AP	070.D-0352	52678.218	600B	-210 ± 43	0.90	118 ± 41	0.81	nnd
HD 74169	MS:A1:AP	272.D-5026	53066.195	600B	-147 ± 44	0.94	1 ± 43	0.89	nnd
HD 74168	MS:B9:AP	072.D-0377	53002.111	600B	-80 ± 67	0.84	13 ± 68	0.89	nnn
HD 74195	MS:B3:SPB	072.D-0377	53002.126	600B	-62 ± 59	0.91	41 ± 58	0.89	nnn
HD 74195	MS:B3:SPB	073.D-0466	53138.972	600B	97 ± 73	0.96	-194 ± 70	0.87	nnn
HD 74195	MS:B3:SPB	073.D-0466	53143.972	600B	160 ± 55	1.01	-226 ± 57	1.12	dnn
HD 74195	MS:B3:SPB	075.D-0295	53455.080	1200g	-7 ± 43	1.05	-5 ± 40	0.91	nnn
HD 74195	MS:B3:SPB	078.D-0140	54108.330	600B	-77 ± 47	0.92	-23 ± 47	0.93	nnn
HD 74196	MS:B7:HEW	072.D-0377	52906.388	600B	223 ± 132	1.04	252 ± 124	0.92	nnn
HD 74195	MS:B3:SPB	075.D-0295	53454.107	1200g	-21 ± 50	0.99	-102 ± 49	0.94	nnn
WD 0839-327	WD:DA6	070.D-0259	52608.319	600B	349 ± 249	0.85	279 ± 287	0.91	n-n
HD 74535	MS:B9:AP	070.D-0352	52678.232	600B	-110 ± 60	0.88	52 ± 58	0.82	nnn
HD 74560	MS:B3:SPB.SB	072.D-0377	53002.141	600B	249 ± 87	0.91	44 ± 85	0.87	dnn
HD 74560	MS:B3:SPB.SB	073.D-0466	53143.986	600B	-150 ± 60	1.05	-106 ± 55	0.87	nnn
HD 74560	MS:B3:SPB.SB	078.D-0140	54108.347	600B	-87 ± 56	0.88	-118 ± 57	0.90	nnn
HD 74575	GS:B1:BCEP	078.D-0140	54082.341	600B	-130 ± 64	0.90	-171 ± 67	1.00	nnn
HD 74575	GS:B1:BCEP	078.D-0140	54109.150	600B	-241 ± 73	1.07	-14 ± 64	0.85	dnd
HD 75049	MS:A0:M.AP	080.D-0170	54464.359	600B	-748 ± 68	2.45	-21 ± 36	0.72	DdD
HD 75049	MS:A0:M.AP	080.D-0170	54482.266	600B	-9240 ± 104	1.54	62 ± 75	0.82	DDD
HD 75049	MS:A0:M.AP	080.D-0170	54483.108	600B	-9622 ± 82	3.22	-80 ± 39	0.75	DDD
HD 75049	MS:A0:M.AP	080.D-0170	54493.203	600B	-1168 ± 64	2.89	-39 ± 32	0.75	DDD
HD 75049	MS:A0:M.AP	080.D-0170	54516.231	600B	-4666 ± 66	2.70	68 ± 35	0.77	DDD
HD 75049	MS:A0:M.AP	080.D-0170	54526.063	600B	-3762 ± 72	2.54	69 ± 38	0.73	DDD
HD 75049	MS:A0:M.AP	080.D-0170	54527.079	600B	-10349 ± 83	3.63	-33 ± 37	0.74	DDD

Table 5. continued.

Star	Classification	Prog. ID	MJD	grism	$\langle B_z \rangle$ (G)	χ^2/ν	$\langle N_z \rangle$ (G)	χ^2/ν	HmT
HD 75049	MS:A0:M.AP	080.D-0170	54532.221	600B	-5978 ± 78	1.76	12 ± 51	0.78	DDD
HD 75049	MS:A0:M.AP	080.D-0170	54539.269	600B	-10249 ± 89	2.66	92 ± 47	0.77	DDD
HD 75049	MS:A0:M.AP	080.D-0170	54543.073	600B	-9645 ± 84	3.34	25 ± 39	0.74	DDD
HD 75049	MS:A0:M.AP	080.D-0170	54546.020	600B	-2016 ± 75	2.06	6 ± 45	0.77	DDD
HD 75049	MS:A0:M.AP	080.D-0170	54555.029	600B	-8661 ± 78	3.83	-56 ± 34	0.75	DDD
HD 75049	MS:A0:M.AP	080.D-0170	54557.117	600B	-1979 ± 66	2.78	14 ± 35	0.78	DDD
HD 75239	MS:B9:AP	074.D-0488	53399.342	600B	-36 ± 75	0.86	-139 ± 78	0.95	nnn
NLTT 20389	WD:DC:HPM	080.D-0521	54485.193	600B					
HD 75989	MS:B9:AP	072.D-0377	52992.341	600B	-337 ± 154	0.89	120 ± 158	0.93	nnn
HD 75989	MS:B9:AP	072.D-0377	53004.284	600B	-175 ± 72	0.81	34 ± 78	0.80	nnn
HD 76534	PM:B2:E	072.C-0447	53062.222	600B	-32 ± 54	1.08	-60 ± 53	1.05	nnn
HD 76534	PM:B2:E	072.C-0447	53063.262	600B	84 ± 49	0.94	76 ± 50	1.04	nnn
HD 76431	SD:B	072.D-0290	53058.255	600B	55 ± 74	0.91	37 ± 73	0.85	nnn
WD 0859-039	WD:DA2	070.D-0259	52674.227	600B	-106 ± 790	1.16	-836 ± 770	1.11	n-n
WD 0859-039	WD:DA2	070.D-0259	52696.219	600B	-1452 ± 739	1.13	-49 ± 688	0.97	n-n
Ve 6-23	PM:OB:LPS	060.A-9203	51880.381	600R					
Ve 6-23	PM:OB:LPS	060.A-9203	54177.162	300V					
Ve 6-23	PM:OB:LPS	060.A-9203	54176.224	300I					
Ve 6-23	PM:OB:LPS	060.A-9203	53863.957	600B					
Ve 6-23	PM:OB:LPS	060.A-9203	54176.055	300I					
Ve 6-23	PM:OB:LPS	073.D-0322	53147.973	300V					
Ve 6-23	PM:OB:LPS	082.D-0695	54830.382	300V					
HD 79351	MS:B2:E	075.D-0507	53455.095	1200g	-196 ± 167	2.06	-216 ± 199	1.99	ndn
PG 0909+276	SD:B	072.D-0290	53058.139	600B	66 ± 179	1.03	-132 ± 215	1.10	nnn
SZ Hya	MS:A:RR	082.D-0342	54781.361	1200B	118 ± 51	1.16	62 ± 46	1.00	nnn
HD 80316	MS:A3:AP	072.D-0377	52992.357	600B	-249 ± 89	0.86	-162 ± 91	0.91	nnn
NLTT 21844	WD:DA7:HPM	080.D-0521	54526.087	600B	-1343 ± 2863	0.76			n-n
HD 298537	MS:A8	074.D-0488	53400.324	600B	-373 ± 165	0.71	139 ± 160	0.66	nnn
HD 83002	MS:B9:AP	074.D-0488	53400.324	600B	-24 ± 58	0.67	-98 ± 56	0.63	nnn
HD 298536	MS:A0	074.D-0488	53400.324	600B	17 ± 157	0.76	-71 ± 152	0.71	nnn
HD 83368	MS:A8:M.AP.ROAP	069.D-0210	52383.036	600B	1002 ± 29	12.11	-3 ± 9	1.19	DDD
HD 83368	MS:A8:M.AP.ROAP	069.D-0210	52383.107	600R	963 ± 56	1.92	57 ± 45	1.01	nDD
WD 0935-371A	WD:DA6	082.D-0736	54786.285	600B					
HD 83625	MS:A0:M.AP	072.D-0377	53008.323	600B	-1245 ± 77	0.97	16 ± 73	0.85	DDD
HD 84041	MS:A5:M.AP	072.D-0377	53002.170	600B	640 ± 52	1.03	-69 ± 49	0.92	DDD
HD 85567	PM:B2:E	072.C-0447	53064.229	600B	-427 ± 209	0.78	114 ± 219	0.84	n-n
HD 85567	PM:B5:E	081.C-0410	54609.012	600B	-223 ± 102	0.78	-10 ± 102	0.80	nnn
LS 1362	CP	072.D-0089	52989.309	600B	-107 ± 384	0.87	-273 ± 501	0.99	nnn
HD 85953	GS:B2:SPB	072.D-0377	53002.152	600B	48 ± 52	0.86	23 ± 52	0.88	nnn
HD 85953	GS:B2:SPB	073.D-0466	53152.971	600B	159 ± 51	0.88	45 ± 65	0.96	ndd
HD 85953	GS:B2:SPB	075.D-0295	53454.139	1200g	-57 ± 26	1.06	19 ± 24	0.91	nnn
HD 85953	GS:B2:SPB	075.D-0295	53455.113	1200g	-7 ± 29	0.94	65 ± 34	0.90	nnn
HD 85953	GS:B2:SPB	078.D-0140	54156.097	600B	13 ± 33	0.96	24 ± 32	0.92	nnn
HD 86181	MS:F0:M.AP	072.D-0377	53002.193	600B	536 ± 58	1.30	75 ± 52	1.03	DDD
HD 86199	MS:B9:M.AP	072.D-0377	53003.345	600B	-800 ± 72	0.96	-43 ± 68	0.85	DDD
WD 0958-073	SD:B	065.H-0293	51729.991	150I					
HD 87241	MS:B9:AP	073.D-0498	53134.080	600B	-7 ± 56	0.96	-21 ± 57	0.96	nnn
HD 87240	MS:B9:AP	070.D-0352	52678.302	600B	-254 ± 43	0.66	-45 ± 43	0.66	DdD
HD 87266	MS:B3	070.D-0352	52678.265	600B	20 ± 29	0.74	-1 ± 27	0.66	nnn
NGC 3114 L54	MS:B9	070.D-0352	52678.302	600B	-108 ± 73	0.70	67 ± 72	0.67	nnn
CPD-59 1698	MS:A1	070.D-0352	52678.265	600B	-9 ± 101	0.71	-129 ± 103	0.75	nnn
CPD-59 1700	MS:A3	070.D-0352	52678.302	600B	265 ± 116	0.70	85 ± 118	0.71	nnn
CPD-59 1703	MS:A0	070.D-0352	52678.265	600B	-117 ± 87	0.67	19 ± 84	0.65	nnn
HD 304841	MS:B8:M.AP	070.D-0352	52678.265	600B	-339 ± 63	0.79	-170 ± 58	0.68	ddD
NGC 3114 AR109	MS:A0	070.D-0352	52678.265	600B	-2634 ± 562	1.13	1980 ± 594	1.26	dnd
HD 304842	MS:B9:AP	070.D-0352	52678.265	600B	347 ± 91	1.10	486 ± 90	1.02	dnd
HD 87405	MS:B9:AP	070.D-0352	52678.265	600B	-66 ± 33	0.73	2 ± 31	0.67	nnn
HD 87403	PM:A1	074.C-0442	53331.339	600B	-24 ± 43	0.89	12 ± 40	0.80	nnn
HD 87752	MS:B9:HGMN	072.D-0377	53008.304	600B	35 ± 99	0.91	-90 ± 98	0.88	nnn
HD 88158	MS:B8:M.AP	072.D-0377	53008.338	600B	320 ± 67	0.90	1 ± 66	0.88	ndd
HD 88385	MS:A0:M.AP	072.D-0377	53010.181	600B	-1160 ± 55	1.28	-26 ± 43	0.78	DDD
HD 88661	MS:B2:P.E	077.D-0406	53889.996	600B	112 ± 114	0.95	-164 ± 118	0.98	nnn
WZ Hya	MS:A:RR	082.D-0342	54782.355	1200B	83 ± 45	1.41	-78 ± 41	1.20	ndn
HD 89103	MS:B9:M.AP	072.D-0377	53010.202	600B	-2136 ± 70	1.14	78 ± 62	0.91	DDD
HD 89385	MS:B9:AP	072.D-0377	53010.218	600B	-93 ± 66	1.01	-91 ± 65	0.98	nnn
HD 89856	??:B9	068.D-0403	52309.389	600R	-131 ± 88	0.81	-32 ± 82	0.74	nnn
HD 298051	MS:A1	068.D-0403	52309.389	600R	-347 ± 144	0.71	6 ± 139	0.66	nnn

Table 5. continued.

Star	Classification	Prog. ID	MJD	grism	$\langle B_z \rangle$ (G)	χ^2/ν	$\langle N_z \rangle$ (G)	χ^2/ν	HmT
10:21:01 –51:53:27	UNCLASSIFIED	068.D-0403	52309.389	600R	893 ± 427	1.13	27 ± 395	0.96	nnn
10:21:05 –51:44:07	UNCLASSIFIED	068.D-0403	52310.359	600R	-2354 ± 765	1.96	1166 ± 794	2.14	ndd
HD 89901	GS:B8	068.D-0403	52310.359	600R	40 ± 117	0.93	-79 ± 107	0.78	nnn
HD 89900	MS:A0	068.D-0403	52310.359	600R	25 ± 98	0.80	61 ± 95	0.76	nnn
10:21:16 –51:51:32	UNCLASSIFIED	068.D-0403	52309.389	600R	-110 ± 177	0.69	-10 ± 178	0.69	nnn
CPD–51 3235	UNCLASSIFIED	068.D-0403	52309.389	600R	-180 ± 103	0.86	9 ± 96	0.74	nnn
HD 89915	MS:B9	068.D-0403	52310.359	600R	-348 ± 319	0.98	-48 ± 329	1.05	nnn
NGC 3228 SC15	UNCLASSIFIED	068.D-0403	52309.389	600R	69 ± 150	0.92	18 ± 138	0.89	nnn
HD 298047	MS:B9	068.D-0403	52310.359	600R	-38 ± 86	0.89	13 ± 76	0.70	nnn
HD 89922	MS:A4	068.D-0403	52309.389	600R	-21 ± 141	0.96	17 ± 135	0.87	nnn
HD 89938	??:A	068.D-0403	52310.359	600R	160 ± 139	0.83	-80 ± 133	0.76	nnn
HD 89937	??:B6	068.D-0403	52310.359	600R	225 ± 563	3.73	-41 ± 501	2.95	nnn
HD 89956	MS:B9	068.D-0403	52310.389	600R	-879 ± 434	1.62	400 ± 445	1.68	nnn
10:21:38 –51:41:44	UNCLASSIFIED	068.D-0403	52310.359	600R	-37 ± 113	0.75	185 ± 115	0.75	nnn
CPD–51 3249	MS:A8	070.D-0352	52679.343	600B	77 ± 64	0.69	-40 ± 66	0.73	nnn
HD 298053	MS:A3:AM	070.D-0352	52679.343	600B	208 ± 38	1.01	19 ± 29	0.60	-DD
HD 298045	??:M3	070.D-0352	52679.343	600B	255 ± 120	0.83	71 ± 113	0.72	-nn
10:21:57 –51:49:06	??:K	070.D-0352	52679.343	600B	34 ± 18	0.91	-41 ± 16	0.72	-nn
HD 298054	??:G0	070.D-0352	52679.343	600B	242 ± 130	1.14	127 ± 133	1.19	nnn
HD 90264	MS:B8	071.D-0308	52824.019	600B	-65 ± 47	1.19	17 ± 40	0.95	nnn
HD 91375	MS:A2	073.D-0464	53116.028	600B	-134 ± 59	0.94	22 ± 58	0.87	nnn
HD 91239	MS:B9:AP	073.D-0464	53118.059	600B	179 ± 109	1.45	194 ± 106	1.37	nnn
HD 91465	MS:B4:E	077.D-0406	53890.044	600B	-128 ± 66	1.04	-84 ± 64	0.97	nnn
CD–34 6792	MS:F:HPM	082.D-0695	54830.376	300V	-763 ± 1187	0.86			nnn
CD–34 6792	MS:F:HPM	082.D-0695	54831.383	300V	1189 ± 1027	0.80			nnn
HD 92106	MS:A0:AP	073.D-0464	53118.080	600B	-15 ± 58	0.68	-49 ± 56	0.64	nnn
HD 92106	MS:A0:AP	072.D-0377	53010.239	600B	-170 ± 107	0.66	-33 ± 105	0.64	nnn
HD 92190	MS:B8	074.D-0488	53400.386	600B	-26 ± 57	0.92	-4 ± 55	0.85	nnn
HD 303107	MS:A0	074.D-0488	53400.386	600B	6 ± 50	0.95	-40 ± 48	0.86	nnn
HD 92287	MS:B3:SPB	072.D-0377	53008.352	600B	-556 ± 89	0.92	334 ± 89	0.92	DnD
HD 92287	MS:B3:SPB	073.D-0466	53134.028	600B	198 ± 106	1.05	-180 ± 106	1.02	nnn
HD 92385	MS:B9:M.AP	072.D-0377	53008.369	600B	-543 ± 56	0.94	-8 ± 55	0.89	DnD
HD 92385	MS:B9:M.AP	072.D-0377	53020.332	600B	-1737 ± 141	1.06	-198 ± 130	0.91	nDD
HD 92499	MS:A2:M.AP	072.D-0377	53010.255	600B	-1649 ± 80	1.86	95 ± 57	0.92	dDD
HD 92499	MS:A2:M.AP	072.D-0377	53011.212	600B	-1451 ± 74	1.51	-4 ± 57	0.90	DDD
Collinder 228 30	MS:B2	073.D-0498	53153.002	600B	601 ± 120	0.69	-158 ± 110	0.58	dDnD
HD 305451	MS:B9	073.D-0498	53153.002	600B	-213 ± 75	0.59	-166 ± 78	0.63	nnn
HD 305535	MS:B2	073.D-0498	53153.002	600B	-3 ± 56	0.66	108 ± 54	0.63	nnn
HD 93030	MS:B0:PSB	072.D-0377	53012.231	600B	-87 ± 101	0.92	245 ± 100	0.90	nnn
HD 93030	MS:B0:PSB	278.D-5056	54181.033	1200B	-18 ± 21	1.63	7 ± 18	1.09	nnn
HD 305543	GS:B1	073.D-0498	53153.002	600B	-46 ± 114	0.65	-123 ± 117	0.68	nnn
WD 1042-690	WD:DA3	070.D-0259	52668.351	600B	-342 ± 728	1.10	-795 ± 908	1.16	n-n
WD 1042-690	WD:DA3	070.D-0259	52674.273	600B	510 ± 756	1.35	1578 ± 768	0.96	n-n
WD 1042-690	WD:DA3	070.D-0259	52695.301	600B	-144 ± 586	0.96	-541 ± 731	1.02	n-n
HD 94509	PM:A0	072.C-0447	53064.266	600B	24 ± 28	1.01	-22 ± 26	0.87	nnn
HD 94509	PM:A0	272.C-5063	53110.217	600B	9 ± 22	1.19	-17 ± 20	1.00	nnn
HD 94509	PM:A0	272.C-5063	53111.999	600B	-8 ± 22	1.22	-7 ± 19	0.93	nnn
HD 94660	MS:A0:M.AP	068.D-0403	52309.365	600B	-2565 ± 61	1.77	-25 ± 46	1.01	DDD
HD 94660	MS:A0:M.AP	068.D-0403	52309.375	600R	-2905 ± 56	1.12	6 ± 33	0.41	DDD
HD 94660	MS:A0:M.AP	070.D-0352	52678.404	600B	-2653 ± 62	1.99	36 ± 42	0.97	DDD
HD 94660	MS:A0:M.AP	072.C-0447	53062.261	600B	-2616 ± 63	1.81	32 ± 46	0.97	DDD
HD 94660	MS:A0:M.AP	072.C-0447	53062.272	600B	-2317 ± 76	1.61	-201 ± 59	0.98	DDD
HD 94660	MS:A0:M.AP	082.D-0342	54782.376	1200B	-2389 ± 51	4.20	-29 ± 31	1.07	DDD
HD 94660	MS:A0:M.AP	082.D-0342	54782.381	1200B	-2061 ± 50	2.82	9 ± 30	1.04	DDD
HD 94660	MS:A0:M.AP	060.A-9203	51991.001	600B	-1980 ± 49	1.23	41 ± 39	0.76	DDD
HD 94660	MS:A0:M.AP	060.A-9203	54181.147	1200B	-1978 ± 34	3.44	-22 ± 20	1.28	DDD
HD 94660	MS:A0:M.AP	060.A-9203	54181.161	600B	-1961 ± 59	1.90	-86 ± 42	1.00	DDD
HD 94660	MS:A0:M.AP	069.D-0210	52383.122	600B	-2653 ± 58	3.11	49 ± 33	1.01	DDD
HD 94660	MS:A0:M.AP	069.D-0210	52383.129	600R	-3262 ± 76	4.30	67 ± 35	0.95	DDD
HD 94660	MS:A0:M.AP	074.C-0442	53332.361	600B	-2528 ± 61	2.78	46 ± 38	1.07	DDD
HD 94660	MS:A0:M.AP	074.C-0442	53332.374	1200g	-2520 ± 38	9.71	-11 ± 13	1.14	DDD
HD 94660	MS:A0:M.AP	074.D-0488	53400.398	600B	-2488 ± 57	2.29	-23 ± 34	0.85	DDD
HD 94660	MS:A0:M.AP	079.D-0697	54311.976	1200B	-2007 ± 146	1.04	-101 ± 175	1.02	DDD
HD 94660	MS:A0:M.AP	081.D-0670	54692.975	1200B	-2029 ± 41	4.55	-33 ± 19	1.02	DDD
HD 94660	MS:A0:M.AP	081.D-0670	54693.969	1200B	-2110 ± 49	2.59	44 ± 29	0.96	DDD

Table 5. continued.

Star	Classification	Prog. ID	MJD	grism	$\langle B_z \rangle$ (G)	χ^2/ν	$\langle N_z \rangle$ (G)	χ^2/ν	HmT
WD 1054-226	WD:DA6:HPM	080.D-0521	54532.264	600B	-3444 ± 1589	0.72			n-n
HD 95881	PM:A1	072.C-0447	53064.292	600B	-39 ± 48	0.86	29 ± 50	0.92	nnn
HD 95881	PM:A1	081.C-0410	54609.993	600B	-101 ± 29	0.84	-31 ± 28	0.79	nnd
HD 96042	PM:B1:E	074.C-0442	53330.367	600B	139 ± 84	0.93	17 ± 82	0.88	nnn
HD 96040	MS:A0:M.AP	074.D-0488	53399.370	600B	-324 ± 51	1.05	25 ± 49	0.99	DdD
HD 96451	MS:A0:AP	073.D-0464	53074.340	600B	2 ± 36	0.91	-67 ± 35	0.90	nnn
HD 96441	MS:A1	060.A-9203	51993.053	600B	-58 ± 69	0.87	4 ± 83	0.86	nnn
HD 96441	MS:A1	079.D-0697	54311.985	1200B	-376 ± 252	1.02	64 ± 303	1.05	nnn
HD 96441	MS:A1	272.C-5063	53112.086	600B	-88 ± 39	0.97	-55 ± 37	0.88	dnn
HD 96441	MS:A1	060.A-9203	51993.012	600B	103 ± 59	0.87	-16 ± 59	0.86	nnn
HD 96653	GS:A0	073.D-0498	53260.995	600B	96 ± 37	0.59	62 ± 37	0.61	nnn
CPD-58 3151	?:G1	073.D-0498	53260.995	600B	-12 ± 51	0.57	8 ± 48	0.51	nnn
HD 96685	MS:B8:E	073.D-0498	53260.995	600B	1 ± 74	0.48	-50 ± 75	0.50	nnn
HD 96729	MS:B9:M.AP	073.D-0498	53260.995	600B	1057 ± 51	0.62	5 ± 47	0.53	DDD
HD 96790	MS:A5	073.D-0498	53260.995	600B	-179 ± 86	0.52	149 ± 83	0.50	nnn
WD 1105-048	WD:DA3	070.D-0259	52641.351	600B	-36 ± 563	0.96	-1031 ± 557	0.94	n-n
WD 1105-048	WD:DA3	070.D-0259	52669.305	600B	3240 ± 646	1.04	-906 ± 648	1.05	D-D
HD 97048	PM:A0:P.SH.E	072.C-0447	53064.323	600B	-129 ± 58	0.97	58 ± 56	0.95	dnn
HD 97048	PM:A0:P.SH.E	074.C-0442	53331.370	600B	-157 ± 85	1.04	73 ± 81	0.95	nnn
HD 97048	PM:A0:P.SH.E	081.C-0410	54609.138	600B	114 ± 63	0.79	123 ± 78	0.79	nnn
HD 97048	PM:A0:P.SH.E	272.C-5063	53110.163	600B	52 ± 61	1.04	-37 ± 64	1.15	nnn
HD 97048	PM:A0:P.SH.E	272.C-5063	53110.188	600B	287 ± 423	1.06	22 ± 438	1.14	nnn
HD 97048	PM:A0:P.SH.E	272.C-5063	53112.047	600B	15 ± 57	1.16	-1 ± 51	0.93	nnn
HD 97048	PM:A0:P.SH.E	272.C-5063	53114.129	600B	-548 ± 172	1.09	-52 ± 162	0.97	dnd
HD 97048	PM:A0:P.SH.E	272.C-5063	53115.131	600B	301 ± 233	1.10			nnn
HD 97048	PM:A0:P.SH.E	272.C-5063	53116.003	600B	-99 ± 52	0.95	44 ± 50	0.90	nnn
HD 303821	MS:A3:AP	074.D-0488	53400.358	600B	-71 ± 66	0.98	230 ± 63	0.88	nnn
HD 97300	PM:B9	081.C-0410	54609.047	600B	91 ± 65	0.85	-91 ± 77	0.79	nnn
HD 97689	MS:A0:AM	073.D-0322	53149.976	300V	368 ± 466	0.79	661 ± 517	1.01	nnn
HD 98340	MS:B9:M.AP	073.D-0464	53074.362	600B	1023 ± 75	0.96	-139 ± 78	1.03	DDD
HD 98922	PM:B9:E	072.C-0447	53064.341	600B	14 ± 90	0.97	102 ± 85	0.85	nnn
HD 99563	MS:F0:M.AP.ROAP	072.D-0377	53012.246	600B	-446 ± 83	0.93	120 ± 82	0.90	nDD
HD 99563	MS:F0:M.AP.ROAP	072.D-0377	53015.225	600B	-561 ± 99	0.98	8 ± 96	0.93	ddD
HD 99563	MS:F0:M.AP.ROAP	269.D-5044	52493.989	600B	-517 ± 192	1.02	-162 ± 182	0.92	nnn
HD 100453	PM:A9:E	074.C-0442	53332.347	600B	37 ± 52	0.83	-36 ± 52	0.84	nnn
HD 100453	PM:A9:E	081.C-0410	54610.022	600B	-8 ± 19	0.82	-16 ± 18	0.75	nnn
HD 100546	PM:B9:E	072.C-0447	53064.356	600B	277 ± 111	1.03	333 ± 114	1.08	nnn
HD 100546	PM:B9:E	081.C-0410	54610.044	600B	-64 ± 42	0.81	-49 ± 52	1.06	n-n
HD 306793	MS:B2:E	080.D-0383	54550.261	600B	-53 ± 61	0.77	43 ± 72	0.78	nnn
CPD-60 3088	MS:B2:HES	080.D-0383	54549.245	600B	-10 ± 47	0.78	-30 ± 57	0.78	nnn
HD 306795	MS:B2:M.HEW	080.D-0383	54550.187	600B	1644 ± 39	0.72	-56 ± 47	0.79	DDD
CPD-60 3098	MS:B2	080.D-0383	54550.187	600B	412 ± 275	0.90	475 ± 352	0.97	nnn
CPD-60 3117	?:F	080.D-0383	54550.375	600B	164 ± 242	0.98	-379 ± 303	1.01	nnn
HD 306797	MS:B4:E	080.D-0383	54550.375	600B	-1 ± 51	0.74	-16 ± 60	0.77	nnn
CPD-60 3120	MS:B3	080.D-0383	54550.067	600B	-63 ± 53	0.71	-9 ± 65	0.73	dnn
CPD-60 3125	MS:B2:E	080.D-0383	54550.017	600B	-155 ± 66	0.76	174 ± 83	0.78	nnn
HD 306798	MS:B2:E	080.D-0383	54549.151	600B	21 ± 38	0.78	45 ± 45	0.74	nnn
11:36:11 -61:34:23	MS:B4	080.D-0383	54549.116	600B	-811 ± 721	1.26	1441 ± 855	1.14	nnn
CPD-60 3128	MS:B2:E	080.D-0383	54549.116	600B	-51 ± 35	0.80	15 ± 42	0.78	nnn
CPD-60 3131	MS:B9	080.D-0383	54549.116	600B	-207 ± 442	0.92	-22 ± 561	1.02	nnn
CD-60 3626	MS:B2:E	080.D-0383	54549.194	600B	1 ± 65	0.97	-51 ± 78	1.00	nnn
CPD-60 3134	MS:B2:HES	080.D-0383	54549.304	600B	-7 ± 45	0.77	-4 ± 55	0.79	nnn
CD-60 3629	MS:B2	080.D-0383	54549.349	600B	-55 ± 31	0.77	11 ± 38	0.81	ndn
CPD-60 3143	MS:B2	080.D-0383	54550.127	600B	0 ± 40	0.81	-91 ± 47	0.77	nnn
HD 306791	MS:B2:E	080.D-0383	54549.021	600B	-111 ± 61	0.74	-59 ± 64	0.81	nnn
CPD-60 3174	MS:B3:HES	080.D-0383	54550.327	600B	211 ± 76	0.83	-29 ± 90	0.81	dnn
HD 100989	MS:B2	080.D-0383	54549.379	600B	9 ± 40	0.81	-24 ± 46	0.73	nnn
HD 101065	MS:F:M.AP.ROAP	069.D-0210	52383.198	600B	-1458 ± 97	74.27	-8 ± 11	0.90	DDD
HD 101065	MS:F:M.AP.ROAP	069.D-0210	52383.260	600R	-1472 ± 64	7.81	2 ± 23	1.01	dDD
HD 101065	MS:F:M.AP.ROAP	079.D-0240	54197.342	600B	-1503 ± 112	5.59	92 ± 42	0.80	dDD
HD 101065	MS:F:M.AP.ROAP	079.D-0240	54209.266	600B	-1255 ± 55	5.59	-6 ± 20	0.73	DDD
HD 101065	MS:F:M.AP.ROAP	079.D-0240	54222.098	600B	-1232 ± 53	8.19	5 ± 16	0.73	DDD
HD 101065	MS:F:M.AP.ROAP	079.D-0240	54232.996	600B	-1237 ± 54	6.54	23 ± 18	0.74	DDD
HD 101065	MS:F:M.AP.ROAP	079.D-0240	54246.985	600B	-1239 ± 57	7.70	-2 ± 18	0.76	DDD
HD 101065	MS:F:M.AP.ROAP	079.D-0240	54254.082	600B	-1264 ± 59	4.62	2 ± 23	0.73	DDD
HD 101065	MS:F:M.AP.ROAP	079.D-0240	54272.028	600B	-1209 ± 53	8.22	28 ± 16	0.74	DDD
HD 101065	MS:F:M.AP.ROAP	079.D-0240	54280.979	600B	-1230 ± 55	5.48	-3 ± 20	0.76	DDD

Table 5. continued.

Star	Classification	Prog. ID	MJD	grism	$\langle B_z \rangle$ (G)	χ^2/ν	$\langle N_z \rangle$ (G)	χ^2/ν	HmT
HD 101065	MS:F:M.AP.ROAP	079.D-0240	54297.033	600B	-1210 ± 55	6.56	-40 ± 19	0.77	DDD
HD 101065	MS:F:M.AP.ROAP	079.D-0240	54306.048	600B	-1184 ± 58	4.17	-24 ± 24	0.73	DDD
HD 101065	MS:F:M.AP.ROAP	270.D-5023	52701.247	600B	-1362 ± 96	120.10	-4 ± 8	0.90	dDD
HD 101412	PM:B9:M	072.C-0447	53062.299	600B	433 ± 163	0.97	-106 ± 164	0.99	dnn
HD 101412	PM:B9:M	081.C-0410	54609.190	600B	-420 ± 41	0.83	-14 ± 41	0.85	DnD
HD 101412	PM:B9:M	081.C-0410	54610.084	600B	-334 ± 38	0.82	33 ± 37	0.83	DnD
WD 1143-013	WD:DA8:HPM	080.D-0521	54554.306	600B	-5761 ± 2676	0.88			n-n
WD 1145-451	WD:DA8:HPM	080.D-0521	54532.241	600B	5874 ± 2714	0.48			n-n
HD 102647	MS:A3:CSD	074.C-0463	53353.366	1200g	72 ± 47	0.98	33 ± 45	0.87	nnn
HD 102647	MS:A3:CSD	074.C-0463	53403.374	1200g	-90 ± 52	0.93	-26 ± 51	0.89	nnn
NLTT 28730	WD:DA6:HPM	080.D-0521	54553.325	600B	1288 ± 2238	0.82			n-n
NLTT 28730	WD:DA6:HPM	080.D-0521	54555.268	600B	2228 ± 2075	0.80			n-n
CD-22 9142	SD:O	073.D-0356	53134.112	600B	956 ± 372	0.94	351 ± 417	0.93	nnn
CD-22 9142	SD:O	073.D-0356	53144.110	600B	23 ± 588	1.06	1387 ± 631	0.96	nnn
HD 104237	PM:A4:M.P.E	072.C-0447	53063.316	600B	102 ± 73	0.97	-51 ± 70	0.92	nnn
HD 104237	PM:A4:M.P.E	072.C-0447	53064.375	600B	-76 ± 62	0.97	38 ± 69	0.98	nnn
HD 104237	PM:A4:M.P.E	074.C-0442	53332.332	600B	79 ± 62	1.03	-7 ± 58	0.92	nnn
HD 104321	MS:A5:SB	074.C-0463	53385.380	1200g	62 ± 26	1.01	3 ± 28	0.92	nnn
WD 1202-232	WD:D6	073.D-0356	53144.146	600B	-687 ± 517	1.12	710 ± 501	1.05	n-n
WD 1202-232	WD:D6	073.D-0356	53147.179	600B	-185 ± 344	0.93	-602 ± 362	1.06	n-n
WD 1202-232	WD:D6	073.D-0356	53150.997	600B	-64 ± 369	0.94	197 ± 379	0.97	n-n
HD 105379	MS:A0:AP	072.D-0377	53011.250	600B	-17 ± 67	0.93	31 ± 68	0.94	nnn
HD 105382	GS:B6:M.HEW	072.D-0377	53011.195	600B	-1114 ± 94	0.87	117 ± 98	0.96	DDD
HD 105382	GS:B6	073.D-0466	53220.016	600B	0 ± 93	0.89			nnn
HD 105382	GS:B6:M.HEW	072.D-0377	53015.246	600B	-721 ± 175	0.93	-270 ± 211	0.94	dnd
HD 105382	GS:B6:M.HEW	073.D-0466	53144.003	600B	-24 ± 66	0.90	-279 ± 83	0.97	nnn
HD 105382	GS:B6:M.HEW	073.D-0466	53224.990	600B	-945 ± 253	1.32	10 ± 246	1.24	dnd
HD 105435	MS:B2:E	075.D-0507	53475.129	1200g	-142 ± 111	0.92	-171 ± 116	1.00	nnn
HD 105435	MS:B2:E	077.D-0406	53869.232	600B	-60 ± 47	0.98	-6 ± 50	1.10	nnn
HD 105770	MS:B9:M.AP	072.D-0377	53011.233	600B	437 ± 96	0.99	75 ± 88	0.84	dnd
HD 105770	MS:B9:M.AP	073.D-0464	53120.145	600B	244 ± 65	0.90	-64 ± 67	0.94	dnd
HD 105999	MS:F1:AP	072.D-0377	53011.270	600B	-32 ± 83	0.86	76 ± 83	0.87	nnn
WD 1209-060	WD:DA8	080.D-0521	54555.305	600B	5253 ± 2882	0.65			n-n
HD 107696	MS:B8:AP	071.D-0308	52824.030	600B	-9 ± 107	0.90	-165 ± 101	0.80	nnn
HD 107696	MS:B8:AP	073.D-0464	53074.375	600B	547 ± 457	1.14	-475 ± 470	1.20	nnn
HD 107969	CP	075.D-0289	53525.093	600B	-431 ± 398	1.10	292 ± 393	1.10	nnn
HD 107969	CP	075.D-0289	53526.072	600B	149 ± 292	1.13	335 ± 297	0.96	nnn
HD 107969	CP	075.D-0289	53527.053	600B	651 ± 345	0.97	374 ± 333	0.89	nnn
HD 108945	MS:A3:M.AP	072.D-0377	53015.335	600B	-55 ± 87	0.97	115 ± 85	0.93	nnn
HD 109085	MS:F2:CSD	074.C-0463	53405.328	1200g	-5 ± 15	0.88	-6 ± 14	0.80	nnn
GJ 473 A	MS:M5:FLS	082.D-0695	54831.365	300V					—
HD 109573	MS:A0:CSD	081.C-0410	54610.116	600B	-7 ± 36	0.77	7 ± 36	0.77	nnn
NLTT 31483	WD:DA9:HPM	080.D-0521	54556.282	600B					—
HD 111123	GS:B0:BCEP	075.D-0295	53455.151	1200g	46 ± 26	1.11	-40 ± 30	0.94	nnn
BS Cru	MS:B1:BCEP	078.D-0140	54155.209	600B	14 ± 96	0.97	-69 ± 94	0.94	nnn
BS Cru	MS:B1:BCEP	078.D-0140	54157.202	600B	81 ± 54	0.87	22 ± 56	0.95	nnn
HD 112244	SG:O8	075.D-0432	53455.190	600B	38 ± 48	1.07	-90 ± 47	0.90	nnn
HD 112244	SG:O8	075.D-0432	53475.174	600B	67 ± 78	1.13	-46 ± 71	0.75	nnn
HD 112244	SG:O8	075.D-0432	53483.104	600B	199 ± 76	0.90	106 ± 70	0.76	nnn
HD 114365	MS:A0:AP	071.D-0308	52824.043	600B	88 ± 68	0.89	-128 ± 84	0.83	nnn
HD 115226	MS:A3:M.AP	073.D-0464	53086.299	600B	703 ± 40	1.23	1 ± 34	0.87	DDD
HD 115226	MS:A3:M.AP	073.D-0464	53074.389	600B	936 ± 203	0.85			ndd
WD 1316-215	WD:DA8:HPM	080.D-0521	54534.384	600B					—
HD 115440	MS:B9:M.AP	073.D-0464	53077.213	600B	3251 ± 56	1.84	12 ± 43	0.89	DDD
HD 115892	MS:A2:CSD	074.C-0463	53405.347	1200g	-54 ± 27	1.24	-29 ± 26	1.11	nnn
HD 116890	MS:B9:AP	071.D-0308	52824.055	600B	-361 ± 66	0.90	101 ± 65	0.88	dDD
HD 117025	MS:A2:M.AP	071.D-0308	52824.067	600B	603 ± 59	1.10	125 ± 55	0.94	dDD
HD 117025	MS:A2:M.AP	073.D-0464	53120.164	600B	728 ± 54	1.57	-92 ± 41	0.93	DDD
WD 1327-083	WD:DA4	073.D-0356	53151.033	600B	-365 ± 467	1.03	-65 ± 584	1.08	n-n
WD 1327-083	WD:DA4	073.D-0356	53153.068	600B	-402 ± 451	0.96	-63 ± 597	1.04	n-n
HD 117555	SG:G5:M.FKCOM	280.D-5075	54568.212	600B	192 ± 24	1.57	28 ± 22	1.36	dDD
HD 117555	SG:G5:M.FKCOM	280.D-5075	54569.231	600B	24 ± 18	0.84	14 ± 17	0.74	nnn
HD 117555	SG:G5:M.FKCOM	280.D-5075	54571.286	600B	138 ± 21	0.84	39 ± 22	0.75	dDD
HD 117555	SG:G5:M.FKCOM	280.D-5075	54575.209	600B	233 ± 20	0.87	10 ± 21	0.73	dDD
HD 117555	SG:G5:M.FKCOM	280.D-5075	54576.131	600B	91 ± 18	0.79	-16 ± 19	0.74	ndd
HD 117555	SG:G5:M.FKCOM	280.D-5075	54577.177	600B	151 ± 22	0.81	3 ± 23	0.77	nDD
HD 117555	SG:G5:M.FKCOM	280.D-5075	54578.165	600B	190 ± 29	0.77	-57 ± 33	0.75	nDD

Table 5. continued.

Star	Classification	Prog. ID	MJD	grism	$\langle B_z \rangle$ (G)	χ^2/ν	$\langle N_z \rangle$ (G)	χ^2/ν	HmT
HD 117555	SG:G5:M.FKCOM	280.D-5075	54579.205	600B	100 \pm 24	0.78	-65 \pm 26	0.76	ndd
HD 117555	SG:G5:M.FKCOM	280.D-5075	54582.186	600B	174 \pm 19	0.80	37 \pm 20	0.74	nDD
HD 117357	GS:B0:E	075.D-0507	53507.995	1200g	125 \pm 104	0.99	-85 \pm 131	1.00	nnn
07:09:18 -32:04:30	??:G	073.D-0516	53134.050	600B					—
07:09:18 -32:04:30	??:G	073.D-0516	53137.010	600B					—
PN A66 36	CP	072.D-0089	53031.287	600B	144 \pm 477	1.04	1642 \pm 502	0.91	nnn
PN A66 36	CP	075.D-0289	53525.004	600B	-35 \pm 160	0.98	-425 \pm 161	1.00	nnn
PN A66 36	CP	075.D-0289	53525.972	600B	198 \pm 213	0.99	-336 \pm 249	0.95	nnn
PN A66 36	CP	075.D-0289	53526.973	600B	258 \pm 224	0.98	-267 \pm 264	0.86	nnn
HD 118913	MS:A0:M.AP	071.D-0308	52824.081	600B	-263 \pm 62	0.94	-88 \pm 59	0.84	dnd
HD 118913	MS:A0:M.AP	073.D-0464	53120.181	600B	-516 \pm 32	1.46	-3 \pm 26	0.95	DDD
HD 119308	MS:A0:M.AP	073.D-0464	53120.204	600B	-293 \pm 48	1.13	13 \pm 41	0.85	dDD
HD 120324	MS:B2:P.E	075.D-0507	53455.222	1200g	286 \pm 342	1.28	-299 \pm 451	1.32	nnn
HD 120324	MS:B2:P.E	077.D-0406	53869.296	600B	-69 \pm 21	0.82	-22 \pm 21	0.75	ndd
HD 120709	MS:B5:PGA	072.D-0377	53015.323	600B	118 \pm 83	0.90	-1 \pm 83	0.95	nnn
CD-46 8926	SD:O	072.D-0290	53058.347	600B	-92 \pm 146	1.16	-14 \pm 155	1.18	nnn
HD 120991	GS:B2:E	075.D-0507	53512.056	1200g	-85 \pm 190	1.65	-71 \pm 192	1.70	-nn
HD 122970	MS:F0:M.AP.ROAP	072.D-0377	53015.350	600B	354 \pm 89	1.03	-130 \pm 84	0.92	ndd
HD 122970	MS:F0:M.AP.ROAP	269.D-5044	52494.006	600B	326 \pm 53	1.03	32 \pm 49	0.88	ddD
CD-47 8861	??:G	073.D-0498	53220.043	600B	-44 \pm 32	0.64	-54 \pm 29	0.53	-nn
CD-47 8868	MS:A0	073.D-0498	53220.043	600B	-24 \pm 66	0.51	54 \pm 64	0.47	nnn
HD 122983	MS:B9	073.D-0498	53220.043	600B	186 \pm 40	0.54	79 \pm 39	0.51	dnd
NGC 5460 73	??:K5	073.D-0498	53199.023	600B	71 \pm 39	0.51	96 \pm 38	0.49	-nn
HD 123183	MS:A0	073.D-0498	53199.023	600B	-470 \pm 112	0.54	71 \pm 108	0.50	dnd
HD 123201B	MS:B9	073.D-0498	53199.023	600B	-70 \pm 70	0.49	92 \pm 71	0.51	nnn
HD 123225	MS:B8	073.D-0498	53199.023	600B	127 \pm 65	0.58	-42 \pm 60	0.49	nnn
HD 123515	MS:B9:SPB	071.D-0308	52824.093	600B	-80 \pm 69	0.87	88 \pm 83	0.87	nnn
HD 123515	MS:B9:SPB	075.D-0295	53454.179	1200g	-47 \pm 28	1.04	13 \pm 26	0.91	nnn
HD 125630	MS:A2:M.AP	071.D-0308	52824.107	600B	735 \pm 52	1.02	103 \pm 49	0.90	DDD
HD 125630	MS:A2:M.AP	073.D-0464	53120.221	600B	73 \pm 44	0.98	-44 \pm 43	0.94	nnn
HD 127493	SD:O	075.D-0352	53571.047	600B	138 \pm 166	0.87	-302 \pm 198	0.95	nnn
WD 1425-811	WD:DA6	073.D-0516	53137.044	600B	440 \pm 1351	1.11	33 \pm 1333	1.08	n-n
HD 127453	MS:B8:M.AP	071.D-0308	52824.121	600B	-261 \pm 72	0.90	-37 \pm 70	0.85	dnd
HD 127753	GS:K5	070.D-0352	52678.328	600B	43 \pm 18	0.91	10 \pm 15	0.68	-nn
CPD-56 6330	MS:A2	070.D-0352	52678.328	600B	85 \pm 252	0.72	317 \pm 255	0.74	nnn
CPD-56 6330	MS:A2	070.D-0352	52678.349	600B	-200 \pm 91	0.77	136 \pm 87	0.72	ndn
HD 127972	MS:B1:E	075.D-0507	53475.222	1200g	-63 \pm 45	0.58	-27 \pm 47	0.48	nnn
HD 127973	MS:B1:E	077.D-0406	53862.327	600B	2 \pm 18	0.84	-12 \pm 16	0.71	nnn
HD 127835	MS:B8	070.D-0352	52678.378	600B	101 \pm 70	0.75	-63 \pm 64	0.63	nnn
CPD-56 6334	MS:B9	070.D-0352	52678.328	600B	-266 \pm 248	0.67	525 \pm 264	0.75	nnn
CPD-56 6334	MS:B9	070.D-0352	52678.349	600B	99 \pm 93	0.73	50 \pm 93	0.74	nnn
HD 127575	MS:B9:M.AP	073.D-0464	53079.388	600B	869 \pm 56	1.05	-74 \pm 53	0.93	DDD
NGC 5662 118	MS:K5	070.D-0352	52678.349	600B	-25 \pm 35	0.72	-47 \pm 33	0.65	-nn
NGC 5662 126	MS:A1	070.D-0352	52678.328	600B	474 \pm 322	0.72	-207 \pm 317	0.70	nnn
NGC 5662 126	MS:A1	070.D-0352	52678.349	600B	223 \pm 99	0.75	27 \pm 99	0.76	nnn
HD 127866	GS:B8	070.D-0352	52678.328	600B	-226 \pm 97	0.65	-37 \pm 101	0.69	nnn
HD 127866	GS:B8	070.D-0352	52678.349	600B	75 \pm 204	0.90	-71 \pm 187	0.75	nnn
CSI-56-14322	MS:A8	070.D-0352	52678.378	600B	521 \pm 207	0.70	162 \pm 195	0.63	dnn
NGC 5662 CLB149	??:K	070.D-0352	52678.378	600B	141 \pm 65	0.77	21 \pm 62	0.70	-nn
NGC 5662 CLB137	MS:A8	070.D-0352	52678.378	600B	-510 \pm 323	0.76	-24 \pm 322	0.76	nnn
HD 127900	GS:B8	070.D-0352	52678.378	600B	16 \pm 43	0.65	-132 \pm 44	0.68	nnn
HD 127924	MS:B8	070.D-0352	52678.378	600B	46 \pm 68	0.68	-62 \pm 67	0.65	nnn
HD 128585	MS:B3:SPB	079.D-0241	54344.981	600B	48 \pm 59	0.76	20 \pm 61	0.80	nnn
HD 128775	MS:B9:M.AP	073.D-0464	53120.236	600B	-311 \pm 54	1.43	-26 \pm 45	1.02	ddD
HD 128974	MS:A0:AP	071.D-0308	52824.144	600B	-46 \pm 52	0.86	16 \pm 54	0.95	nnn
HD 128898	MS:A7:M.AP.ROAP	069.D-0210	52383.300	600B	-311 \pm 27	3.92	1 \pm 15	1.21	DDD
HD 128898	MS:A7:M.AP.ROAP	069.D-0210	52383.325	600R	-436 \pm 107	1.20	-67 \pm 103	1.10	ndd
HD 129557	GS:B3:BCEP	078.D-0140	54158.228	600B	25 \pm 37	0.96	13 \pm 38	0.88	nnn
HD 129929	MS:B2:BCEP	075.D-0295	53572.053	1200g	-46 \pm 38	0.99	-38 \pm 37	0.93	nnn
HD 129929	MS:B2:BCEP	078.D-0140	54177.217	600B	52 \pm 63	0.98	-23 \pm 64	0.84	nnn
HD 129929	MS:B2:BCEP	079.D-0241	54343.980	600B	-29 \pm 33	0.76	6 \pm 38	0.72	nnn
HD 130158	MS:B9:AP	071.D-0308	52824.176	600B	4 \pm 65	0.96	-107 \pm 66	0.82	nnn
HD 130158	MS:B9:AP	073.D-0464	53116.312	600B	1 \pm 46	1.02	66 \pm 55	1.00	nnn
NLT 38356	WD:DA7:HPM	080.D-0521	54556.356	600B	1107 \pm 2255	1.00	1640 \pm 2301	1.03	n-n
HD 130557	MS:B9:AP	071.D-0308	52853.058	600B	-39 \pm 62	0.84	20 \pm 61	0.84	nnn
HD 130557	MS:B9:AP	073.D-0464	53144.267	600B	-26 \pm 42	0.98	-98 \pm 44	1.06	nnn
HD 129899	MS:A0:M.AP	073.D-0464	53120.295	600B	579 \pm 39	1.15	41 \pm 35	0.92	DDD

Table 5. continued.

Star	Classification	Prog. ID	MJD	grism	$\langle B_z \rangle$ (G)	χ^2/ν	$\langle N_z \rangle$ (G)	χ^2/ν	HmT
HD 131120	MS:B7:HEW	071.D-0308	52824.160	600B	-57 ± 118	0.99	-35 ± 119	1.00	nnn
HD 131120	MS:B7:HEW	072.D-0377	53020.357	600B	46 ± 50	0.78	-82 ± 51	0.82	nnn
HD 131120	MS:B7:HEW	072.D-0377	53030.366	600B	148 ± 109	0.85	-84 ± 134	0.86	nnn
HD 131120	MS:B7:HEW	073.D-0466	53225.027	600B	83 ± 50	0.97	-61 ± 47	0.88	nnn
HD 131120	MS:B7:HEW	073.D-0466	53234.102	600B	-54 ± 86	1.50	-7 ± 90	1.61	nnn
HD 131058	MS:B3:SPB	075.D-0295	53454.220	1200g	-99 ± 57	1.09	-94 ± 54	0.97	nnn
HD 132200	MS:B2:BCEP	079.D-0241	54343.994	600B	-62 ± 62	0.77	-200 ± 80	0.78	nnn
HD 132322	MS:A7:M.AP	073.D-0464	53111.311	600B	393 ± 33	1.79	8 ± 25	1.05	dDD
HD 132947	PM:A0	072.C-0447	53064.419	600B	329 ± 116	1.23	-316 ± 117	1.25	nnn
HD 13405	MS:A6:M.AP	073.D-0464	53144.301	600B	319 ± 36	1.13	-30 ± 33	0.95	nDD
HD 133792	MS:A0:AP	071.D-0308	52853.070	600B	89 ± 55	0.86	-82 ± 54	0.81	nnn
HD 133792	MS:A0:AP	073.D-0464	53120.312	600B	66 ± 36	1.17	-16 ± 31	0.87	nnn
HD 135344B	PM:F8:CSD	081.C-0410	54609.243	600B	-14 ± 17	0.79	16 ± 17	0.75	nnn
HD 135344B	PM:F8:CSD	081.C-0410	54610.144	600B	1 ± 17	0.83	-29 ± 16	0.75	nnn
HD 135240	GS:O7	075.D-0432	53475.243	600B	11 ± 70	0.97	-42 ± 66	0.85	nnn
HD 135240	GS:O7	075.D-0432	53487.263	600B	-15 ± 61	0.99	17 ± 59	0.93	nnn
HD 135240	GS:O7	075.D-0432	53553.103	600B	-74 ± 65	0.93	140 ± 64	0.90	nnn
HD 135591	GS:O7	075.D-0432	53487.242	600B	-44 ± 53	1.07	14 ± 50	0.97	nnn
HD 135591	GS:O7	075.D-0432	53553.081	600B	4 ± 55	1.08	49 ± 57	1.05	nnn
HD 135591	GS:O7	075.D-0432	53571.066	600B	37 ± 107	0.77	109 ± 112	0.84	nnn
HD 135591	GS:O7	075.D-0432	53571.081	600B	38 ± 65	0.97	-6 ± 67	0.99	nnn
NLTT 40020	MS:G5:HPM	080.D-0521	54555.342	600B	919 ± 896	0.74			nnn
HD 136504	MS:B2:M.BCEP.SB	079.D-0241	54344.999	600B	-137 ± 38	0.80	79 ± 45	0.73	nnd
HD 136933	MS:A0:AP	071.D-0308	52823.220	600B	-186 ± 61	0.96	-23 ± 64	0.95	ndd
HD 137432	MS:B4:E	075.D-0507	53532.162	1200g	-101 ± 47	1.86	-39 ± 47	1.83	nnn
HD 137949	MS:F3:M.AP.ROAP	069.D-0210	52383.370	600B	2682 ± 69	38.86	19 ± 11	1.00	DDD
HD 137949	MS:F3:M.AP.ROAP	069.D-0210	52383.408	600R	2871 ± 64	7.07	18 ± 24	1.01	DDD
HD 137949	MS:F3:M.AP.ROAP	079.D-0240	54209.285	600B	2502 ± 40	3.81	63 ± 18	0.78	DDD
HD 137949	MS:F3:M.AP.ROAP	079.D-0240	54230.282	600B	2342 ± 78	4.16	91 ± 35	0.85	DDD
HD 137949	MS:F3:M.AP.ROAP	079.D-0240	54272.049	600B	2457 ± 41	3.59	-14 ± 19	0.76	DDD
HD 137949	MS:F3:M.AP.ROAP	079.D-0240	54280.997	600B	2512 ± 44	2.79	-25 ± 23	0.77	DDD
HD 137949	MS:F3:M.AP.ROAP	079.D-0240	54308.016	600B	2417 ± 41	3.53	12 ± 19	0.74	DDD
HD 138764	MS:B6:SPB	072.D-0377	52904.016	600B	169 ± 81	0.84	-28 ± 83	0.88	nnn
HD 138764	MS:B6:SPB	075.D-0295	53454.234	1200g	11 ± 168	1.16	66 ± 169	1.19	nnn
HD 138769	MS:B3:SPB.P	072.D-0377	52904.015	600B	27 ± 62	0.31	-190 ± 63	0.32	nnn
HD 138769	MS:B3:SPB.P	073.D-0466	53144.019	600B	-432 ± 53	0.98	243 ± 60	0.94	DdD
HD 138769	MS:B3:SPB.P	073.D-0466	53202.028	600B	-157 ± 211	0.83			nnn
HD 138769	MS:B3:SPB.P	073.D-0466	53202.046	600B	-605 ± 218	1.19	250 ± 216	1.14	dnn
HD 138769	MS:B3:SPB.P	073.D-0466	53225.002	600B	-425 ± 130	0.82	-94 ± 130	0.81	nnd
HD 138769	MS:B3:SPB.P	073.D-0466	53227.130	600B	-364 ± 317	0.95			nnn
HD 138769	MS:B3:SPB.P	073.D-0466	53234.117	600B	-42 ± 45	0.92	112 ± 46	0.97	nnn
HD 138769	MS:B3:SPB.P	072.D-0377	52908.022	600B	-243 ± 75	0.72	-133 ± 77	0.75	nnd
NLTT 40636	MS:G:HPM	080.D-0521	54555.382	600B	-2802 ± 1184	0.77			dnn
NLTT 40636	MS:G:HPM	080.D-0521	54557.340	600B	-1246 ± 1165	0.75			nnn
HD 138758	MS:B9:M.AP	073.D-0464	53086.328	600B	468 ± 33	1.14	-66 ± 30	0.92	DDD
HD 139614	PM:A7:E	072.D-0377	52904.040	600B	-78 ± 64	0.91	-25 ± 62	0.88	nnn
HD 139614	PM:A7:E	081.C-0410	54610.201	600B	-19 ± 20	0.82	3 ± 20	0.78	nnn
HD 139614	PM:A7:E	074.C-0463	53405.373	1200g	29 ± 22	1.28	-14 ± 20	1.08	nnn
LSE 125	CP	075.D-0289	53525.236	600B	-168 ± 119	1.17	-139 ± 125	1.08	nnn
LSE 125	CP	075.D-0289	53526.208	600B	277 ± 143	0.94	-399 ± 176	0.97	nnn
LSE 125	CP	075.D-0289	53527.266	600B	453 ± 236	1.09			nnn
HD 140873	GS:B8:SPB.SB	073.D-0466	53151.192	600B	27 ± 52	0.98	48 ± 50	0.90	nnn
HD 140873	GS:B8:SPB.SB	075.D-0295	53454.247	1200g	-158 ± 91	0.98	-41 ± 96	1.08	nnn
HD 140873	GS:B8:SPB.SB	075.D-0295	53572.083	1200g	-248 ± 146	1.11	486 ± 147	1.14	nnn
HD 140873	GS:B8:SPB.SB	078.D-0140	54179.298	600B	11 ± 55	0.87	212 ± 52	0.80	nnn
HD 140873	GS:B8:SPB.SB	079.D-0241	54344.012	600B	-36 ± 36	0.79	-35 ± 35	0.77	nnn
HD 141569	PM:B9:E	072.C-0447	53062.343	600B	-65 ± 46	1.18	-233 ± 39	0.81	nnn
HD 142378	MS:B2	079.D-0241	54344.024	600B	92 ± 48	0.71	-111 ± 63	0.80	nnn
HD 142666	PM:A8:E	072.C-0447	53063.355	600B	32 ± 46	1.09	-40 ± 43	0.95	nnn
HD 143309	GS:B8:SPB	073.D-0466	53151.220	600B	-94 ± 84	1.13	209 ± 96	0.98	nnn
HD 143309	GS:B8:SPB	073.D-0466	53225.056	600B	172 ± 90	0.91	88 ± 83	0.85	nnn
HD 143309	GS:B8:SPB	073.D-0466	53234.016	600B	15 ± 56	0.99	38 ± 66	0.92	nnn
HD 143309	SG:B8:SPB	075.D-0295	53454.280	1200g	35 ± 42	1.02	-27 ± 39	0.93	nnn
HD 144432	PM:A9:E	072.D-0377	52900.991	600B	70 ± 56	0.96	-31 ± 56	0.95	nnn
HD 144432	PM:A9:E	081.C-0410	54609.384	600B	5 ± 33	0.84	15 ± 37	0.83	nnn
HD 144432	PM:A9:E	072.C-0447	53062.401	600B	-42 ± 29	1.73	30 ± 26	1.48	nnn
HD 144432	PM:A9:E	074.C-0463	53447.352	1200g	-122 ± 21	1.26	-3 ± 19	1.01	dDD

Table 5. continued.

Star	Classification	Prog. ID	MJD	grism	$\langle B_z \rangle$ (G)	χ^2/ν	$\langle N_z \rangle$ (G)	χ^2/ν	HmT
HD 144667	PM:A1	079.D-0241	54344.101	600B	-91 ± 44	0.85	101 ± 41	0.75	nnn
HD 144668	PM:A7:E.DSCT	072.C-0447	53063.402	600B	15 ± 24	1.08	41 ± 22	0.90	nnn
HD 144668	PM:A7:E.DSCT	072.D-0377	52901.007	600B	-77 ± 85	0.94	-239 ± 85	0.94	nnn
HD 144668	PM:A7:E.DSCT	073.D-0464	53120.254	600B	43 ± 42	0.99	43 ± 40	0.98	nnn
HD 144668	PM:A7:E.DSCT	075.D-0295	53461.405	1200g	51 ± 103	1.01	113 ± 101	0.97	nnn
HD 144668	PM:A7:E.DSCT	081.C-0410	54610.238	600B	-89 ± 29	0.83	29 ± 27	0.77	nnd
HD 144668	PM:A7:E.DSCT	074.C-0463	53447.379	1200g	434 ± 234	1.23	162 ± 244	1.34	nnn
HD 145102	MS:B9:AP	071.D-0308	52763.315	600B	-70 ± 77	0.88	-70 ± 73	0.82	nnn
NGC 6025 129	MS:A0	073.D-0498	53199.086	600B	-43 ± 50	0.50	-36 ± 50	0.50	nnn
CPD-57 7817	MS:B8:M.AP	073.D-0498	53199.086	600B	-620 ± 50	0.54	20 ± 48	0.49	DdD
TYC8719-717-1	MS:B7	073.D-0498	53199.086	600B	30 ± 61	0.52	12 ± 60	0.51	nnn
HD 146484	MS:B7	070.D-0352	52679.371	600B	-150 ± 82	0.78	78 ± 78	0.71	nnn
HD 146555	MS:A0:M.AP	070.D-0352	52679.371	600B	475 ± 93	0.78	284 ± 85	0.66	dnd
NGC 6087 91	MS:A8	070.D-0352	52679.371	600B	-75 ± 200	0.77	-317 ± 202	0.79	nnn
16:20:05 -57:53:28	??:M	070.D-0352	52679.371	600B	-56 ± 82	0.76	-149 ± 83	0.80	-nn
CPD-57 7883	??:M	070.D-0352	52679.371	600B	66 ± 26	0.90	-3 ± 25	0.83	-nn
HD 147084	GS:A4:V	077.D-0556	53975.968	1200B	54 ± 22	1.32	8 ± 19	1.01	nnn
WD 1620-391	WD:DA2	069.D-0210	52383.426	600B	297 ± 766	0.99			n-n
WD 1620-391	WD:DA2	069.D-0210	52383.431	600R	703 ± 1112	1.11			n-n
WD 1620-391	WD:DA2	073.D-0356	53136.301	600B	177 ± 338	0.85	-677 ± 353	0.78	n-n
WD 1620-391	WD:DA2	073.D-0356	53143.322	600B	-56 ± 498	1.07	99 ± 506	1.02	n-n
WD 1620-391	WD:DA2	073.D-0356	53147.255	600B	-5 ± 296	0.88	-91 ± 328	0.90	n-n
WD 1620-391	WD:DA2	073.D-0356	53151.070	600B	9 ± 416	0.95	1025 ± 450	0.96	n-n
WD 1620-391	WD:DA2	080.D-0521	54529.391	600B	-3134 ± 2204	0.78			n-n
LS IV -12 1	SD:O	075.D-0352	53566.068	600B	206 ± 231	1.07	-412 ± 272	0.99	nnn
HD 147869	MS:A1:AP	071.D-0308	52763.327	600B	-77 ± 64	0.83	86 ± 66	0.88	nnn
HD 147869	MS:A1:AP	073.D-0464	53144.318	600B	-33 ± 36	0.95	42 ± 37	0.99	nnn
HD 148112	MS:A0:AP	071.D-0308	52763.338	600B	-111 ± 54	0.92	131 ± 56	0.99	nnn
HD 148184	MS:B1:P.E	075.D-0507	53532.224	1200g	23 ± 56	0.69	137 ± 65	0.93	-nn
HD 148184	MS:B1:P.E	077.D-0406	53862.380	600B	54 ± 52	1.07	-104 ± 44	0.74	-nn
HD 148259	MS:B2:E	075.D-0507	53532.195	1200g	248 ± 134	1.55	-38 ± 130	1.48	nnn
HD 148259	MS:B2:E	075.D-0507	53572.104	1200g	14 ± 56	1.10	75 ± 52	0.92	nnn
HD 148898	MS:A6:AP	071.D-0308	52763.349	600B	204 ± 62	0.93	-97 ± 60	0.87	ndd
HD 148937	MS:O6:M.FP	080.D-0383	54550.416	600B	-142 ± 79	0.78	20 ± 96	0.79	nnn
HD 149382	SD:OB	075.D-0352	53458.390	600B	74 ± 688	1.16	768 ± 733	1.33	nnn
HD 149257	SG:B1	073.D-0498	53199.116	600B	159 ± 60	0.52	-120 ± 60	0.52	dnn
HD 149277	MS:B2:M.HES	073.D-0498	53199.116	600B	2298 ± 97	0.53	94 ± 90	0.48	DDD
HD 149822	MS:B9:M.AP	071.D-0308	52763.361	600B	-712 ± 49	1.08	17 ± 43	0.87	DDD
HD 149757	MS:O9:E	081.C-0410	54609.345	600B	118 ± 61	0.79	10 ± 65	0.93	nnn
HD 149764	MS:A0:M.AP	071.D-0308	52763.374	600B	-1188 ± 67	0.88	20 ± 68	0.90	DdD
HD 149764	MS:A0:M.AP	073.D-0464	53120.331	600B	73 ± 50	1.51	-48 ± 44	0.93	nnn
HD 150193	PM:A0:E	081.C-0410	54609.093	600B	-245 ± 39	0.83	-1 ± 39	0.83	DdD
CD-48 11050	MS:A2	073.D-0498	53199.145	600B	-81 ± 85	0.53	-82 ± 84	0.51	nnn
CD-48 11050	MS:A2	073.D-0498	53210.119	600B	-45 ± 52	0.48	82 ± 50	0.43	nnn
CD-48 11051	MS:B1:M.HES	073.D-0498	53199.145	600B	-2196 ± 97	0.56	82 ± 93	0.51	DDD
CD-48 11051	MS:B1:M.HES	073.D-0498	53210.119	600B	-2011 ± 65	0.58	-90 ± 60	0.48	DDD
CD-48 11059	MS:B3	073.D-0498	53199.145	600B	314 ± 145	0.52	-142 ± 144	0.52	nnn
CD-48 11059	MS:B3	073.D-0498	53210.119	600B	136 ± 94	0.53	-49 ± 91	0.50	nnn
CD-48 11060	MS:B3	073.D-0498	53199.145	600B	-6 ± 116	0.48	-17 ± 119	0.51	nnn
CD-48 11060	MS:B3	073.D-0498	53210.119	600B	-83 ± 76	0.48	-64 ± 79	0.53	nnn
HD 150562	MS:A5:M.AP	079.D-0240	54208.382	600B	1853 ± 46	1.50	-4 ± 33	0.76	DDD
HD 150562	MS:A5:M.AP	079.D-0240	54238.251	600B	1904 ± 47	1.57	16 ± 33	0.78	DDD
HD 150562	MS:A5:M.AP	079.D-0240	54247.083	600B	1878 ± 44	1.63	-38 ± 30	0.76	DDD
HD 150549	MS:A0:AP	071.D-0308	52763.386	600B	-78 ± 61	1.05	55 ± 56	0.91	nnn
HD 150549	MS:A0:AP	073.D-0464	53116.386	600B	-65 ± 41	0.87	-6 ± 39	0.82	nnn
HD 150549	MS:A0:AP	073.D-0464	53120.350	600B	-80 ± 32	0.95	26 ± 32	0.90	nnn
HD 151525	MS:B9:M.AP	071.D-0308	52733.395	600B	17 ± 78	0.88	-41 ± 92	0.83	nnn
HD 151525	MS:B9:M.AP	071.D-0308	52763.397	600B	205 ± 71	0.94	-118 ± 68	0.86	nnn
HD 151804	SG:O8	075.D-0432	53476.371	600B	31 ± 197	0.98	-115 ± 218	1.02	nnn
HD 151804	SG:O8	075.D-0432	53571.025	600B	-142 ± 100	1.00	-124 ± 94	0.89	nnn
HD 151804	SG:O8	075.D-0432	53596.061	600B	288 ± 69	0.91	-231 ± 68	0.89	ndd
HD 152404	PM:F5:E	081.C-0410	54609.311	600B	-42 ± 19	0.80	-24 ± 19	0.76	nnn
HD 152408	SG:O8:P.E	075.D-0432	53556.214	600B	-52 ± 129	1.22	121 ± 110	0.88	nnn
HD 152408	SG:O8:P.E	075.D-0432	53571.103	600B	195 ± 280	1.08	-219 ± 244	0.82	nnn
HD 152408	SG:O8:P.E	075.D-0432	53596.081	600B	9 ± 116	1.06	77 ± 102	0.85	nnn
HD 152635	GS:B7:SPB	079.D-0241	54344.041	600B	-99 ± 30	0.84	37 ± 30	0.86	dnd
HD 152511	MS:B5:M.SPB	079.D-0241	54344.116	600B	600 ± 51	0.74	113 ± 62	0.75	DnD

Table 5. continued.

Star	Classification	Prog. ID	MJD	grism	$\langle B_z \rangle$ (G)	χ^2/ν	$\langle N_z \rangle$ (G)	χ^2/ν	HmT
HD 152511	MS:B5:M.SPB	081.C-0410	54610.223	600B	113 ± 35	0.91	-43 ± 33	0.80	dnd
HD 152511	MS:B5:M.SPB	060.A-9203	54608.158	600B	69 ± 33	0.85	-68 ± 36	0.87	nnn
HD 152511	MS:B5:M.SPB	081.C-0410	54609.433	600B	429 ± 49	0.66	144 ± 48	0.62	DnD
HD 153261	MS:B2:E	075.D-0507	53532.252	1200g	72 ± 96	0.78	-173 ± 87	0.66	nnn
HD 322676	MS:A0	073.D-0498	53219.234	600B	-176 ± 97	0.49	117 ± 96	0.48	nnn
HD 323673	MS:A0	073.D-0498	53219.234	600B	-182 ± 81	0.54	-68 ± 83	0.57	nnn
HD 153948	MS:A2:M.AP	073.D-0498	53219.234	600B	209 ± 54	0.58	39 ± 55	0.59	nnd
HD 153716	MS:B5	079.D-0241	54344.057	600B	-70 ± 48	0.78	-79 ± 58	0.78	nnn
PN H 2-1	CP	075.D-0289	53525.325	600B					—
PN H 2-1	CP	075.D-0289	53527.202	600B					—
HD 154072	CP	075.D-0289	53526.295	600B	7 ± 169	1.21	-233 ± 190	1.14	nnn
HD 154072	CP	075.D-0289	53527.323	600B	13 ± 193	1.00	503 ± 201	0.98	nnn
HD 154708	MS:A2:M.AP.ROAP	073.D-0464	53120.376	600B	9227 ± 141	37.11	-43 ± 24	1.10	DDD
HD 154708	MS:A2:M.AP.ROAP	075.D-0295	53487.308	1200g	7178 ± 109	50.59	-34 ± 15	0.95	DDD
HD 154708	MS:A2:M.AP.ROAP	075.D-0295	53570.998	1200g	9001 ± 193	2.63	-158 ± 142	1.43	DDD
HD 154708	MS:A2:M.AP.ROAP	079.D-0240	54197.369	600B	9516 ± 168	10.01	-11 ± 46	0.79	DDD
HD 154708	MS:A2:M.AP.ROAP	079.D-0240	54209.307	600B	8853 ± 82	13.87	-30 ± 19	0.80	DDD
HD 154708	MS:A2:M.AP.ROAP	079.D-0240	54215.279	600B	8357 ± 78	10.33	-40 ± 21	0.79	DDD
HD 154708	MS:A2:M.AP.ROAP	079.D-0240	54223.173	600B	7542 ± 79	14.08	38 ± 18	0.81	DDD
HD 154708	MS:A2:M.AP.ROAP	079.D-0240	54238.283	600B	7084 ± 76	4.79	9 ± 29	0.77	DDD
HD 154708	MS:A2:M.AP.ROAP	079.D-0240	54247.172	600B	8556 ± 81	6.31	17 ± 27	0.74	DDD
HD 154708	MS:A2:M.AP.ROAP	079.D-0240	54254.121	600B	7097 ± 77	3.63	39 ± 35	0.78	DDD
HD 154708	MS:A2:M.AP.ROAP	079.D-0240	54258.249	600B	8314 ± 79	6.69	1 ± 25	0.75	DDD
HD 154708	MS:A2:M.AP.ROAP	079.D-0240	54270.309	600B	7152 ± 72	9.38	21 ± 19	0.75	DDD
HD 154708	MS:A2:M.AP.ROAP	079.D-0240	54279.166	600B	8761 ± 81	14.53	9 ± 18	0.79	DDD
HD 154708	MS:A2:M.AP.ROAP	079.D-0240	54287.225	600B	6996 ± 115	1.52	80 ± 84	0.82	DDD
HD 154708	MS:A2:M.AP.ROAP	079.D-0240	54305.153	600B	8730 ± 83	11.07	16 ± 22	0.80	DDD
HD 154708	MS:A2:M.AP.ROAP	079.D-0240	54307.021	600B	7777 ± 73	13.41	46 ± 17	0.77	DDD
HD 154708	MS:A2:M.AP.ROAP	079.D-0240	54297.302	600B	7112 ± 78	3.53	32 ± 34	0.74	DDD
HD 155379	MS:A0	071.D-0308	52763.410	600B	106 ± 67	0.85	67 ± 83	0.88	nnn
HD 155379	MS:A0	073.D-0464	53137.393	600B	29 ± 38	0.97	-33 ± 39	1.01	ndn
HD 155806	MS:O7:E	075.D-0432	53476.398	600B	2 ± 112	0.90	-71 ± 108	0.82	nnn
HD 155806	MS:O7:E	075.D-0432	53532.306	600B	47 ± 59	1.09	9 ± 57	1.02	nnn
HD 155806	MS:O7:E	075.D-0432	53556.235	600B	-70 ± 89	0.85	-100 ± 116	0.95	nnn
HD 155806	MS:O7:E	075.D-0507	53532.283	1200g	38 ± 66	1.07	126 ± 64	0.99	nnn
HD 155806	MS:O7:E	080.D-0383	54549.403	600B	-123 ± 80	0.74	57 ± 99	0.74	nnn
HD 157056	MS:B2:BCEP	075.D-0295	53532.324	1200g	-18 ± 25	1.10	-27 ± 24	1.02	nnn
HD 157056	MS:B2:BCEP	075.D-0295	53572.122	1200g	-45 ± 48	0.91	-97 ± 48	0.88	nnn
HD 157751	MS:B9:M.AP	071.D-0308	52793.271	600B	4108 ± 76	2.80	-14 ± 43	0.93	DDD
HD 157751	MS:B9:M.AP	073.D-0464	53116.404	600B	3889 ± 67	3.99	14 ± 38	1.27	DDD
HD 158643	PM:A0	081.C-0410	54609.275	600B	-74 ± 29	0.81	-24 ± 30	0.74	nnn
HD 158427	MS:B2:E	077.D-0406	53869.353	600B	-27 ± 38	1.05	-12 ± 41	1.23	nnn
NGC 6383 28	MS:A0	073.D-0498	53220.182	600B	77 ± 126	0.74	-80 ± 122	0.69	nnn
NGC 6383 700	MS:A3:P	073.D-0498	53220.182	600B	130 ± 121	0.74	251 ± 121	0.72	nnn
NGC 6383 26	PM:A2:E.P	073.D-0498	53220.182	600B	4 ± 153	0.68	-110 ± 145	0.60	nnn
HD 317857	MS:A1:M.AP	073.D-0498	53210.161	600B	-1688 ± 74	1.44	-22 ± 46	0.56	DDD
NGC 6383 87	PM:A5:E.P	073.D-0498	53220.182	600B	-77 ± 93	0.62	57 ± 94	0.63	nnn
HD 317846	MS:B5	073.D-0498	53210.161	600B	-44 ± 53	0.55	-53 ± 53	0.55	nnn
NGC 6383 102	MS:B8	073.D-0498	53210.161	600B	277 ± 91	0.66	66 ± 77	0.49	nnd
HD 317852	MS:F2:P	073.D-0498	53220.182	600B	1 ± 60	0.65	30 ± 57	0.58	nnn
HD 159217	MS:A0	077.D-0556	53976.193	600B	115 ± 50	0.90	-87 ± 51	0.92	nnn
HD 159312	MS:A0	077.D-0556	53976.178	600B	156 ± 77	0.97	98 ± 79	1.04	nnn
WD 1733-544	WD:DA8	073.D-0516	53199.178	600B	3554 ± 4260	1.34	4070 ± 3882	1.11	n-n
NGC 6396 PPM48	GS:B5	070.D-0352	52679.394	600B	-562 ± 225	0.77	293 ± 228	0.76	nnn
NGC 6396 PPM93	GS:B	070.D-0352	52679.394	600B	-62 ± 247	0.68	-322 ± 258	0.75	nnn
17:37:37 -35:04:20	??:F	070.D-0352	52679.394	600B	665 ± 374	0.76	-262 ± 359	0.77	nnn
TYC7384-506-1	??:F	070.D-0352	52679.394	600B	-78 ± 93	0.72	-325 ± 90	0.68	nnn
CD-34 11864	??:M4	070.D-0352	52679.394	600B	53 ± 40	0.77	-102 ± 39	0.72	-nn
HD 160124	MS:B3:SPB	073.D-0466	53151.259	600B	30 ± 54	0.90	23 ± 54	0.94	nnn
HD 160124	MS:B3:SPB	075.D-0295	53520.234	1200g	20 ± 78	1.12	117 ± 76	1.06	nnn
HD 160124	MS:B3:SPB	075.D-0295	53600.109	1200g	78 ± 46	0.87	38 ± 56	0.89	nnn
HD 160124	MS:B3:SPB	075.D-0295	53604.109	1200g	55 ± 35	0.96	-16 ± 37	0.82	nnn
HD 318107	MS:B8:M.AP	073.D-0498	53211.986	600B	5878 ± 67	2.13	-39 ± 31	0.47	DDD
HD 318108	MS:B9	073.D-0498	53211.986	600B	-112 ± 61	0.53	-20 ± 59	0.50	nnn
HD 318109	MS:A0	073.D-0498	53211.986	600B	-29 ± 71	0.58	87 ± 64	0.48	nnn
CD-32 13089	MS:A4	073.D-0498	53234.056	600B	34 ± 63	0.56	-29 ± 60	0.51	nnn
CD-32 13093	MS:A0	073.D-0498	53234.056	600B	-125 ± 83	0.50	25 ± 83	0.51	nnn

Table 5. continued.

Star	Classification	Prog. ID	MJD	grism	$\langle B_z \rangle$ (G)	χ^2/ν	$\langle N_z \rangle$ (G)	χ^2/ν	HmT
V976 Sco	MS:A4	073.D-0498	53234.056	600B	-209 ± 139	0.54	-206 ± 137	0.53	nnn
HD 318100	MS:B9:M.AP	073.D-0498	53234.056	600B	363 ± 51	0.52	75 ± 52	0.54	DnD
NGC 6405 322	??:F5	073.D-0498	53220.098	600B	93 ± 46	0.52	-30 ± 46	0.53	nnn
HD 318099	MS:A0	073.D-0498	53234.056	600B	-40 ± 65	0.54	43 ± 61	0.47	nnn
CD-32 13119	MS:A8:AP	073.D-0498	53220.098	600B	-62 ± 28	0.58	-25 ± 28	0.60	nnn
HD 318095	MS:A1	073.D-0498	53220.098	600B	83 ± 46	0.52	-59 ± 47	0.52	nnn
HD 160578	GS:B1:BCEP	075.D-0295	53532.346	1200g	13 ± 33	1.19	-79 ± 31	1.06	nnn
HD 160578	GS:B1:BCEP	075.D-0295	53604.127	1200g	47 ± 41	0.96	-56 ± 39	0.87	nnn
CD-28 13479	GS:B2	060.A-9203	53948.239	600B	888 ± 1403	1.07			nnn
HD 160917	MS:B9	075.D-0289	53527.450	600B	101 ± 68	0.95	-21 ± 74	0.99	nnn
HD 161044	CP	075.D-0289	53525.396	600B	-167 ± 111	1.15	-68 ± 113	1.17	-nn
HD 161044	CP	075.D-0289	53526.442	600B	-15 ± 396	1.33	38 ± 409	1.39	-nn
HD 161044	CP	075.D-0289	53527.425	600B	123 ± 384	1.30	-15 ± 355	1.16	-nn
HD 160468	MS:F2:AP	073.D-0464	53116.362	600B	-55 ± 61	2.48	47 ± 62	2.62	nnn
HD 160468	MS:F2:AP	073.D-0464	53134.319	600B	-48 ± 40	1.48	-40 ± 34	1.10	nnn
GJ 2131 A	MS:M1	073.D-0516	53192.133	600B	181 ± 84	0.94	-62 ± 87	1.01	-nn
GJ 2131 A	MS:M1	073.D-0516	53193.150	600B	138 ± 124	0.42	-70 ± 123	0.42	-nn
HD 161277	MS:B9:AP	073.D-0464	53134.341	600B	66 ± 37	1.00	-54 ± 44	0.94	nnn
HD 161459	MS:A2:M.AP.ROAP	269.D-5044	52476.123	600B	-2118 ± 79	2.16	46 ± 57	1.15	DDD
HD 161783	MS:B2:SPB.SB.EB	073.D-0466	53151.281	600B	70 ± 50	0.78	-78 ± 55	0.97	nnn
HD 161783	MS:B2:SPB.SB.EB	075.D-0295	53487.333	1200g	-77 ± 40	0.95	38 ± 45	0.88	nnn
HD 161783	MS:B2:SPB.SB.EB	075.D-0295	53598.108	1200g	-185 ± 122	0.90	-277 ± 117	0.84	nnn
HD 161783	MS:B2:SPB.SB.EB	075.D-0295	53599.118	1200g	-3 ± 45	0.95	-65 ± 43	0.86	nnn
HD 162305North	MS:B9:AP	073.D-0498	53220.275	600B	18 ± 60	0.91	28 ± 61	0.95	nnn
HD 162305South	MS:B9:AP	073.D-0498	53220.244	600B	-66 ± 59	0.89	-109 ± 58	0.87	nnn
HD 162305	MS:B9:AP	073.D-0498	53274.097	600B	178 ± 76	0.86	-138 ± 79	0.93	nnn
17:52:04 -34:55:08	?:K	073.D-0498	53240.073	600B	218 ± 125	0.57	-77 ± 128	0.60	-nn
HD 320765	MS:A2	073.D-0498	53240.073	600B	-32 ± 62	0.47	92 ± 63	0.49	nnn
HD 320764	MS:A1	073.D-0498	53240.073	600B	-136 ± 67	0.48	-155 ± 68	0.51	nnn
HD 162678	MS:B9	073.D-0498	53219.275	600B	2 ± 27	0.55	-13 ± 30	0.59	nnn
HD 162724	MS:B9	073.D-0498	53219.275	600B	-57 ± 38	0.49	-7 ± 41	0.49	nnn
HD 162725	MS:A0:M.AP	073.D-0498	53219.275	600B	-44 ± 25	0.50	-24 ± 26	0.47	nnn
HD 162725	MS:A0:M.AP	080.D-0383	54549.413	600B	58 ± 35	0.76	0 ± 42	0.74	nnn
HD 162978	SG:O7	075.D-0432	53556.258	600B	2 ± 63	0.91	-4 ± 64	0.95	nnn
HD 162978	SG:O7	075.D-0432	53595.116	600B	68 ± 74	1.02	-121 ± 69	0.89	nnn
HD 162978	SG:O7	075.D-0432	53604.144	600B	44 ± 66	0.75	30 ± 72	0.90	nnn
HD 163472	MS:B2:M.BCEP	073.D-0466	53151.298	600B	-201 ± 43	0.93	85 ± 43	0.92	ndd
HD 163336	MS:A0	077.D-0556	53976.163	600B	60 ± 48	0.94	86 ± 50	1.04	nnn
HD 163296	PM:A1:E	081.C-0410	54610.255	600B	-8 ± 44	0.75	-64 ± 45	0.79	nnn
HD 163296	PM:A1:E	074.C-0463	53279.016	1200g	-56 ± 34	1.08	-68 ± 34	0.95	nnn
HD 163254	MS:B2:SPB	079.D-0241	54344.069	600B	-50 ± 51	0.73	-128 ± 62	0.70	nnn
HD 164245	MS:B7	079.D-0241	54345.140	600B	-14 ± 44	0.77	54 ± 55	0.75	nnn
HD 164249	MS:F5:CSD	081.C-0410	54610.301	600B	-42 ± 19	0.90	30 ± 21	0.75	nnn
HD 164794	MS:O4	075.D-0432	53520.356	600B	21 ± 65	1.04	-31 ± 64	1.03	nnn
HD 164794	MS:O4	075.D-0432	53594.120	600B	199 ± 76	0.96	116 ± 74	0.91	nnn
HD 164794	MS:O4	075.D-0432	53595.096	600B	-27 ± 69	0.85	97 ± 76	1.03	nnn
V426 Oph	WD:CV	079.D-0697	54311.080	1200B					—
V426 Oph	WD:CV	081.D-0670	54693.058	1200B					—
V426 Oph	WD:CV	081.D-0670	54694.052	1200B					—
HD 166197	MS:B1	079.D-0241	54345.154	600B	-56 ± 51	0.77	-68 ± 62	0.73	nnn
HD 166469	MS:A0:AP	073.D-0464	53136.273	600B	-2 ± 42	0.93	-17 ± 42	0.94	nnn
BD-14 4922	GS:O9	067.D-0306	52048.283	600R	970 ± 547	0.98			nnn
BD-14 4922	GS:O9	067.D-0306	52078.270	600R	1876 ± 875	0.89			nnn
HD 166469	MS:A0:AP	071.D-0308	52793.291	600B	-27 ± 56	1.12	51 ± 55	1.09	nnn
HD 166473	MS:A5:M.AP.ROAP	079.D-0240	54209.327	600B	2296 ± 41	2.79	-20 ± 22	0.80	DDD
HD 166473	MS:A5:M.AP.ROAP	079.D-0240	54247.193	600B	2257 ± 50	1.70	49 ± 34	0.78	DDD
HD 166473	MS:A5:M.AP.ROAP	079.D-0240	54250.396	600B	2273 ± 43	2.52	-10 ± 23	0.75	DDD
HD 166473	MS:A5:M.AP.ROAP	079.D-0240	54308.285	600B	2404 ± 42	3.06	12 ± 21	0.78	DDD
HD 167263	GS:O9	075.D-0432	53594.142	600B	131 ± 84	1.02	24 ± 88	1.12	nnn
HD 167263	GS:O9	075.D-0432	53595.015	600B	-46 ± 61	1.14	-5 ± 57	0.99	nnn
HD 167263	GS:O9	075.D-0432	53596.112	600B	-7 ± 54	0.96	47 ± 54	0.93	nnn
HD 167771	GS:O7	075.D-0432	53520.377	600B	-99 ± 65	0.93	-44 ± 60	0.81	nnn
HD 167771	GS:O7	075.D-0432	53594.164	600B	-121 ± 116	1.25	-70 ± 113	1.18	nnn
HD 167771	GS:O7	075.D-0432	53594.240	600B	47 ± 38	0.84	-26 ± 37	0.84	nnn
HD 167771	GS:O7	075.D-0432	53595.066	600B	39 ± 87	1.13	-123 ± 80	0.93	nnn
HD 168957	MS:B3:E	075.D-0507	53572.158	1200g	-30 ± 71	1.26	46 ± 68	1.15	nnn
HD 168856	MS:B9:M.AP	073.D-0464	53144.341	600B	-525 ± 42	0.98	22 ± 51	0.95	DDD

Table 5. continued.

Star	Classification	Prog. ID	MJD	grism	$\langle B_z \rangle$ (G)	χ^2/ν	$\langle N_z \rangle$ (G)	χ^2/ν	HmT
HD 169033	MS:B5	079.D-0241	54344.144	600B	-50 ± 43	0.77	154 ± 52	0.77	nnn
HD 169142	PM:A9:E	081.C-0410	54610.175	600B	20 ± 24	0.75	60 ± 25	0.76	nnn
HD 169820	MS:B9:SPB	073.D-0466	53151.312	600B	55 ± 57	0.89	-78 ± 59	0.93	nnn
HD 169820	MS:B9:SPB	075.D-0295	53520.333	1200g	-16 ± 52	0.90	111 ± 52	0.89	nnn
HD 169820	MS:B9:SPB	075.D-0295	53597.112	1200g	44 ± 40	1.03	48 ± 38	0.92	nnn
HD 169820	MS:B9:SPB	079.D-0241	54345.124	600B	-49 ± 41	0.75	69 ± 50	0.75	nnn
HD 169959A	MS:A0:M.AP	073.D-0498	53192.159	600B	-541 ± 53	0.89	110 ± 54	0.92	DnD
HD 169467	MS:B3:SPB	079.D-0241	54345.166	600B	-49 ± 39	0.92	66 ± 43	0.81	nnn
HD 170054	MS:B7:AP	073.D-0498	53244.114	600B	-23 ± 73	0.93	12 ± 73	0.83	nnn
HD 170054	MS:B7:AP	073.D-0498	53271.057	600B	-12 ± 63	0.79	34 ± 67	0.90	nnn
VV Ser	PM:B:SH.E	081.C-0410	54610.332	600B	-135 ± 131	0.90	49 ± 126	0.81	nnn
WD 1826-045	WD:DA6	073.D-0516	53193.179	600B	-2467 ± 1477	1.51	-301 ± 1479	1.50	n-n
BD-19 5044 F	MS:B8	073.D-0498	53240.107	600B	23 ± 82	0.56	-75 ± 79	0.52	nnn
BD-19 5045	MS:B5	073.D-0498	53240.107	600B	26 ± 57	0.54	-24 ± 53	0.49	nnn
BD-19 5044 L	MS:B8:M.AP	073.D-0498	53240.107	600B	-287 ± 100	0.54	46 ± 97	0.50	nnn
BD-19 5044 M	MS:B8	073.D-0498	53240.107	600B	-51 ± 103	0.51	-161 ± 98	0.47	nnn
BD-19 5046	MS:A1	073.D-0498	53240.107	600B	138 ± 61	0.55	30 ± 56	0.47	nnn
HD 170836	MS:B8:M.AP	073.D-0498	53240.143	600B	-637 ± 112	0.53	57 ± 109	0.50	DnD
HD 170836	MS:B8:M.AP	073.D-0498	53245.193	600B	-637 ± 70	0.50	-55 ± 69	0.48	DdD
HD 170836	MS:B8:M.AP	073.D-0498	53274.121	600B	438 ± 83	0.64	37 ± 76	0.63	ddD
HD 170835	MS:B5	073.D-0498	53240.143	600B	-293 ± 187	0.51	-61 ± 194	0.56	nnn
HD 170835	MS:B5	073.D-0498	53245.193	600B	-69 ± 125	0.52	33 ± 124	0.52	nnn
HD 170835	MS:B5	073.D-0498	53274.121	600B	-51 ± 159	0.65	-306 ± 149	0.64	nnn
HD 170860A	MS:B8:AP	073.D-0498	53221.278	600B	27 ± 84	0.88	-102 ± 83	0.87	nnn
HD 171184	MS:A0:M.AP	071.D-0308	52880.028	600B	119 ± 40	0.88	-27 ± 40	0.87	dnn
HD 171184	MS:A0:M.AP	073.D-0464	53144.368	600B	-32 ± 42	1.30	32 ± 41	1.26	nnn
HD 171034	MS:B2:BCEP	079.D-0241	54344.131	600B	9 ± 33	0.83	99 ± 34	0.87	nnn
HD 171279	MS:A0:AP	073.D-0464	53144.393	600B	-54 ± 34	1.10	-65 ± 31	0.93	nnn
HD 171858	SD:B	075.D-0352	53512.357	600B	-28 ± 132	0.85	42 ± 166	0.88	nnn
HD 172032	MS:A9:AP	073.D-0464	53151.105	600B	-148 ± 38	1.12	40 ± 35	0.97	ndd
BD-12 5133	MS:B1	060.A-9203	52822.396	600B	-38 ± 1237	1.08	-1008 ± 1224	1.06	nnn
BD-12 5133	MS:B1	060.A-9203	52900.106	600B	-18 ± 1090	0.92			nnn
HD 172910	MS:B2:BCEP	079.D-0241	54345.178	600B	-50 ± 35	0.80	-7 ± 43	0.78	nnn
HD 172555	MS:A7:CSD	081.C-0410	54610.287	600B	-29 ± 24	0.78	-19 ± 24	0.76	nnn
WD 1845+019	WD:DA2	073.D-0356	53131.395	600B	244 ± 811	1.00	532 ± 953	0.93	n-n
WD 1845+019	WD:DA2	073.D-0356	53136.389	600B	-41 ± 692	0.88	565 ± 894	1.05	n-n
HD 174240	MS:A1	077.D-0556	53976.208	600B	18 ± 50	0.96	2 ± 49	0.96	nnn
HD 175744	MS:B9:AP	071.D-0308	52880.054	600B	101 ± 64	0.87	98 ± 78	0.88	nnn
HD 175744	MS:B9:AP	071.D-0308	52901.019	600B	319 ± 88	1.01	-120 ± 87	0.98	nnd
HD 175640	GS:B9	071.D-0308	52901.032	600B	20 ± 92	1.04	-112 ± 91	1.01	nnn
HD 175640	GS:B9	072.D-0377	52901.043	600B	83 ± 82	0.96	22 ± 101	0.92	nnn
HD 176386	PM:B9:E	081.C-0410	54610.272	600B	-87 ± 41	0.77	-41 ± 41	0.78	nnn
TY Cra	PM:B8:E	074.C-0442	53331.030	600B	-79 ± 170	1.37	105 ± 157	1.18	n-n
TY Cra	PM:B8:E	074.C-0442	53332.028	1200g	145 ± 131	1.08	81 ± 119	0.90	nnn
CD-51 11879	SD:O	075.D-0352	53512.395	600B	359 ± 247	0.81	-53 ± 298	0.82	nnn
HD 176387	MS:A:RR	082.D-0342	54781.007	1200B	-149 ± 48	1.23	-89 ± 45	1.20	nnd
HD 172690	MS:A0:M.AP	073.D-0464	53134.368	600B	222 ± 51	1.06	-41 ± 51	1.01	dnd
HD 172690	MS:A0:M.AP	071.D-0308	52793.314	600B	-254 ± 79	0.91	92 ± 78	0.89	nnd
HD 176196	MS:B9:M.AP	071.D-0308	52793.329	600B	338 ± 69	0.85	-37 ± 68	0.80	dnd
HD 176196	MS:B9:M.AP	073.D-0464	53134.389	600B	175 ± 51	1.20	75 ± 50	1.13	dnd
HD 177863	MS:B8:SPB	073.D-0466	53193.211	600B	-16 ± 45	0.98	-71 ± 44	0.94	nnn
HD 177863	MS:B8:SPB	075.D-0295	53597.128	1200g	-35 ± 30	1.00	12 ± 29	0.92	nnn
HD 179218	PM:A0:E	081.C-0410	54609.360	600B	-57 ± 30	0.78	-7 ± 29	0.77	nnn
HD 179588	MS:B9:SPB	079.D-0241	54343.135	600B	38 ± 42	0.78	-65 ± 41	0.75	nnn
HD 179761	MS:A0	071.D-0308	52822.280	600B	-219 ± 84	0.92	163 ± 86	0.97	dnn
HD 180642	GS:B1:BCEP	079.D-0241	54343.159	600B	-9 ± 26	0.74	41 ± 27	0.80	nnn
HD 180642	GS:B1:BCEP	079.D-0241	54344.084	600B	119 ± 36	0.75	-2 ± 43	0.78	ndd
HD 181558	GS:B5:SPB	073.D-0466	53193.251	600B	-63 ± 39	0.91	-16 ± 39	0.89	nnn
HD 181558	GS:B5:SPB	073.D-0466	53227.184	600B	67 ± 56	0.99	78 ± 52	0.83	nnn
HD 181558	GS:B5:SPB	073.D-0466	53274.145	600B	4 ± 115	0.95	-126 ± 113	0.91	nnn
HD 181558	GS:B5:SPB	073.D-0466	53275.144	600B	67 ± 50	0.94	37 ± 52	0.88	nnn
HD 181558	GS:B5:SPB	075.D-0295	53519.378	1200g	17 ± 43	1.00	12 ± 52	0.94	nnn
HD 181558	GS:B5:SPB	075.D-0295	53520.397	1200g	-37 ± 37	1.07	26 ± 34	0.94	nnn
HD 181558	GS:B5:SPB	079.D-0241	54344.167	600B	-109 ± 36	0.76	-23 ± 44	0.76	nnd
WD 1919+145	WD:DA5	073.D-0356	53132.324	600B	-1455 ± 754	1.06	-769 ± 938	1.05	n-n
WD 1919+145	WD:DA5	073.D-0356	53136.351	600B	-812 ± 764	0.98	426 ± 784	1.04	n-n
HD 181616	SG:B8:SB.CSD	279.D-5042	54333.020	1200B	-9 ± 9	3.19	8 ± 5	1.08	-nn

Table 5. continued.

Star	Classification	Prog. ID	MJD	grism	$\langle B_z \rangle$ (G)	χ^2/ν	$\langle N_z \rangle$ (G)	χ^2/ν	HmT
HD 181616	SG:B8:SB.CSD	279.D-5042	54343.098	1200B	-60 ± 8	2.66	13 ± 6	1.31	-DD
HD 181616	SG:B8:SB.CSD	279.D-5042	54361.071	1200B	8 ± 13	1.52	9 ± 10	1.02	-nn
HD 181616	SG:B8:SB.CSD	075.D-0507	53520.415	1200g	-10 ± 16	2.17	8 ± 11	0.99	-nn
HD 182255	GS:B6:SPB	075.D-0295	53514.317	1200g	26 ± 184	1.66	-255 ± 184	1.66	nnn
HD 182255	GS:B6:V	073.D-0466	53193.234	600B	127 ± 45	0.99	-37 ± 45	0.97	nnn
HD 181327	MS:F5:CSD	081.C-0410	54610.364	600B	0 ± 17	0.98	48 ± 14	0.72	nnn
HD 182180	MS:B2:M.HES	081.D-2005	54652.328	1200B	-2431 ± 183	0.93	-23 ± 179	0.88	DDD
HD 182180	MS:B2:M.HES	081.D-2005	54656.078	1200B	-2154 ± 186	1.04	305 ± 173	0.92	DDD
HD 182180	MS:B2:M.HES	081.D-2005	54656.146	1200B	778 ± 166	1.33	426 ± 134	0.91	ddd
HD 182180	MS:B2:M.HES	081.D-2005	54661.327	1200B	-1421 ± 215	1.18	-216 ± 197	1.00	DnD
HD 182180	MS:B2:M.HES	081.D-2005	54669.187	1200B	-62 ± 182	1.14	587 ± 153	0.79	nnn
HD 182180	MS:B2:M.HES	081.D-2005	54669.327	1200B	2836 ± 199	1.21	-4 ± 187	1.07	DDD
HD 182761	MS:A0	077.D-0556	53976.080	600B	6 ± 62	0.86	-44 ± 61	0.83	nnn
HD 183133	MS:B2:SPB	079.D-0241	54344.179	600B	97 ± 41	0.71	17 ± 53	0.80	nnn
HD 183806	MS:A0:M.AP	071.D-0308	52793.345	600B	-36 ± 43	0.91	-27 ± 46	1.02	nnn
HD 183806	MS:A0:M.AP	073.D-0464	53120.424	600B	131 ± 33	1.14	-2 ± 33	0.90	dnd
HD 185256	MS:F0:M.AP.ROAP	269.D-5044	52476.175	600B	-771 ± 58	1.33	-57 ± 49	0.93	DDD
HD 186122	MS:B9:HGMN	071.D-0308	52822.312	600B	88 ± 66	0.80	14 ± 80	0.92	nnn
HD 186117	MS:A0:AP	073.D-0464	53134.413	600B	-120 ± 39	1.19	-41 ± 36	1.05	ndd
HD 186117	MS:A0:AP	073.D-0464	53140.329	600B	21 ± 37	1.09	26 ± 33	0.90	nnn
HD 186219	GS:A4	077.D-0556	53976.243	600B	76 ± 25	0.93	-30 ± 24	0.84	ndd
HD 187474	MS:A0:M.AP	069.D-0210	52530.969	600R	-2471 ± 116	1.82	73 ± 96	0.96	DDD
HD 188001	SG:O7	075.D-0432	53520.434	600B	93 ± 57	1.04	71 ± 56	1.00	nnn
HD 188001	SG:O7	075.D-0432	53594.199	600B	119 ± 38	0.75	-16 ± 38	0.79	nnd
HD 188001	SG:O7	075.D-0432	53595.149	600B	63 ± 62	1.26	-78 ± 56	1.04	nnn
HD 188001	SG:O7	075.D-0432	53597.149	600B	-21 ± 68	0.88	29 ± 68	0.89	nnn
HD 188042	MS:A5:M.AP	060.A-9203	52130.168	600R	1964 ± 35	1.66	-46 ± 27	0.93	DDD
HD 188042	MS:A5:M.AP	060.A-9203	52130.176	600B	1909 ± 42	3.58	55 ± 20	0.81	DDD
HD 188042	MS:A5:M.AP	060.A-9203	52130.270	600B	1987 ± 51	5.08	129 ± 20	0.81	DDD
HD 188112	MS:B9	075.D-0352	53565.291	600B	157 ± 749	1.34	720 ± 873	1.17	n-n
CD-23 15853	SD:O	075.D-0352	53533.347	600B	-292 ± 566	0.81	-508 ± 653	0.79	n-n
WD 1952-206	WD:DA6	073.D-0516	53251.088	600B	1240 ± 1138	1.05	-1880 ± 1151	1.07	n-n
WD 1953-011	WD:DA6:M	067.D-0306	52048.303	600R	-40265 ± 1422	1.77			D-D
WD 1953-011	WD:DA6:M	067.D-0306	52048.396	600R	-37616 ± 1466	1.18			D-D
WD 1953-011	WD:DA6:M	067.D-0306	52076.173	600R	-30772 ± 2124	1.86			D-D
WD 1953-011	WD:DA6:M	067.D-0306	52076.385	600R	-22868 ± 3477	2.28			D-D
WD 1953-011	WD:DA6:M	067.D-0306	52078.225	600R	-30838 ± 2119	1.63			D-D
WD 1953-011	WD:DA6:M	067.D-0306	52078.381	600R	-43903 ± 1998	2.14			D-D
WD 1953-011	WD:DA6:M	067.D-0306	52079.174	600R	-38077 ± 2995	3.45			D-D
WD 1953-011	WD:DA6:M	067.D-0306	52079.394	600R	-22884 ± 3662	2.08			D-D
WD 1953-011	WD:DA6:M	067.D-0306	52087.123	600R	-44542 ± 1664	1.76			D-D
WD 1953-011	WD:DA6:M	067.D-0306	52087.172	600R	-41605 ± 2025	2.47			D-D
WD 1953-011	WD:DA6:M	067.D-0306	52087.225	600R	-40904 ± 1368	1.73			D-D
WD 1953-011	WD:DA6:M	067.D-0306	52087.270	600R	-37784 ± 1498	0.87			D-D
HD 226868	SG:O9:XRB	079.D-0549	54270.267	1200B	-15 ± 55	1.00	48 ± 51	0.88	nnn
HD 226868	SG:O9:XRB	079.D-0549	54271.281	1200B	5 ± 43	1.05	-47 ± 41	0.93	nnn
HD 226868	SG:O9:XRB	079.D-0549	54272.262	1200B	30 ± 41	1.00	39 ± 40	0.93	nnn
HD 226868	SG:O9:XRB	079.D-0549	54277.311	1200B	13 ± 55	1.04	70 ± 54	0.99	nnn
HD 226868	SG:O9:XRB	079.D-0549	54281.210	1200B	47 ± 38	1.04	-8 ± 35	0.89	dnn
HD 226868	SG:O9:XRB	079.D-0549	54291.268	1200B	150 ± 37	1.17	-48 ± 33	0.94	ndd
HD 226868	SG:O9:XRB	381.D-0138	54662.213	1200B	32 ± 48	1.04	-43 ± 47	0.99	nnn
HD 226868	SG:O9:XRB	381.D-0138	54663.187	1200B	156 ± 44	1.04	-82 ± 41	0.90	ndd
HD 226868	SG:O9:XRB	381.D-0138	54664.194	1200B	99 ± 46	1.08	-67 ± 43	0.97	nnn
HD 226868	SG:O9:XRB	381.D-0138	54665.195	1200B	57 ± 39	1.13	-58 ± 33	0.90	nnn
HD 226868	SG:O9:XRB	381.D-0138	54671.207	1200B	-20 ± 35	0.83	-50 ± 30	0.65	nnn
HD 226868	SG:O9:XRB	381.D-0138	54672.230	1200B	107 ± 41	1.17	-56 ± 36	0.91	nnn
HD 226868	SG:O9:XRB	381.D-0138	54678.178	1200B	44 ± 36	1.00	86 ± 35	0.94	nnn
V1674 Cyg	GS:F8:V	079.D-0549	54269.283	1200B	-28 ± 23	1.52	23 ± 22	1.04	dnn
V1674 Cyg	GS:F8:V	079.D-0549	54270.267	1200B	-6 ± 22	1.25	15 ± 22	1.23	nnn
V1674 Cyg	GS:F8:V	079.D-0549	54271.281	1200B	20 ± 26	1.40	-12 ± 25	1.30	nnn
V1674 Cyg	GS:F8:V	079.D-0549	54272.262	1200B	-4 ± 23	1.27	-21 ± 21	1.07	nnn
V1674 Cyg	GS:F8:V	079.D-0549	54277.311	1200B	-56 ± 62	5.80	-45 ± 57	5.04	nnn
V1674 Cyg	GS:F8:V	079.D-0549	54281.210	1200B	116 ± 22	1.45	30 ± 21	1.31	ddD
V1674 Cyg	GS:F8:V	079.D-0549	54291.268	1200B	18 ± 18	1.23	57 ± 17	1.16	nnn
V1674 Cyg	GS:F8:V	381.D-0138	54662.213	1200B	-94 ± 44	3.67	66 ± 42	3.35	nnn
V1674 Cyg	GS:F8:V	381.D-0138	54663.187	1200B	31 ± 27	1.66	32 ± 26	1.48	nnn
V1674 Cyg	GS:F8:V	381.D-0138	54664.194	1200B	-68 ± 57	4.16	-1 ± 54	3.77	nnn

Table 5. continued.

Star	Classification	Prog. ID	MJD	grism	$\langle B_z \rangle$ (G)	χ^2/ν	$\langle N_z \rangle$ (G)	χ^2/ν	HmT
V1674 Cyg	GS:F8:V	381.D-0138	54665.195	1200B	-25 ± 21	1.37	-12 ± 19	1.10	nnn
V1674 Cyg	GS:F8:V	381.D-0138	54672.230	1200B	-18 ± 16	1.34	-29 ± 14	1.11	nnn
V1674 Cyg	GS:F8:V	381.D-0138	54678.178	1200B	61 ± 18	1.32	-7 ± 17	1.19	ndd
HD 190073	PM:A2:M.P.E	074.C-0442	53330.016	600B	239 ± 204	1.21	-346 ± 181	0.95	nnn
HD 190073	PM:A2:M.P.E	074.C-0442	53330.030	1200g					—
HD 190073	PM:A2:M.P.E	075.D-0507	53514.369	1200g	103 ± 63	1.14	-33 ± 53	0.80	nnn
HD 190073	PM:A2:M.P.E	075.D-0507	53519.404	1200g	29 ± 80	1.18	3 ± 72	0.96	nnn
HD 190073	PM:A2:M.P.E	075.D-0507	53596.151	1200g	44 ± 73	1.17	-11 ± 71	1.09	nnn
HD 190073	PM:A2:M.P.E	081.C-0410	54609.411	600B	14 ± 73	1.00	59 ± 81	0.76	nnn
HD 191295	GS:B7:SPB	079.D-0241	54343.181	600B	-45 ± 30	0.77	53 ± 35	0.73	nnn
HD 191295	GS:B7:SPB	079.D-0241	54345.218	600B	15 ± 35	0.73	102 ± 43	0.77	nnn
WD 2007-303	WD:DA4	067.D-0306	52076.437	600R	1056 ± 2814	0.94			n-n
WD 2007-303	WD:DA4	073.D-0356	53132.382	600B	312 ± 361	1.08	383 ± 339	0.95	n-n
WD 2007-303	WD:DA4	073.D-0356	53138.373	600B	-452 ± 394	0.88	670 ± 531	1.06	n-n
HD 190290	MS:A0:M.AP.ROAP	073.D-0498	53193.349	600B	2747 ± 100	4.41	11 ± 46	0.93	DDD
HD 190290	MS:A0:M.AP.ROAP	269.D-5044	52494.042	600B	3469 ± 103	5.16	77 ± 43	0.90	DDD
HD 190290	MS:A0:M.AP.ROAP	269.D-5044	52498.032	600B	3417 ± 116	2.69	76 ± 67	0.90	DDD
HD 192674	MS:B9:AP	073.D-0464	53137.362	600B	102 ± 38	0.99	-21 ± 37	0.90	nnn
WD 2014-575	WD:DA2	073.D-0356	53140.360	600B	592 ± 1071	1.00	-388 ± 1295	0.97	n-n
WD 2014-575	WD:DA2	073.D-0356	53184.273	600B	-5213 ± 2235	1.19			n-n
WD 2014-575	WD:DA2	073.D-0356	53185.107	600B	223 ± 1106	1.02	722 ± 1509	1.21	n-n
HD 193756	MS:A9:APROAP	269.D-5044	52498.074	600B	-131 ± 39	1.54	-14 ± 34	1.16	ndd
HD 194783	GS:B8	071.D-0308	52793.361	600B	37 ± 62	0.94	11 ± 60	0.87	nnn
HD 196470	MS:A2:M.AP.ROAP	269.D-5044	52476.233	600B	1366 ± 43	1.74	-5 ± 32	0.98	DDD
WD 2039-202	WD:DA3	060.A-9203	53869.443	600B	-3183 ± 1816	1.61	3053 ± 1920	1.81	n-n
WD 2039-202	WD:DA3	073.D-0322	53148.420	300V	502 ± 655	0.82	-134 ± 678	0.86	n-n
WD 2039-202	WD:DA3	073.D-0356	53143.362	600B	-106 ± 639	1.10	300 ± 706	0.91	n-n
WD 2039-202	WD:DA3	073.D-0356	53167.393	600B	685 ± 390	0.98	821 ± 457	0.97	n-n
HD 199180	MS:A0:M.AP	071.D-0308	52822.344	600B	-398 ± 64	0.97	49 ± 60	0.84	nDD
HD 199728	MS:B9:M.AP	071.D-0308	52822.357	600B	-158 ± 59	0.81	40 ± 60	0.84	nnn
RV Cap	MS:A:RR	082.D-0342	54783.080	1200B	-131 ± 72	1.25	-67 ± 72	1.26	nnn
HD 201018	MS:A2:M.AP	073.D-0464	53151.371	600B	582 ± 41	1.97	14 ± 28	0.92	DDD
HD 201601	MS:A9:M.AP.ROAP	060.A-9203	53335.011	600I	-594 ± 57	1.61	-38 ± 44	0.96	DDD
HD 201601	MS:A9:M.AP.ROAP	077.D-0556	53976.260	600B	-1281 ± 61	1.91	-27 ± 48	1.21	DDD
HD 201601	MS:A9:M.AP.ROAP	077.D-0556	53976.268	1200B	-1459 ± 30	6.16	-2 ± 16	1.18	DDD
HD 201601	MS:A9:M.AP.ROAP	069.D-0210	52531.045	600R	-1714 ± 51	6.91	86 ± 19	1.03	DDD
HD 201484	MS:A:RR	082.D-0342	54783.127	1200B	-75 ± 49	1.22	53 ± 46	1.13	nnn
WD 2105-820	WD:DA6.M	073.D-0516	53199.317	600B	9117 ± 1400	1.18	-1914 ± 1509	1.37	D-D
WD 2105-820	WD:DA6.M	073.D-0516	53227.209	600B	9599 ± 846	1.02	-1 ± 864	1.07	D-D
WD 2105-820	WD:DA6.M	073.D-0516	53192.269	600B	8254 ± 1327	1.42	-417 ± 1210	1.16	D-D
WD 2105-820	WD:DA6.M	073.D-0516	53193.278	600B	10612 ± 984	1.16	-910 ± 1007	1.22	D-D
WD 2105-820	WD:DA6.M	073.D-0516	53197.294	600B	7173 ± 1534	1.21	809 ± 1521	1.19	d-d
HD 202149	MS:B9:HG	073.D-0464	53137.413	600B	40 ± 36	1.01	46 ± 37	1.08	nnn
HD 202627	MS:A1:AP	071.D-0308	52793.374	600B	-117 ± 60	0.94	141 ± 56	0.83	nnn
HD 202671	MS:B7:HEW.MN	073.D-0464	53151.411	600B	-18 ± 51	0.95	-55 ± 50	0.96	nnn
WD 2115-560	WD:DA6	073.D-0516	53199.342	600B	-1114 ± 1080	1.18	-1562 ± 974	0.96	n-n
WD 2115-560	WD:DA6	073.D-0516	53227.238	600B	304 ± 928	1.09	-103 ± 915	1.05	n-n
HD 203932	MS:A5:APROAP	269.D-5044	52498.112	600B	-298 ± 60	0.97	7 ± 59	0.92	dnd
HD 205805	GS:B7	075.D-0352	53533.384	600B	-130 ± 115	0.93	-210 ± 138	0.97	nnn
HD 206540	MS:B5:SPB	075.D-0295	53514.416	1200g	-42 ± 41	0.80	112 ± 40	0.78	nnn
HD 206540	MS:B5:SPB	079.D-0241	54344.220	600B	-33 ± 29	0.76	-37 ± 29	0.75	nnn
HD 206653	MS:B9:AP	071.D-0308	52793.394	600B	37 ± 54	0.81	-4 ± 57	0.88	nnn
JL 87	SD:B	075.D-0352	53597.196	600B	-120 ± 143	0.94	-125 ± 177	0.95	nnn
HD 205879	MS:B8:SPB	079.D-0241	54343.226	600B	90 ± 47	0.79	-86 ± 58	0.77	nnn
WD 2148+286	SD:O	075.D-0352	53533.414	600B	-114 ± 400	0.76	-914 ± 548	0.87	nnn
WD 2149+021	WD:DA3	073.D-0356	53183.278	600B	-340 ± 669	1.10	301 ± 805	1.09	n-n
WD 2149+021	WD:DA3	073.D-0356	53196.346	600B	139 ± 545	0.83	1200 ± 695	0.92	n-n
WD 2149+021	WD:DA3	073.D-0356	53222.200	600B	102 ± 509	1.01	835 ± 569	0.87	n-n
HD 208057	MS:B3:E.SPB	073.D-0466	53192.308	600B	-170 ± 53	0.93	-86 ± 64	0.94	ndd
HD 208057	MS:B3:E.SPB	075.D-0295	53597.166	1200g	-124 ± 35	0.98	36 ± 34	0.93	ndd
WD 2151-015	WD:DA6	073.D-0516	53240.174	600B	661 ± 2297	1.36	4329 ± 2256	1.27	n-n
WD 2151-015	WD:DA6	073.D-0516	53251.124	600B	-1692 ± 926	0.96	667 ± 915	0.95	n-n
WD 2151-015	WD:DA6	073.D-0516	53252.120	600B	-703 ± 1668	1.27	-4305 ± 1814	1.51	n-n
WD 2153-512	WD:DQ7	082.D-0736	54786.073	600B					—
BV Aqr	MS:A:RR	082.D-0342	54782.074	1200B	-10 ± 46	1.18	-34 ± 44	1.11	nnn
HD 209409	MS:B7:E	077.D-0406	53955.185	600B	-70 ± 47	1.15	-56 ± 41	0.79	nnn
HD 209409	MS:B7:E	380.D-0480	54432.027	1200B	-77 ± 32	0.75	1 ± 29	0.64	nnn

Table 5. continued.

Star	Classification	Prog. ID	MJD	grism	$\langle B_z \rangle$ (G)	χ^2/ν	$\langle N_z \rangle$ (G)	χ^2/ν	HmT
HD 209409	MS:B7:E	380.D-0480	54433.008	1200B	-63 ± 39	0.94	-21 ± 32	0.67	nnn
HD 209459	MS:B9	071.D-0308	52822.381	600B	-24 ± 65	0.95	52 ± 63	0.91	nnn
WD 2211-495	WD:DA1	073.D-0356	53140.401	600B	-69 ± 1076	0.85	-1592 ± 1209	0.85	n-n
WD 2211-495	WD:DA1	073.D-0356	53185.246	600B	-1445 ± 1124	0.80	-2103 ± 1282	0.79	n-n
HD 212385	MS:A3:M.AP	071.D-0308	52822.413	600B	338 ± 43	0.96	23 ± 41	0.89	nDD
HD 212385	MS:A3:M.AP	073.D-0464	53184.297	600B	639 ± 40	2.02	-17 ± 28	1.02	DDD
HD 212643	MS:A0	074.C-0442	53332.051	600B	194 ± 67	0.85	161 ± 71	0.94	nnn
WD 2226-210	WD:CP:DA0	075.D-0289	53527.386	600B	-194 ± 1174	1.16			nnn
WD 2226-210	WD:CP:DA0	075.D-0289	53526.387	600B	3148 ± 969	1.07	-2074 ± 1014	1.20	dnd
HD 213637	MS:F1:M.AP.ROAP	079.D-0240	54230.382	600B	753 ± 87	1.74	-23 ± 59	0.81	nDD
HD 213637	MS:F1:M.AP.ROAP	079.D-0240	54248.387	600B	693 ± 35	0.89	81 ± 32	0.75	DDD
HD 213637	MS:F1:M.AP.ROAP	079.D-0240	54269.420	600B	767 ± 26	1.11	21 ± 22	0.75	DDD
HD 213637	MS:F1:M.AP.ROAP	079.D-0240	54279.198	600B	755 ± 38	0.93	24 ± 33	0.72	DDD
HD 213637	MS:F1:M.AP.ROAP	079.D-0240	54288.365	600B	772 ± 38	0.92	74 ± 35	0.78	DDD
HD 213637	MS:F1:M.AP.ROAP	079.D-0240	54297.404	600B	831 ± 35	0.93	15 ± 31	0.74	DDD
HD 213637	MS:F1:M.AP.ROAP	079.D-0240	54305.186	600B	697 ± 39	0.91	-19 ± 35	0.74	DDD
HD 213637	MS:F1:M.AP.ROAP	079.D-0240	54316.150	600B	642 ± 40	0.82	19 ± 39	0.78	DDD
HD 213637	MS:F1:M.AP.ROAP	269.D-5044	52498.150	600B	856 ± 45	1.39	-42 ± 36	0.92	DDD
HD 215789	MS:A2:SB	077.D-0556	53976.290	600B	16 ± 84	0.88	19 ± 86	0.93	nnn
HD 215573	MS:B6:SPB	072.D-0377	52900.080	600B	196 ± 64	0.99	34 ± 63	0.96	nnd
HD 215573	MS:B6:SPB	073.D-0466	53191.222	600B	-17 ± 44	1.00	23 ± 42	0.94	nnn
HD 215573	MS:B6:SPB	073.D-0466	53192.290	600B	-73 ± 36	0.79	63 ± 35	0.75	nnn
HD 215573	MS:B6:SPB	075.D-0295	53506.416	1200g	50 ± 38	0.79	25 ± 44	0.72	nnn
HD 215573	MS:B6:SPB	075.D-0295	53522.420	1200g	67 ± 95	1.76	22 ± 94	1.73	nnn
HD 215573	MS:B6:SPB	079.D-0241	54345.232	600B	56 ± 39	0.77	60 ± 49	0.79	nnn
HD 215573	MS:B6:SPB	078.D-0140	54042.020	600B	225 ± 68	0.92	50 ± 68	0.93	nnd
HD 215573	MS:B6:SPB	079.D-0241	54343.245	600B	-37 ± 32	0.75	106 ± 40	0.77	nnn
LP 877-23	SD:G	060.A-9203	52476.268	600B	-419 ± 553	1.02			nnn
HD 217186	MS:A1	077.D-0556	53976.330	600B	101 ± 45	0.83	-20 ± 59	0.92	nnn
HD 217522	MS:F:M.AP.ROAP	060.A-9203	53335.026	600I	-520 ± 63	1.56	65 ± 59	0.93	DDD
HD 217522	MS:F:M.AP.ROAP	269.D-5044	52498.183	600B	-938 ± 70	1.50	123 ± 53	0.88	DDD
HD 217522	MS:F:M.AP.ROAP	069.D-0210	52531.236	600R	-1063 ± 44	6.99	46 ± 17	1.10	dDD
HD 218495	MS:A2:M.AP.ROAP	269.D-5044	52519.225	600B	-1169 ± 56	1.20	-22 ± 50	0.95	DDD
HD 218994	MS:A:M.AP	079.D-0241	54343.203	600B	430 ± 30	0.89	-2 ± 34	0.78	DDD
HD 219571	GS:F1:D	074.C-0463	53279.040	1200g	81 ± 29	1.25	34 ± 34	1.11	ndn
WD 2317-054	SD:O:HPM	080.D-0521	54400.015	600B	-857 ± 3266	0.81			n-n
IP Peg	WD:CV	079.D-0697	54311.313	1200B					—
IP Peg	WD:CV	081.D-0670	54693.286	1200B					—
IP Peg	WD:CV	081.D-0670	54694.270	1200B					—
WD 2322+137	WD:DA9:HPM	080.D-0521	54400.030	600B					—
HD 221507	MS:B9:HGMN	072.D-0377	52900.092	600B	-178 ± 59	0.94	-47 ± 59	0.94	nnn
HD 221760	MS:A2:AP	071.D-0308	52793.415	600B	-26 ± 75	0.91	219 ± 75	0.90	nnn
HD 221760	MS:A2:AP	073.D-0464	53184.314	600B	-36 ± 31	0.80	2 ± 30	0.75	nnn
WD 2333-049	WD:DA6	073.D-0516	53274.201	600B	4478 ± 5423	1.10			n-n
NLTT 57760	WD:DZ:HPM	080.D-0521	54419.090	600B					—
CD-35 15910	SD:B	075.D-0352	53598.378	600B	258 ± 239	0.99	-371 ± 251	1.10	nnn
HD 223640	MS:B9:M.AP	071.D-0308	52822.427	600B	-32 ± 59	0.80	-59 ± 63	0.94	nnn
HD 224361	MS:A1	077.D-0556	53976.313	600B	-83 ± 81	1.06	-144 ± 82	1.08	nnn
HD 224392	MS:A1	077.D-0556	53976.347	600B	-57 ± 43	0.77	42 ± 48	0.74	nnn
HD 224686	MS:B9:E	077.D-0406	53869.405	600B	30 ± 17	0.82	31 ± 17	0.77	nnn
HD 224686	MS:B9:E	380.D-0480	54432.065	1200B	58 ± 33	0.82	46 ± 30	0.70	nnn